MINISTÉRIO DA EDUCAÇÃO
UNIVERSIDADE FEDERAL DE SERGIPE
PRÓ-REITORIA DE PÓS-GRADUAÇÃO E PESQUISA
PROGRAMA DE PÓS-GRADUAÇÃO EM ZOOTECNIA

TRANSCRIPTOMA DE CODORNAS JAPONESAS É MODULADO POR TEMPERATURA EMBRIONÁRIA E DESAFIO IMUNE

Juliana dos Santos Conceição

SÃO CRISTÓVÃO – SE
2025

TRANSCRIPTOMA DE CODORNAS JAPONESAS É MODULADO POR TEMPERATURA EMBRIONÁRIA E DESAFIO IMUNE

Juliana dos Santos Conceição
Zootecnista

Dissertação apresentada ao Colegiado do Programa de Pós-Graduação Integrado em Zootecnia, como requisito parcial para a obtenção do Título de Mestre em Zootecnia.

Orientador (a): Ana Paula Del Vesco

SÃO CRISTÓVÃO – SE
2025

FICHA CATALOGRÁFICA

MANIPULAÇÃO TÉRMICA E RESPOSTA IMUNE A LIPOPOLISSACARÍDEO EM CODORNAS PÓS-ECLOSÃO

Comissão Examinadora da Defesa de Dissertação de
Juliana dos Santos Conceição

Aprovada em 28 de Julho de 2025

_____
Profa. Dra. Ana Paula Del Vesco (UFRB/UFS)
Orientadora

_____
Profa. Dra. Eliane Gasparino (UEM)
Examinador Interno

_____
Prof. Dr. Júlio Cesar Polonio (UEM)
Examinador Externo

SÃO CRISTÓVÃO – SE
2025

DEDICATÓRIA

À todos os pesquisadores que, mesmo enfrentando batalhas silenciosas com a saúde mental, seguem resistindo, criando, investigando e contribuindo para o avanço da ciência. Que nunca lhes faltem acolhimento, reconhecimento e esperança.

AGRADECIMENTOS

A lista de agradecimentos é extensa e sou profundamente grata por isso.

Agradeço, em primeiro lugar, ao Senhor Jesus, meu Pai, Amigo, Conselheiro e amado Irmão. Sem Ele, nada seria. É por Sua graça que sigo adiante e por Sua vontade que pessoas tão especiais cruzaram meu caminho e me acompanharam nesta jornada.

Aos meus pais, Zenilda e Jair, meu mais sincero reconhecimento. Vocês fizeram o possível e o impossível para que eu chegasse até aqui. Tudo o que sou devo, em grande parte, ao amor e dedicação de vocês. Às minhas irmãs, Ana Júlia e Alícia, que me ensinaram o verdadeiro significado do amor, meu carinho eterno.

À minha tia Elisângela, à minha avó Dona Josefina e à minha prima Maria Eduarda, obrigada por sempre me ouvirem com paciência e bom humor, oferecendo conselhos e acolhimento nos momentos em que mais precisei.

Ao meu companheiro de vida, Marcelo, minha gratidão por nunca deixar de acreditar em mim. Sua presença constante e apoio incondicional foram fundamentais em cada etapa deste projeto.

Aos meus grandes e melhores amigos, Lenilson, Moisés e Amanda, obrigada por serem a família que escolhi. A amizade de vocês é um presente que carrego com orgulho e afeto.

Aos meus queridos amigos Peterson, Marisa e Vanicleide, obrigada por todo apoio e carinho, sempre terão um lugar especial no meu coração.

À minha orientadora, professora Ana Paula, que se tornou também uma mãe e amiga: você sempre diz que sou "fora da curva", mas isso se deve, em grande parte, à você, que é uma inspiração como profissional e ser humano. Sua orientação firme e generosa foi essencial para este trabalho.

Às queridas, Thais e Angélica, doutoras por mérito e amigas por bênção, agradeço pela parceria, pelos conselhos, pelos puxões de orelha e por acreditarem em mim. Nada disso seria possível sem vocês.

À banca examinadora, composta pela professora Dra. Eliane e pelo professor Dr. Julio, agradeço imensamente. Dra. Eliane, minha sincera gratidão pela leitura atenta e pelas contribuições valiosas ao longo do desenvolvimento deste projeto. Admiro profundamente o seu trabalho e sinto-me verdadeiramente honrada por tê-la na minha banca.

EPÍGRAFE

"Venham a mim, todos os que estão cansados e sobrecarregados, e eu darei descanso a vocês."
Matheus 11:28

LISTA DE FIGURAS

LISTA DE FIGURAS DO CAPÍTULO 1

LISTA DE TABELAS DO CAPÍTULO 1

LISTA DE FLUXOGRAMAS DO CAPÍTULO 1

SUMÁRIO

TRANSCRIPTOMA DE CODORNAS JAPONESAS É MODULADO POR TEMPERATURA EMBRIONÁRIA E DESAFIO IMUNE

RESUMO: A embriogênese é um período crítico de programação, pois fatores ambientais podem modular a fisiologia dos organismos. Em aves, a temperatura de incubação tem sido amplamente desenvolvida como um indutor de respostas genéticas que influenciam o desenvolvimento embrionário e a resposta aos desafios pós-eclosão. Nesse contexto, o presente estudo teve como objetivo investigar os efeitos da manipulação térmica embrionária sobre a resposta imune de codornas japonesas (*Coturnix coturnix japonica*) desafiadas com lipopolissacarídeo (LPS) após a eclosão, utilizando análise de transcriptoma (RNA-seq). Para isso, foi realizado um experimento em esquema fatorial 2x2, com duas temperaturas de incubação: temperatura controle (CTL - 37,5°C) e alta temperatura (AT - 39°C) e dois status de inoculação: codornas inoculadas com LPS (LPS) e codornas não inoculadas com LPS (SLPS). Os ovos permaneceram nas respectivas temperaturas dos tratamentos durante todo o período de incubação e, 25 dias após a eclosão, os pintainhos foram desafiados com LPS ou solução salina (placebo). Posteriormente a inoculação, o tecido do jejuno foi coletado para a análise de expressão gênica via RNA-seq. A temperatura de incubação reduziu significativamente ($p<0,05$) as taxas de eclosão, mas não afetou ($p>0,05$) o desempenho morfológico dos embriões sobreviventes. O LPS induziu alterações significavas ($p<0,05$) no baço, indicando ativação do sistema imunológico. A análise transcriptômica revelou genes diferencialmente expressos (p-ajustado$<0,05$) associados a processos metabólicos, resposta imune e estresse oxidativo, com padrões distintos entre os contrastes avaliados (CTL+LPS *vs* CTL+SLPS e AT+LPS vs AT+SLPS). Em condição controle, o LPS induziu a expressão diferencial de 41 genes, destacando *IL1R2*, *IL18BP* e *S100A12*, relacionados à modulação inflamatória, integridade da barreira mucosa e metabolismo energético. Em aves incubadas sob alta temperatura, o LPS desencadeou amplas alterações, com ativação de vias associadas à inflamação, homeostase lipídica, controle proteico, metabolismo energético (glicólise, pentoses e ciclo de Krebs) e tráfego vesicular, enquanto suprimia genes cruciais para imunidade adaptativa, angiogênese, diferenciação celular e regulação epigenética. Um conjunto conservado de genes inflamatórios (*MMP7, PI3, SLC6A14*) foi regulado (p-ajustado$<0,05$) em ambas as condições térmicas, sugerindo ativação de mecanismos centrais de defesa. Conclui-se que a alta temperatura durante a incubação compromete a eclosão, mas não o fenótipo da progênie; contudo, modula de forma profunda a resposta molecular ao LPS, alterando vias inflamatórias, metabólicas e regenerativas, o que pode impactar a adaptação intestinal a estresses futuros.

Palavras chave: coturnicultura; epigenética; expressão gênica; inflamação; reprogramação embrionária.

JAPANESE QUAIL TRANSCRIPTOME IS MODULATED BY EMBRYONIC TEMPERATURE AND IMMUNE CHALLENGE

ABSTRACT: Embryogenesis is a critical programming period, as environmental factors can modulate the physiology of organisms. In birds, incubation temperature has been widely studied as an inducer of genetic responses that influence embryonic development and response to post-hatch challenges. In this context, the present study aimed to investigate the effects of embryonic thermal manipulation on the immune response of Japanese quails (*Coturnix coturnix japonica*) challenged with lipopolysaccharide (LPS) after hatching, using transcriptome analysis (RNA-seq). For this purpose, an experiment was carried out in a 2x2 factorial design, with two incubation temperatures: control temperature (CTL - 37.5°C) and high temperature (AT - 39°C) and two inoculation statuses: quails inoculated with LPS (LPS) and quails not inoculated with LPS (SLPS). Eggs remained at the respective treatment temperatures throughout the incubation period, and 25 days after hatching, chicks were challenged with LPS or saline (placebo). After inoculation, jejunal tissue was collected for gene expression analysis via RNA-seq. Incubation temperature significantly reduced ($p<0.05$) hatching rates but did not affect ($p>0.05$) the morphological performance of surviving embryos. LPS induced significant changes ($p<0.05$) in the spleen, indicating immune system activation. Transcriptomic analysis revealed differentially expressed genes (adjusted $p<0.05$) associated with metabolic processes, immune response, and oxidative stress, with distinct patterns between the contrasts evaluated (CTL+LPS *vs.* CTL+SLPS and AT+LPS *vs.* AT+SLPS). Under control conditions, LPS induced the differential expression of 41 genes, notably *IL1R2*, *IL18BP*, and *S100A12*, related to inflammatory modulation, mucosal barrier integrity, and energy metabolism. In birds incubated at high temperature, LPS triggered broad changes, activating pathways associated with inflammation, lipid homeostasis, protein control, energy metabolism (glycolysis, pentose and Krebs cycles), and vesicular trafficking, while suppressing genes crucial for adaptive immunity, angiogenesis, cellular differentiation, and epigenetic regulation. A conserved set of inflammatory genes (*MMP7, PI3, SLC6A14*) was upregulated (adjusted $p<0.05$) under both thermal conditions, suggesting activation of central defense mechanisms. We conclude that high temperature during incubation compromises hatching, but not the phenotype of the offspring; However, it profoundly modulates the molecular response to LPS, altering inflammatory, metabolic, and regenerative pathways, which may impact intestinal adaptation to future stresses.

Key words: embryonic reprogramming; epigenetics; gene expression; inflammation; quail farming.

INTRODUÇÃO GERAL

A embriogênese é um processo complexo e dinâmico, caracterizado por eventos celulares e moleculares que culminam na formação de um organismo completo. Em aves, esse processo ocorre inteiramente dentro do ovo, onde o embrião se desenvolve a partir de interações coordenadas entre os anexos embrionários, como saco vitelínico, âmnio, alantoide e cório (Jiang *et al*., 2023). Durante esse período, fatores ambientais, influenciam de modo crucial na regulação do crescimento embrionário e na modulação de mecanismos genéticos que afetam a fisiologia das aves ao longo da vida (Bednarczyk *et al*., 2021).

Dentre os fatores ambientais que influenciam a embriogênese, a temperatura tem sido amplamente estudada devido ao seu impacto direto na taxa metabólica, na eclodibilidade dos ovos e na sobrevivência neonatal das aves (Ebtsam *et al.*, 2023). Com isso, a manipulação térmica embrionária tem se mostrado como estratégia promissora na indução de respostas genéticas para aumentar a tolerância ao estresse térmico e melhorar a eficiência produtiva. Essas modificações envolvem processos de regulação e expressão gênica (David *et al*., 2019).

Existe um termo chamado plasticidade fenotípica que está associado à adaptação ao calor quando as aves são expostas a desafio térmicos durante a incubação (Raza *et al*., 2021). Esse mecanismo pode impactar no modo como as aves respondem a diferentes desafios futuros, incluindo a forma como lida contra microorganismos (Alma *et al.*, 2024). Nesse sentido, a exposição ao lipopolissacarídeo (LPS) é bastante utilizada como mecanismo para induzir estresse imunológico em animais (Yousefi; Jonaidi; Sadeghi, 2021). O LPS ativa a resposta inflamatória via receptores, como a via Toll-like 4 (*TLR4*), desencadeando a produção de citocinas pró-inflamatórias e modulando a expressão de genes associados à imunidade inata de aves (Koutsos e Klasing, 2001). Evidências sugerem que o estresse imunológico induzido por LPS pode influenciar mecanismos epigenéticos, afetando a expressão de genes relacionados à resposta ao estresse e ao metabolismo celular, o que pode comprometer o desempenho e a sobrevivência das aves (Bi *et al*., 2022).

Nesse contexto, o estudo do transcriptoma, conjunto completo de transcrições gênicas ativas em uma célula ou tecido em determinada condição, surge como uma ferramenta essencial para compreender como os estímulos ambientais e imunológicos influenciam a regulação da expressão gênica (Wang, Gerstein e Snyder, 2008). A análise transcriptômica permite identificar genes diferencialmente expressos, elucidar vias metabólicas e inflamatórias ativadas, e revelar mecanismos moleculares que participam da adaptação e resposta fisiológica das aves frente a diferentes desafios.

Nesse trabalho, hipotetizamos que a manipulação térmica durante a embriogênese de codornas resultará em alterações significativas nos perfis de expressão gênica em resposta ao desafio com LPS pós-eclosão. Para investigar nossa hipótese, ovos de codornas japonesas foram submetidos a duas temperaturas de incubação: controle (CTL) e alta temperatura (AT). Aos 25 dias de idade, as aves provenientes de ambas temperaturas foram submetidas à inoculação com lipopolissacarídeo (LPS) ou com solução placebo (SLPS). Após 3,5 horas da inoculação, as aves foram abatidas e o tecido do jejuno foi coletado para a análise molecular. A escolha do jejuno se justifica por sua importância como principal sítio de absorção de nutrientes, além de desempenhar papel-chave na imunidade de mucosa e atuar como barreira contra patógenos, sendo altamente responsivo a estressores ambientais e inflamatórios (Maaike Vancamelbeke e Vermeire, 2017). Os resultados deste trabalho contribuem para a compreensão de como fatores ambientais moldam a regulação molecular do desenvolvimento em aves, fornecendo informações para otimizar práticas de manejo e melhorar a resiliência dos animais a desafios externos.

REVISÃO DE LITERATURA

Desenvolvimento embrionário das aves

As codornas são amniotas e ovíparas, com o desenvolvimento das membranas embrionárias ocorrendo dentro do ovo (Farner, 1960; Griffith *et al*., 2017). Esse processo é sustentado pelos membranas extraembrionárias, como o saco vitelínico, âmnio, alantoide e cório (Jiang *et al*., 2023). O desenvolvimento do embrião dentro do ovo representa entre 35% e 40% da vida total do indivíduo e ocorre em três etapas principais: embriogênese (E3 a E7 – do terceiro ao sétimo dia embrionário), crescimento (E8 a E14 – do oitavo ao décimo quarto dia embrionário) e maturação (a partir do décimo quarto dia embrionário) (Hamburger; Hamilton, 1992; Meng *et al*., 2021).

O ovo recém-formado contém todos os componentes necessários para o desenvolvimento adequado do embrião, com exceção de calor e oxigênio (Griffith *et al*., 2017; Jiang *et al*., 2023). O oxigênio é fornecido por difusão através dos poros da casca, enquanto o calor é gerado pela temperatura de incubação, geralmente mantido pela sua matriz (Huang; Arai; Kawahara, 2015). As estruturas básicas que compõem o ovo incluem o blastodisco (ou blastômero), gema, albúmen, membranas da casca, casca e cutícula (Starck; Stewart; Blackburn, 2021).

Através da mitose, o blastômero, célula-mãe, divide-se em duas células-filhas no momento em que o ovo entra no istmo (Bednarczyk *et al*., 2021). Após 20 minutos, ocorre outra divisão, seguida por uma terceira divisão ainda no istmo, formando um total de oito células. Cerca de cinco horas após a fertilização, o zigoto atinge o útero, alcançando o estágio de 16 células. Durante as 17 horas seguintes, as divisões celulares continuarão resultando na formação de 256 células, que é o blastoderme indiferenciado do período de pré-gástrula. O blastoderme é composto pelo epiblasto, que dará origem ao embrião, e pelo hipoblasto, responsável pelas estruturas extraembrionárias.

Enquanto as divisões celulares prosseguem no útero, ocorre a formação da casca do ovo, cuja função é proteger o embrião contra invasões microbianas, variações de calor, respiração e transpiração através dos poros. As membranas da casca são delgadas, flexíveis e compostas por colágeno, ovoqueratina e glicoproteínas. Elas são semipermeáveis, permitindo a troca de gases e água. Já a cutícula é um filme que cobre toda a casca, formando uma barreira contra a invasão bacteriana e a perda excessiva de água (Liu *et al*., 2017).

A gema diferencia-se em duas partes: a branca, rica em proteínas que nutrem o embrião, e a amarela, rica em lipídios (Meng *et al*., 2021). Além disso, contém imunoglobulinas (IgG), que conferem imunidade materna ao embrião. O albúmen, por sua vez, desempenha um papel fundamental na proteção física do conteúdo interno do ovo e serve como principal fonte de água e minerais (Meng *et al*., 2021).

O saco vitelino é a primeira membrana a se formar (Gadelha *et al*., 2021), proveniente da ectoderme, tendo função nutricional e absortiva, pois absorve a gema, formando o vitelo, que é utilizado para nutrir o embrião e participa junto com a membrana corioalantoide para o processo de troca gasosa (Mortola, 2009). O âmnio é um saco membranoso, preenchido por líquido amniótico que é formado a partir de um dobramento da ectoderme e acompanhado pela mesoderme somática (Vanderley; Santana, 2015). É o anexo que possui maior relação com o embrião, pois se encontra envolto ao feto e tem função de proteger contra choques mecânicos e contra microrganismos. O alantoide é formado na endoderme a partir do divertículo da parede ventral do intestino, fazendo o depósito de excreção do ovo (Mortola, 2009; Vanderley; Santana, 2015; Monteiro, 2017). O cório forma a parede externa do blastocisto, formado por duas camadas de trofoblasto e pela mesoderme extraembrionária, unindo-se ao alantoide para desempenhar função respiratória e está localizado logo abaixo da casca (Gabrielli; Accili, 2010).

De acordo com alguns autores Bekoff (1981); Hamburger e Hamilton, (1992); e Watt *et al*. (1993), o desenvolvimento embrionário de aves (Figura 1) ocorre da seguinte forma: Antes da postura, o blastoderme inicia sua diferenciação em duas camadas germinativas, marcando o início da gastrulação. A camada acima do blastocele origina o epiblasto (ectoderma), enquanto a camada abaixo da origem do hipoblasto (endoderma). Após a postura, o embrião, que antes estava a uma temperatura de 40-41°C no corpo da ave, sofre resfriamento. Nesse estágio inicial, o embrião se tornou um organismo pecilotérmico, sendo fortemente influenciado pela temperatura ambiental.

Nas primeiras 24 horas de incubação, começa a se formar o trato alimentar, a prega neural, o cérebro e os sistemas nervosos, da cabeça e dos olhos. Em até 48 horas, o embrião se posiciona no lado esquerdo, os vasos sanguíneos começam a se formar, o coração inicia os nervos e o tubo neural se desenvolve a partir do fechamento do canal neural. Também ocorre a formação da vesícula auditiva e as três regiões do cérebro, além dos primeiros sinais de formação do ânus.

Até 72 horas, surgem os vestígios da cauda, os botões dos membros superiores e inferiores, as narinas e o cristalino dos olhos. Aos quatro dias (E4), completa-se a formação das membranas extraembrionárias (âmnio, cório e alantoide), e o embrião posiciona-se ao lado esquerdo. Aos cinco dias (E5), o embrião cresceu significativamente, os olhos tornam-se visíveis (grandes e pretos), e forma-se o proventrículo e a moela. Aos sete dias (E7), os dígitos das asas e pernas tornam-se proeminentes, o abdômen aumenta devido ao desenvolvimento das vísceras, e o coração já está na cavidade torácica. A alantoide cobre completamente a gema, e inicia-se a formação das penas.

Aos dez dias (E10), o bico resistente, e os poros da pele tornam-se visíveis. O corpo e o pescoço começam a adquirir a forma característica da ave, e o embrião é coberto por uma penugem fina. No 14º dia (E14), o embrião posiciona a cabeça em direção à câmara de ar. No 15º dia (E15), o intestino penetra na cavidade abdominal. Aos 19 dias (E19), o saco vitelino começa a ser absorvido, e o embrião ocupa quase totalmente o ovo, exceto pela câmara de ar.

No 20º dia (E20), o saco vitelino está completamente absorvido, o alantoide seco, e o embrião rompe o âmnio, iniciando a respiração pela câmara de ar. Por fim, no 21º dia (E21), o pintainho bica a casca, eclode, seca suas penas e cicatriza o umbigo.

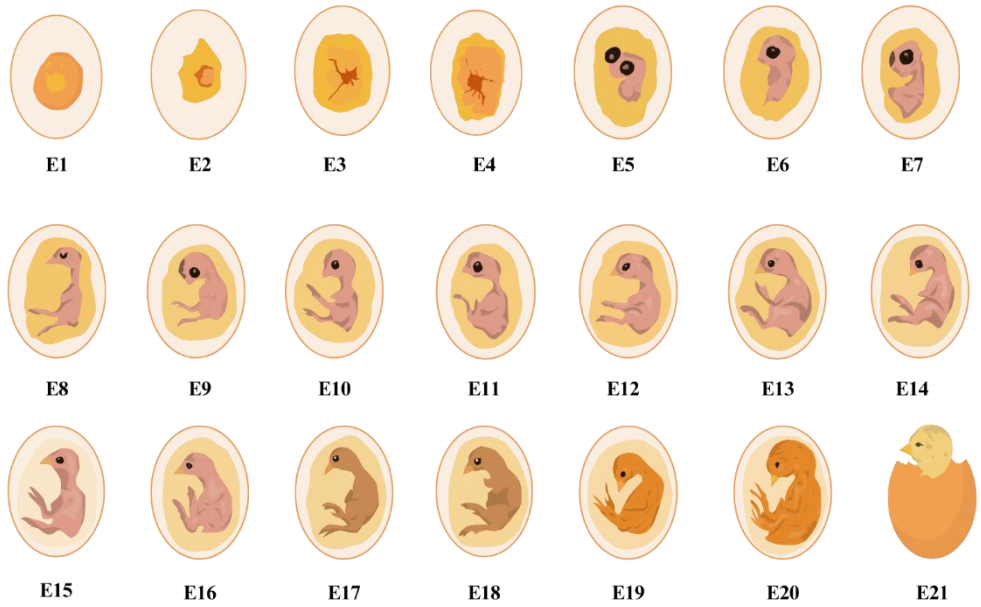

Figura 1. Desenvolvimento embrionário de aves

Figura adaptada de BEKOFF (1981); HAMBURGER E HAMILTON, (1992) e WATT *et al.* (1993). Representação do desenvolvimento embrionário do pintainho. A imagem representa o estágio de desenvolvimento com a referente contagem do 1° dia do embrião (E1) ao 21° dia do embrião (E21).

Influência da temperatura na embriogênese das aves

A temperatura ideal para codornas em fase de postura varia entre 22 e 24°C, caracterizando a zona termoneutra (Barros *et al*., 2024). Durante o período de incubação, de acordo com Ebtsam *et al.* (2023), a temperatura ideal está entre 37,5°C e 37,8°C. A manipulação térmica de pintainhos pode induzir adaptações epigenéticas que influenciam a saúde e o desenvolvimento das aves, uma vez que variações térmicas afetam funções orgânicas e podem comprometer o desempenho (Bednarczyk *et al*., 2021).

Como estratégia de adaptação, a indústria avícola adota o condicionamento térmico, que consiste na aclimatação precoce ao calor, aplicada durante a embriogênese ou no período pós-natal. Quando realizado corretamente, esse método pode aumentar a termotolerância das aves em ambientes quentes. A temperatura de incubação também influencia os sistemas termorreguladores, incluindo os sistemas nervoso periférico e central, permitindo melhor resposta ao estresse térmico na vida adulta (Tzschentke, 2008; Ebtsam *et al.*, 2023).

Alguns estudos investigaram o impacto da manipulação térmica no desenvolvimento embrionário de frangos de corte. David *et al*. (2019) analisaram amostras de hipotálamo e músculo de aves aos 35 dias, utilizando imunoprecipitação da cromatina, e identificaram

modificações epigenéticas nas marcas H3K4me3 e H3K27me3. Essas alterações estavam associadas à regulação de genes do desenvolvimento neural, sugerindo que a manipulação térmica pode influenciar a neurogênese e aumentar a resistência ao estresse térmico na fase adulta. Já Al-Zghoul; Mohammad (2020) avaliaram os efeitos da intervenção térmica entre os dias embrionários 8 e 16 (E8-E16) e sua relação com a resposta ao estresse térmico crônico na fase adulta. Eles observaram que frangos expostos ao calor apresentaram menor expressão de enzimas antioxidantes e alterações nos níveis de mRNA de fatores de choque térmico, possivelmente devido a modificações epigenéticas induzidas pela modulação térmica.

A determinação do momento ideal para a aclimatação térmica é fundamental, sendo promissor o período anterior ao décimo dia embrionário, pois antecede a formação completa da resposta ao estresse pelo eixo adrenal (Collin *et al*., 2007). Após o 13º dia embrionário, a aclimatação também se mostra relevante, pois coincide com o aumento da produção de tri-iodotironina (T3), hormônio essencial para a termorregulação (Yahav *et al*., 2004). Os efeitos do condicionamento térmico incluem a redução da temperatura corporal, observada até 28 dias após a eclosão (Tona *et al*., 2008). Para melhorar a termotolerância sem comprometer a eclodibilidade, a exposição de embriões entre os dias E7 e E16 a 39,5°C por 12 horas diárias foi identificada como uma estratégia eficaz (Loyau *et al*., 2014).

Além da manipulação térmica embrionária, a intervenção pós-natal também contribui para a regulação térmica das aves, preparando-as para enfrentar desafios térmicos na fase adulta. A exposição ao calor moderado nos primeiros dias de vida auxilia na manutenção da temperatura corporal e melhora o desempenho sob altas temperaturas (Persson; Cuív; NORD, 2024). Esse condicionamento térmico pós-natal também favorece a eficiência alimentar, aumentando a ingestão e a conversão de ração em ganho de peso, fator essencial para a viabilidade econômica da criação (Bilal *et al*., 2021).

Fora da zona térmica ideal, as aves enfrentam dificuldades para manter a homeostase, entrando em estado de estresse térmico, que pode ser agudo ou crônico. Esse estresse desencadeia respostas comportamentais, bioquímicas e fisiológicas, prejudicando o desempenho produtivo. Para mitigar o excesso de calor, codornas reduzem a ingestão alimentar, aumentam o consumo de água, passam mais tempo deitadas e mantêm as asas abertas (Wasti; Sah; Mishra, 2020). Atrelado a isso, o calor excessivo induz estresse oxidativo e alterações fisiológicas, incluindo aumento da relação heterófilo/linfócito e dos níveis plasmáticos de glicose, colesterol e glicocorticoides (Vesco *et al*., 2020).

O metabolismo celular gera espécies reativas de oxigênio (ERO) e nitrogênio (ERN), essenciais para funções como a transcrição de citocinas e o transporte de íons. Entretanto, temperaturas elevadas aumentam a demanda energética e, consequentemente, a produção dessas espécies reativas, podendo levar ao estresse oxidativo e danos celulares, incluindo peroxidação lipídica e apoptose (Chaudhary; Mishra, 2024). Para neutralizar esses efeitos, o organismo ativa mecanismos antioxidantes regulatórios, incluindo enzimas como superóxido dismutase (SOD), glutationa peroxidase (GPx) e catalase (CAT), além de antioxidantes não enzimáticos, como vitamina E e ácido ascórbico (Madkour *et al*., 2022).

Outro mecanismo de resposta ao estresse térmico envolve a síntese de proteínas de choque térmico (HSPs), que auxiliam na manutenção celular, no dobramento de proteínas e na resposta imune. A HSP70, em particular, tem sido associada à maior tolerância ao calor em aves comerciais (Al Amaz; Mishra, 2024).

Estudos indicam que variações térmicas durante a incubação afetam a epigenética e o desenvolvimento das aves. Corbett *et al*. (2020) demonstraram que o aumento da temperatura da casca do ovo altera o perfil de metilação do DNA cardíaco e reduz o peso do coração na eclosão. Já Al-Zghoul; Sukker; Ababneh, (2019) verificaram que a manipulação térmica embrionária modula a expressão de genes antioxidantes, como NADPH oxidase 4 (*NOX4)*, Glutationa peroxidase (*GPx2)*, Superóxido dismutase (*SOD2)*, promovendo ajustes epigenéticos que melhoram a resistência ao estresse oxidativo ao longo da vida das aves.

Atuação do lipopolissacarídeo como indutor de estresse imunológico

As bactérias Gram-negativas são responsáveis por diversas patologias associadas à inflamação local ou sistêmica. Como estratégia experimental, são utilizadas em experimentos *in vitro* e *in vivo* (Fock; Parnova, 2021). Em sua parede celular, encontra-se o lipopolissacarídeo (LPS), um componente patogênico conhecido por estimular a comunidade de elementos imunológicos (Yousefi; Jonaidi; Sadeghi, 2021). Além de suas propriedades antigênicas e citotóxicas, o LPS desempenha papéis importantes na resistência aos medicamentos e na proteção das bactérias. Sua estrutura é formada por três domínios: o antígeno O, o oligossacarídeo central e o lipídeo A. O antígeno O varia entre cepas bacterianas e é utilizado para sorotipagem, enquanto o lipídeo A, um ácido graxo de cadeia longa, é o principal componente imunoestimulante, capaz de induzir impulso intestinal e ativar a imunidade inata do hospedeiro (Wang *et al*., 2022; Arayamethakorn *et al*., 2023). A *Escherichia coli* e a

Salmonela enterica sorovar Typhimurium contém a porção do lipídeo A hexa-acilado que é altamente imunoestimulatório (Maldonado; Sá-Correia; Valvano, 2016).

Quando o sinal é percebido, ele é passado intracelular e leva a ativação do fator de transcrição nuclear (NF-kB) e a indução da resposta de fase aguda (RFA). A proteína de ligação a LPS (LBP) o reconhece e transfere a informação para o cluster de diferenciação 14 (CD14), que é uma glicoproteína encontrada em macrófagos, neutrófilos e monócitos. Além de sinalizar a presença do complexo LPS-LBP, o CD14 funciona como uma proteína de superfície mediando a internalização do LPS, sinalizando para outros receptores, como a glicoproteína secretada de diferenciação mieloide 2 (MD2). A MD2 forma um complexo com o domínio extracelular do receptor Toll like 4 (TLR4) e esse complexo recruta proteínas adaptadoras (Triantafilou; Triantafilou, 2002; Pålsson-Mcdermott; O'Neill, 2004; Wyns *et al*., 2015). Por fim, a cascata de sinalização libera o fator de transcrição nuclear a fim de se ligar aos promotores dos genes que irão atuar na resposta da fase aguda. Essa resposta é realizada por citocinas pró-inflamatórias interleucina-1 β (IL-1β), fator de necrose tumoral-α (TNF-α) e interleucina-6 (IL-6) (Rivier; Chizzonite; Vale, 1989; Zetterström *et al*., 1998; Koutsos; Klasing, 2001). Essas respostas são produzidas principalmente pelos macrófagos, mas os neutrófilos e células endoteliais também contribuem para a elevação dos tecidos inflamados.

Além da resposta inflamatória, o LPS também causa danos sistêmicos em diversos órgãos, incluindo fígado, duodeno, jejuno, baço e íleo (Li *et al*., 2017; Yu *et al*., 2022; Tong *et al*., 2022, 2023). Estudos em frangos de corte mostram que injeções repetidas de LPS por via intraperitoneal induzem estresse imunológico, impactando o crescimento inicial dessas aves (Webel; Johnson; Baker, 1998; Li *et al*., 2015; Wu; Wang; Qi, 2017) e causando danos à mucosa intestinal (Jiang *et al*., 2019). Além disso, o desafio do LPS pode desencadear estresse oxidativo, um fator adicional na redução do desempenho, diminuição do consumo de alimentos e aumento do catabolismo de nutrientes (Bi *et al*., 2022; Xu *et al*., 2022; Hu *et al*., 2023).

Foi relatado em alguns estudos que um fator estressante pode preparar o hospedeiro para desafios futuros. Em 1969 Gross e Colmano notaram que os frangos submetidos a um estresse social foram resistentes a *Escherichia coli*. Shanmugasundaram, Wick e Lilburn (2018) observaram que a manipulação térmica embrionária (38°C versus 37,5°C) de E11 a E21 aumentou *HSP70* em embriões de pato ao E25. Posteriormente, Shanmugasundaram, Wick e Lilburn (2019), inocularam patinhos de Pequim (*Anas platyrhynchos domesticus*) incubados em diferentes temperaturas com LPS de *Salmonella Enteritidis*, os achados sugeriram que o

estresse por temperatura de incubação pode ser benéfico para o sistema imunológico na pós-eclosão de aves.

Estudo das respostas moleculares

Dentre os diversos métodos disponíveis para estudar as respostas moleculares dos organismos submetidos a diferentes condições biológicas, como estresse por temperatura e estresse imunológico, surgiu o sequenciamento de RNA. O sequenciamento de mRNA (RNA-seq) é um método avançado de análise genômica que permite estudar o transcriptoma, ou seja, o conjunto completo de moléculas de mRNA em uma célula, tecido ou organismo em um determinado momento (Panichnantakul *et al*., 2016).

Atualmente, a tecnologia mais utilizada para RNA-seq é o sequenciamento por síntese (SBS – Sequencing By Synthesis) da Illumina (Figura 5), um método de sequenciamento de nova geração (NGS) que permite a análise abrangente do transcriptoma, incluindo expressão gênica, splicing alternativo, fusões gênicas e descoberta de novos transcritos (Lybecker; Henderson, 2017).

O processo começa com a extração do RNA total, seguida pelo enriquecimento do RNA mensageiro (mRNA) por meio da captura de sequências poli(A) usando beads revestidos com oligonucleotídeos de timina (dT). Em seguida, o RNA é fragmentado por meio de métodos químicos ou enzimáticos. Esses fragmentos são convertidos em cDNA de fita dupla, e adaptadores de sequenciamento são ligados às suas extremidades, permitindo a identificação da amostra e a hibridização na flow cell (célula de fluxo) do sequenciador Illumina (Liang; Zeng, 2015; Sheng *et al*., 2016).

Na flow cell, os fragmentos de cDNA são amplificados por PCR em ponte (bridge amplification), gerando clusters de DNA idênticos que serão sequenciados. O sequenciamento por síntese (SBS) ocorre pela adição cíclica de nucleotídeos marcados com corantes fluorescentes, onde cada base incorporada emite um sinal óptico detectado por imagens de alta resolução (Liang; Zeng, 2015; Sheng *et al*., 2016).

Os sinais são processados computacionalmente, gerando leituras curtas (reads) que são posteriormente alinhadas a um genoma ou transcriptoma de referência usando ferramentas bioinformáticas. Por fim, a quantificação da expressão gênica é realizada, permitindo comparações entre diferentes condições experimentais, identificação de isoformas alternativas e detecção de variantes.

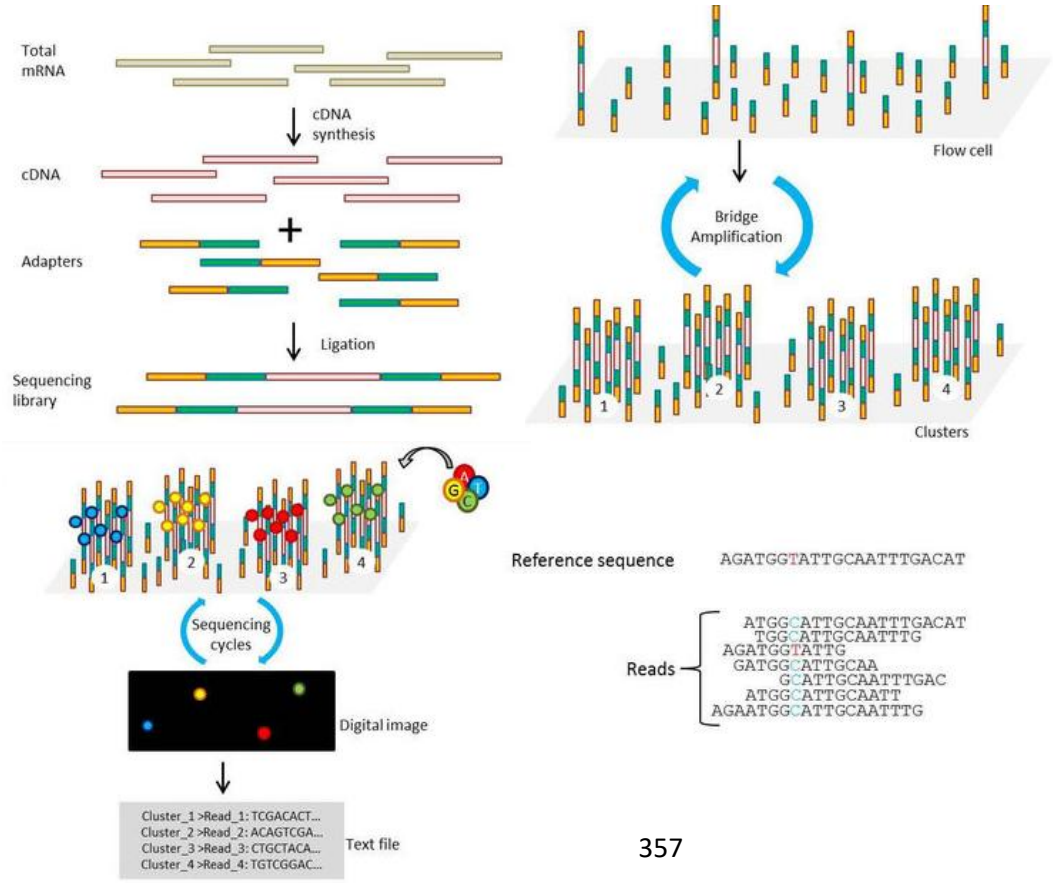

Figura 2. Fluxograma da metodologia Illumina de RNA-seq

Fonte: Adaptado de Juarez, Paulo. (2017).

A análise de expressão diferencial (DE) em RNA-seq identifica genes cujos níveis de transcrição variam significativamente entre condições experimentais (controle *vs* tratamento) (Lang *et al*., 2017). Essa abordagem é fundamental para elucidar mecanismos moleculares em condições biológicas específicas, como respostas a estímulos, doenças ou alterações ambientais. Os principais parâmetros utilizados para determinar a expressão diferencial incluem o log2 fold change (log2FC), o padj (p-valor ajustado) e a taxa de descoberta falsa (FDR), cada um fornecendo informações distintas e complementares sobre a relevância biológica e estatística das diferenças observadas (Van *et al*., 2018).

O log2FC quantifica a magnitude da diferença de expressão entre dois grupos em uma escala logarítmica (base 2) (Lang *et al*., 2017). Quando é maior que zero (>0) indica que o gene está superexpresso na condição experimental, já quando é menor do que zero (<0), indica que o gene está subexpresso. Embora essa medida indique diretamente alteração na expressão gênica, a interpretação deve ser feita juntamente com as outras medidas de significância estatística (Lang *et al*., 2017).

Já o padj (p-valor ajustado) é uma versão corrigida do p-valor bruto, projetada para controlar o erro estatístico em testes múltiplos. O método mais comum para calcular o padj em RNA-seq é o FDR (False Discovery Rate), que estima a proporção de falsos positivos entre os genes declarados significativos (Guo *et al*., 2023). Quando o padj é menor do que 0,05, o gene é considerado diferencialmente expresso com um FDR de 5%, ou seja, entre todos os genes com padj < 0,05, espera-se que até 5% sejam falsos positivos. Mas quando ele é igual ou maior do que 0,05, a diferença na expressão não é estatisticamente significativa.

Após identificar genes diferencialmente expressos (DEGs - Differentially Expressed Genes), uma série de análises subsequentes são realizadas para interpretar seu significado biológico, validar resultados e gerar hipóteses funcionais. O processo inicia-se com análises bioinformáticas que buscam caracterizar os DEGs em termos funcionais, seguindo-se por abordagens experimentais para confirmação dos achados e, finalmente, pela integração dos resultados em modelos biológicos compreensíveis.

A primeira etapa consiste em análises de enriquecimento funcional, particularmente através de ontologias gênicas (GO) e vias metabólicas (Yin *et al*., 2016). Estas análises permitem classificar os DEGs em categorias biológicas relevantes, como processos celulares, funções moleculares ou componentes celulares. Ferramentas como DAVID e clusterProfiler são frequentemente empregadas para identificar termos GO ou vias de sinalização significativamente enriquecidos entre os DEGs. Paralelamente, análises de redes de interação proteína-proteína, realizadas em plataformas como STRING e visualizadas no Cytoscape, ajudam a identificar proteínas centrais (hubs) que podem desempenhar papeis-chave nos processos biológicos alterados (Yin *et al*., 2016; Yuan *et al*., 2019).

A validação experimental constitui uma etapa crítica do processo. Técnicas como qPCR são amplamente utilizadas para confirmar os padrões de expressão observados no RNA-seq, sendo geralmente selecionados os genes com maiores magnitudes de alteração e significância estatística. A integração com outros dados ômicos representa um avanço importante na interpretação dos resultados. A correlação de dados de transcriptômica com proteômica ou metabolômica pode revelar até que ponto as alterações observadas em nível de RNA se traduzem em mudanças funcionais na célula. Ferramentas de análise multi-ômica, como o IPA (Ingenuity Pathway Analysis), facilitam esta integração, permitindo construir modelos mais completos das vias biológicas afetadas (Chen, 2023).

Na fase final de interpretação, os resultados são sintetizados em modelos biológicos coerentes. Diagramas de vias metabólicas ou de sinalização, gerados através de ferramentas como PathVisio ou KEGG Mapper, ajudam a visualizar como os DEGs se inserem em processos biológicos conhecidos. Esta etapa culmina na formulação de hipóteses testáveis sobre os mecanismos subjacentes às condições experimentais estudadas (Yuan *et al*., 2019).

As aplicações práticas destes achados são diversas. Em estudos translacionais, os DEGs podem ser investigados como potenciais biomarcadores para diagnóstico ou prognóstico de doenças. Em pesquisa básica, eles podem apontar para novos alvos terapêuticos ou mecanismos patogênicos até então desconhecidos. A comparação de DEGs entre diferentes condições experimentais ou mesmo entre espécies pode ainda revelar princípios conservados ou especializados da regulação gênica.

É importante notar que todo este processo deve ser conduzido com atenção às limitações inerentes à técnica. A mera identificação de DEGs não estabelece relação causal, sendo necessários experimentos funcionais adicionais para comprovar o papel específico de cada gene nos fenótipos observados. Além disso, a interpretação dos dados deve sempre considerar o contexto biológico mais amplo, integrando informações da literatura existente para evitar conclusões prematuras.

REFERÊNCIAS

AL AMAZ, S.; MISHRA, B. Embryonic thermal manipulation: a potential strategy to mitigate heat stress in broiler chickens for sustainable poultry production. **Journal of Animal Science and Biotechnology/Journal of animal science and biotechnology**, v. 15, n. 1, 4 jun. 2024. DOI: https://doi.org/10.1186/s40104-024-01028-1

ALMA, L.; MCELHANY, P.; CRIM, R. N.; NEWTON, J. A.; MAHER, M.; MICKETT, J. B.; PADILLA-GAMIÑO, J. L. Phenotypic plasticity and carryover effects in an ecologically important bivalve in response to changing environments. **Frontiers in Marine Science**, v. 11, 13 mar. 2024. DOI: https://doi.org/10.3389/fmars.2024.1178507

AL-ZGHOUL, M. B.; MOHAMMAD SALEH, K. M. Effects of thermal manipulation of eggs on the response of jejunal mucosae to posthatch chronic heat stress in broiler chickens. **Poultry Science**, v. 99, n. 5, p. 2727–2735, maio 2020. DOI: 10.1016/j.psj.2019.12.038

AL-ZGHOUL, M.B.; H. SUKKER; M.M. ABABNEH. Effect of thermal manipulation of broilers embryos on the response to heat-induced oxidative stress. **Poultry Science**, v. 98, n. 2, p. 991–1001, 17 ago. 2018. DOI: 10.3382/ps/pey379

ARAYAMETHAKORN; TANAPORN UENGWETWANIT; NITSARA KAROONUTHAISIRI; PAWADEE METHACANON; WANILADA RUNGRASSAMEE. Comparative effects of different bacterial lipopolysaccharides on modulation of immune levels to improve survival of the black tiger shrimp. **Journal of Invertebrate Pathology**, v. 197, p. 107872–107872, 21 dez. 2022. DOI: 10.1016/j.jip.2022.107872

BARROS, H. S. S. *et al*. Functional oil in the feeding of heat-stressed Japanese quail. **Poultry Science**, v. 103, n. 10, 1 out. 2024. DOI: 10.1016/j.psj.2024.104041

BEDNARCZYK, M.; ALEKSANDRA DUNISLAWSKA; KATARZYNA STADNICKA; GROCHOWSKA, E. Chicken embryo as a model in epigenetic research. **Poultry Science**, v. 100, n. 7, p. 101164–101164, 27 mar. 2021. DOI: https://doi.org/10.1016/j.psj.2021.101164

BEKOFF, A. Embryonic development of chick motor behaviour. **Trends in Neurosciences**, v. 4, p. 181–184, jan. 1981. DOI: https://doi.org/10.1016/0166-2236(81)90059-X

BI, S.; QU, Y.; SHAO, J.; ZHANG, J.; LI, W.; ZHANG, L.; NI, J.; CAO, L. Ginsenoside Rg3 Ameliorates Stress of Broiler Chicks Induced by Escherichia coli Lipopolysaccharide. **Frontiers in Veterinary Science**, v. 9, 8 abr. 2022. DOI: 10.3389/fvets.2022.878018

BILAL, R. M.; HASSAN, F.; FARAG, M. R.; NASIR, T. A.; RAGNI, M.; MAHGOUB, H. A. M.; MAHMOUD ALAGAWANY. Thermal stress and high stocking densities in poultry farms: Potential effects and mitigation strategies. **Journal of Thermal Biology**, v. 99, p. 102944–102944, 6 abr. 2021. DOI: 10.1016/j.jtherbio.2021.102944

CHAUDHARY, A.; MISHRA, B. Systemic effects of heat stress on poultry performances, transcriptomics, epigenetics and metabolomics, along with potential mitigation

strategies. **World s Poultry Science Journal**, p. 1–37, 14 jun. 2024. DOI: 10.1080/00439339.2024.2364884

CHEN, Y. *et al.* Gene set enrichment analysis and ingenuity pathway analysis to verify the impact of Wnt signaling in psoriasis treated with Taodan granules. **American Journal of Translational Research**, v. 15, n. 1, p. 422, 15 jan. 2023. PMCID: PMC9908442

COLLIN, A. *et al*. Effects of Thermal Manipulation During Early and Late Embryogenesis on Thermotolerance and Breast Muscle Characteristics in Broiler Chickens. **Poultry Science**, v. 86, n. 5, p. 795–800, maio 2007. DOI: 10.1093/ps/86.5.795

CORBETT, R. J.; PAS, M. F. W. TE; BRAND, H. VAN DEN; GROENEN, M. A. M.; CROOIJMANS, R. P. M. A.; ERNST, C. W.; MADSEN, O. Genome-Wide Assessment of DNA Methylation in Chicken Cardiac Tissue Exposed to Different Incubation Temperatures and CO2 Levels. **Frontiers in Genetics**, v. 11, 28 out. 2020. DOI: https://doi.org/10.3389/fgene.2020.558189

DAVID, S. A. *et al*. Thermal Manipulation During Embryogenesis Impacts H3K4me3 and H3K27me3 Histone Marks in Chicken Hypothalamus. **Frontiers in Genetics**, v. 10, 26 nov. 2019. DOI: 10.3389/fgene.2019.01207

EBTSAM IRAQI; HADY, A. A.; ELSAYED, N.; KHALIL, H.; EL-SAADANY, A.; KARIM EL-SABROUT. Effect of thermal manipulation on embryonic development, hatching process, and chick quality under heat-stress conditions. **Poultry Science**, v. 103, n. 1, p. 103257–103257, 29 out. 2023. DOI: https://doi.org/10.1016/j.psj.2023.103257

FARNER, D. S. The Avian Embryo Alexis L. Romanoff. **The Auk,** v. 77, n. 3, p. 358–359, jul. 1960.

FOCK, E. M.; PARNOVA, R. G. Protective Effect of Mitochondria-Targeted Antioxidants against Inflammatory Response to Lipopolysaccharide Challenge: A Review. **Pharmaceutics**, v. 13, n. 2, p. 144–144, 22 jan. 2021. DOI: 10.3390/farmacêutica13020144

GABRIELLI, M. G.; ACCILI, D. The Chick Chorioallantoic Membrane: A Model of Molecular, Structural, and Functional Adaptation to Transepithelial Ion Transport and Barrier Function during Embryonic Development. **Journal of Biomedicine and Biotechnology**, v. 2010, p. 1–12, 2010. DOI: 10.1155/2010/940741

GADELHA, A. I. B. B. *et al*. Os anexos embrionários de aves: revisão de literatura. **Research, Society and Development**, v. 10, n. 2, p. e54310212498, 28 fev. 2021. DOI: http://dx.doi.org/10.33448/rsd-v10i2.12498

GRIFFITH, O. W.; BRANDLEY, M. C.; WHITTINGTON, C. M.; BELOV, K.; THOMPSON, M. B. Comparative genomics of hormonal signaling in the chorioallantoic membrane of oviparous and viviparous amniotes. **General and Comparative Endocrinology**, v. 244, p. 19–29, 22 abr. 2016. DOI: 10.1016/j.ygcen.2016.04.017

GROSS, W. B.; COLMANO, G. The Effect of Social Isolation on Resistance to Some Infectious Diseases. **Poultry Science**, v. 48, n. 2, p. 514–520, mar. 1969.

GUO, X.; NING, J.; CHEN, Y.; LIU, G.; ZHAO, L.; FAN, Y.; SUN, S. Recent advances in differential expression analysis for single-cell RNA-seq and spatially resolved transcriptomic studies. **Briefings in Functional Genomics**, v. 23, n. 2, p. 95–109, 5 abr. 2023. DOI: https://doi.org/10.1093/bfgp/elad011

HAMBURGER, V.; HAMILTON, H. L. A series of normal stages in the development of the chick embryo. **Developmental Dynamics**, v. 195, n. 4, p. 231–272, 1 dez. 1992.

HU, W.; BI, S.; SHAO, J.; QU, Y.; ZHANG, L.; LI, J.; CHEN, S.; MA, Y.; CAO, L. Ginsenoside Rg1 and Re alleviates inflammatory responses and oxidative stress of broiler chicks challenged by lipopolysaccharide. **Poultry Science**, v. 102, n. 4, p. 102536, abr. 2023. DOI: 10.1016/j.psj.2023.102536

HUANG, W.; ARAI, F.; KAWAHARA, T. Egg-in-Cube: Design and Fabrication of a Novel Artificial Eggshell with Functionalized Surface. **PLoS ONE**, v. 10, n. 3, p. e0118624–e0118624, 13 mar. 2015. DOI: 10.1371/journal.pone.0118624

JIANG, B.; HE, Y.; ELSLER, A.; WANG, S.; KEATING, J. N.; SONG, J.; KEARNS, S. L.; BENTON, M. J. Extended embryo retention and viviparity in the first amniotes. **Nature Ecology & Evolution**, v. 7, n. 7, p. 1131–1140, 12 jun. 2023. DOI: https://doi.org/10.1038/s41559-023-02074-0

JIANG, J.; QI, L.; LV, Z.; JIN, S.; WEI, X.; SHI, F. Dietary Stevioside Supplementation Alleviates Lipopolysaccharide-Induced Intestinal Mucosal Damage through Anti-Inflammatory and Antioxidant Effects in Broiler Chickens. **Antioxidants**, v. 8, n. 12, p. 575, 21 nov. 2019. DOI: 10.3390/antiox8120575

JUAREZ, P. Regulatory mechanisms of mexEF-oprN efflux operon in Pseudomonas aeruginosa: from mutations in clinical isolates to its induction as response to electrophilic stress. **Hal.science**, 15 dez. 2017.

KOUTSOS, E. A.; KLASING, K. C. The acute phase response in Japanese quail (Coturnix coturnix japonica). **Comparative Biochemistry and Physiology Part C Toxicology & Pharmacology**, v. 128, n. 2, p. 255–263, 1 fev. 2001. DOI: 10.1016/s1532-0456(00)00199-x

LANG, B. J. *et al*. A Workflow Guide to RNA-seq Analysis of Chaperone Function and Beyond. **Methods in Molecular Biology**, p. 233–252, 26 nov. 2017. DOI: 10.1007/978-1-4939-7477-1_18

LI, N.; ANSARI, A. R.; SUN, Z.; HUANG, H.; CUI, L.; HU, Y.; ZHAO, X.; ZHONG, J.; ABDEL-KAFY, E.-S. M.; LIU, H. Toll like receptor 4 signaling pathway participated in Salmonella lipopolysaccharide-induced spleen injury in young chicks. **Microbial Pathogenesis**, v. 112, p. 288–294, nov. 2017. DOI: 10.1016/j.micpath.2017.10.004

LI, Y.; ZHANG, H.; CHEN, Y. P.; YANG, M. X.; ZHANG, L. L.; LU, Z. X.; ZHOU, Y. M.; WANG, T. Bacillus amyloliquefaciens supplementation alleviates immunological stress in lipopolysaccharide-challenged broilers at early age. **Poultry Science**, v. 94, n. 7, p. 1504–1511, 26 maio 2015. DOI: 10.3382/ps/pev124

LIANG, H.; ZENG, E. RNA-Seq Experiment and Data Analysis. **Methods in molecular biology**, p. 99–114, 19 nov. 2015. DOI: 10.1007/978-1-4939-3127-9_9

LIU, Z.; SONG, L.; LU, L.; ZHANG, X.; ZHANG, F.; WANG, K.; LINHARDT, R. J. Comparative proteomics of matrix fractions between pimpled and normal chicken eggshells. **Journal of Proteomics**, v. 167, p. 1–11, 26 jul. 2017. DOI: 10.1016/j.jprot.2017.07.015

LOYAU, T. *et al*. Cyclic variations in incubation conditions induce adaptive responses to later heat exposure in chickens: A review. **Animal**, v. 9, n. 1, p. 76–85, 30 jul. 2014. DOI: https://doi.org/10.1017/S1751731114001931

LYBECKER; HENDERSON, K. Borrelia burgdorferi Transcriptome Analysis by RNA-Sequencing. **Methods in molecular biology**, p. 127–136, 14 out. 2017. DOI: 10.1007/978-1-4939-7383-5_11

MAAIKE VANCAMELBEKE; VERMEIRE, S. The intestinal barrier: a fundamental role in health and disease. **Expert Review of Gastroenterology & Hepatology**, v. 11, n. 9, p. 821–834, 26 jun. 2017. DOI: 10.1080/17474124.2017.1343143

MADKOUR, M. *et al*. Mitigating the detrimental effects of heat stress in poultry through thermal conditioning and nutritional manipulation. **Journal of Thermal Biology Elsevier Ltd**., 1 jan. 2022.

MALDONADO, R. F.; SÁ-CORREIA, I.; VALVANO, M. A. Lipopolysaccharide modification in Gram-negative bacteria during chronic infection. **FEMS Microbiology Reviews**, v. 40, n. 4, p. 480–493, jul. 2016.

MENG, Y.; QIU, N.; GUYONNET, V.; MINE, Y. Omics as a Window To Unravel the Dynamic Changes of Egg Components during Chicken Embryonic Development. **Journal of Agricultural and Food Chemistry**, v. 69, n. 44, p. 12947–12955, 28 out. 2021. DOI: 10.1021/acs.jafc.1c05883

MONTEIRO, A. P. **Histologia e Embriologia Comparada.** 1° ed. Londrina. Disponível em: <https://cm-kls-content.s3.amazonaws.com/201701/INTERATIVAS_2_0/HISTOLOGIA_E_EMBRIOLOGIA_COMPARADA/U1/LIVRO_UNICO.pdf>.

MORTOLA, J. P. Gas exchange in avian embryos and hatchlings. **Comparative Biochemistry and Physiology Part A: Molecular & Integrative Physiology**, v. 153, n. 4, p. 359–377, ago. 2009. DOI: 10.1016/j.cbpa.2009.02.041

PÅLSSON-MCDERMOTT, E. M.; LUKE. Signal transduction by the lipopolysaccharide receptor, Toll-like receptor-4. **Immunology**, v. 113, n. 2, p. 153–162, 17 set. 2004. DOI: 10.1111/j.1365-2567.2004.01976.x

PANICHNANTAKUL; PUDCHALALUCK e COLAB. RNA-Seq as a Tool to Study the Tumor Microenvironment. **Methods in Molecular Biology**, p. 311–337, 2016. DOI: https://pubmed.ncbi.nlm.nih.gov/27581031/

PERSSON, E.; Ó CUÍV, C.; NORD, A. Thermoregulatory consequences of growing up during a heatwave or a cold snap in Japanese quail. **Journal of Experimental Biology**, v. 227, n. 2, 15 jan. 2024. DOI: https://doi.org/10.1242/jeb.246876

RAZA, S. H. A.; ABDELNOUR, S. A.; DHSHAN, A. I. M.; HASSANIN, A. A.; NORELDIN, A. E.; ALBADRANI, G. M.; ABDEL-DAIM, M. M.; CHENG, G.; ZAN, L. Potential role of specific microRNAs in the regulation of thermal stress response in livestock. Journal of Thermal Biology, v. 96, p. 102859, fev. 2021. DOI: 10.1016/j.jtherbio.2021.102859

RIVIER, C.; CHIZZONITE, RICHARD.; VALE, WYLIE. In the Mouse, the Activation of the Hypothalamic Pituitary-Adrenal Axis by a Lipopolysaccharide (Endotoxin) Is Mediated through Interleukin-1*. **Endocrinology**, v. 125, n. 6, p. 2800–2805, dez. 1989.

SHANMUGASUNDARAM, R.; WICK, M.; LILBURN, M. S. Effect of embryonic thermal manipulation on heat shock protein 70 expression and immune system development in Pekin duck embryos. **Poultry Science**, v. 97, n. 12, p. 4200–4210, dez. 2018. DOI: https://doi.org/10.3382/ps/pey298

SHANMUGASUNDARAM, R.; WICK, M.; LILBURN, M. S. Effect of embryonic thermal manipulation on heat shock protein 70 (HSP70) expression and subsequent immune response to post-hatch lipopolysaccharide challenge in Pekin ducklings. **Poultry Science**, v. 98, n. 2, p. 722–733, fev. 2019. DOI: https://doi.org/10.3382/ps/pey460

SHENG, Q. *et al*. Multi-perspective quality control of Illumina RNA sequencing data analysis. **Briefings in Functional Genomics,** p. elw035–elw035, 29 set. 2016. DOI: 10.1093/bfgp/elw035

STARCK, J. M.; STEWART, J. R.; BLACKBURN, D. G. Phylogeny and evolutionary history of the amniote egg. **Journal of Morphology**, v. 282, n. 7, p. 1080–1122, 26 jul. 2021. DOI: 10.1002/jmor.21380

TONA, K.; O. ONAGBESAN; BRUGGEMAN, V.; COLLIN, A.; BERRI, C.; DUCLOS, M. J.; S. TESSERAUD; J. BUYSE; E. DECUYPERE; S. YAHAV. Effects of heat conditioning at d 16 to 18 of incubation or during early broiler rearing on embryo physiology, post-hatch growth performance and heat tolerance. **Archiv für Geflügelkunde**, v. 72, n. 2, p. 75–83, 1 abr. 2008. DOI: 10.1016/S0003-9098(25)00883-5

TONG, Y.; YU, C.; XIE, Z.; ZHANG, X.; YANG, Z.; WANG, T. Trans-anethole ameliorates lipopolysaccharide-induced acute liver inflammation in broilers via inhibiting NF-κB

672 signaling pathway. **Poultry Science**, v. 101, n. 8, p. 101962–101962, 13 maio 2022. DOI:
673 10.1016/j.psj.2022.101962
674
675 TONG, Y.; YU, C.; CHEN, S.; ZHANG, X.; YANG, Z.; WANG, T. Trans-anethole exerts
676 protective effects on lipopolysaccharide-induced acute jejunal inflammation of broilers via
677 repressing NF-κB signaling pathway. **Poultry Science**, v. 102, n. 2, p. 102397, fev. 2023.
678 DOI: 10.1016/j.psj.2022.102397
679
680 TRIANTAFILOU, M.; TRIANTAFILOU, K. Lipopolysaccharide recognition: CD14, TLRs
681 and the LPS-activation cluster. **Trends in Immunology**, v. 23, n. 6, p. 301–304, jun. 2002.
682 DOI: 10.1016/s1471-4906(02)02233-0
683
684 TZSCHENTKE, B. Monitoring the development of thermoregulation in poultry embryos and
685 its influence by incubation temperature. **Computers and Electronics in Agriculture**, v. 64, n.
686 1, p. 61–71, nov. 2008.
687
688 VAN DEN BERGE, K. *et al*. Observation weights unlock bulk RNA-seq tools for zero
689 inflation and single-cell applications. **Genome Biology**, v. 19, n. 1, 26 fev. 2018. DOI:
690 10.1186/s13059-018-1406-4
691
692 VANDERLEY, S. B. S. C.; SANTANA, H. C. I. **Histologia e Embriologia Animal**
693 **Comparada**. 2° ed. [s.l: s.n.].
694
695 VESCO, A. P.; KHATLAB, A. S.; SANTANA, T. P.; POZZA, P. C.; AMÉLIA, M.; BRITO, C.
696 O.; BARBOSA, L. T.; GASPARINO, E. Heat stress effect on the intestinal epithelial function
697 of broilers fed methionine supplementation. **Livestock Science**, v. 240, p. 104152–104152, 23
698 jun. 2020. DOI: https://doi.org/10.1016/j.livsci.2020.104152
699
700 WANG, Z.; GERSTEIN, M.; SNYDER, M. RNA-Seq: a revolutionary tool for
701 transcriptomics. **Nature Reviews Genetics**, v. 10, n. 1, p. 57–63, 18 nov. 2008.
702 DOI: 10.1038/nrg2484
703
704 WANG, Z.; WU, Q.; LIAO, G.; FAN, L. New insights into the regulation mechanism of
705 Litopenaeus vannamei hepatopancreas after lipopolysaccharide challenge using transcriptome
706 analyses. **Fish & Shellfish Immunology**, v. 128, p. 466–473, 18 ago. 2022. DOI:
707 10.1016/j.fsi.2022.08.014
708
709 WASTI, S.; SAH, N.; MISHRA, B. Impact of heat stress on poultry health and performances,
710 and potential mitigation strategies. **Animals**, v. 10, n. 8, p. 1–19, 1 ago. 2020. DOI:
711 10.3390/ani10081266
712
713 WATT, J. M.; PETITTE, J. N.; ETCHES, R. J. Early development of the chick embryo.
714 **Journal of Morphology**, v. 215, n. 2, p. 165–182, 6 fev. 1993. DOI:
715 10.1002/jmor.1052150205
716
717 WEBEL, D. M.; JOHNSON, R. W.; BAKER, D. H. Lipopolysaccharide-Induced Reductions
718 in Food Intake Do Not Decrease the Efficiency of Lysine and Threonine Utilization for

Protein Accretion in Chickens. **The Journal of Nutrition**, v. 128, n. 10, p. 1760–1766, out. 1998. DOI: 10.1093/jn/128.10.1760

WU, Q. J.; WANG, Y. Q.; QI, Y. X. Influence of procyanidin supplementation on the immune responses of broilers challenged with lipopolysaccharide. **Animal Science Journal**, v. 88, n. 7, p. 983–990, 6 jul. 2017. DOI: 10.1111/asj.12729

WYNS, H.; PLESSERS, E.; DE BACKER, P.; MEYER, E.; CROUBELS, S. In vivo porcine lipopolysaccharide inflammation models to study immunomodulation of drugs. **Veterinary Immunology and Immunopathology**, v. 166, n. 3-4, p. 58–69, ago. 2015. DOI: 10.1016/j.vetimm.2015.06.001

YAHAV, S.; COLLIN, A.; SHINDER, D.; PICARD, M. Thermal manipulations during broiler chick embryogenesis: effects of timing and temperature. **Poultry Science**, v. 83, n. 12, p. 1959–1963, 1 dez. 2004. DOI: 10.1093/ps/83.12.1959

YIN, H.; WANG, S.; ZHANG, Y.-H.; CAI, Y.-D.; LIU, H. Analysis of Important Gene Ontology Terms and Biological Pathways Related to Pancreatic Cancer. **BioMed Research International**, v. 2016, p. 1–10, 1 jan. 2016. DOI: 10.1155/2016/7861274

YOUSEFI, M.; JONAIDI, H.; SADEGHI, B. Influence of peripheral lipopolysaccharide (LPS) on feed intake, body temperature and hypothalamic expression of neuropeptides involved in appetite regulation in broilers and layer chicks. **British Poultry Science**, v. 62, n. 1, p. 110–117, 2021. DOI: 10.1080/00071668.2020.1813254

YU, J.; HU, G.; CAO, H.; GUO, X. Quercetin Ameliorates Lipopolysaccharide-Induced Duodenal Inflammation through Modulating Autophagy, Programmed Cell Death and Intestinal Mucosal Barrier Function in Chicken Embryos. **Animals**, v. 12, n. 24, p. 3524–3524, 13 dez. 2022. DOI: https://doi.org/10.3390/ani12243524

YUAN, F.; PAN, X.; CHEN, L.; ZHANG, Y.-H.; HUANG, T.; CAI, Y.-D. Analysis of Protein–Protein Functional Associations by Using Gene Ontology and KEGG Pathway. **BioMed Research International**, v. 2019, p. 1–10, 18 jul. 2019. DOI: 10.1155/2019/4963289

ZETTERSTRÖM, M.; SUNDGREN-ANDERSSON, A. K.; ÖSTLUND, P.; BARTFAI, T. Delineation of the Proinflammatory Cytokine Cascade in Fever Induction[a]. **Annals of the New York Academy of Sciences**, v. 856, n. 1, p. 48–52, set. 1998. DOI: 10.1111/j.1749-6632.1998.tb08311.x

CAPÍTULO 1 – ARTIGO 1

Combined effects of incubation temperature and lipopolysaccharide exposure on immune response modulation in the quail gut

Juliana dos Santos Conceição[1]*, Angélica de Souza Khatlab[3], Eliane Gasparino[3], Thais Pacheco Santana[2], Amanda Silva Carvalho[1], Marcus Vinicius de Aragão Batista[4], Marcelo Santana Filho[5], Simone Eliza Facioni Guimaraes[6], Jodnes Sobreira Vieira[2], Ana Paula Del Vesco[1,2]

[1]*Integrated Graduate Program in Animal Science, Federal University of Sergipe, São Cristóvão, Sergipe, Brazil*

[2]*Department of Animal Science, Federal University of Sergipe, São Cristóvão, Sergipe, Brazil*

[3]*Department of Animal Science, State University of Maringá, Maringá, Paraná, Brazil*

[4] *Department of Biology, Federal University of Sergipe, São Cristóvão, Sergipe, Brazil*

[5]*Postgraduate Program in Biotechnology, Federal University of Sergipe, São Cristóvão, Sergipe, Brazil*

[6]*Department of Animal Science, Federal University of Viçosa, Viçosa, Minas Gerais, Brazil*

*Corresponding author, *E-mail address:* lijuanay@gmail.com

Summary: Embryogenesis is a critical programming window in birds, during which environmental factors can reshape gene expression and influence adaptive capacity after hatching. This study evaluated the effects of embryonic thermal manipulation on the intestinal transcriptomic response of Japanese quail (*Coturnix coturnix japonica*) challenged with lipopolysaccharide (LPS). A 2×2 factorial design was applied, including two incubation temperatures (control – 37.5 °C; high – 39 °C) and two challenge conditions (LPS and saline

solution). At 25 days post-hatch, jejunum samples were collected after inoculation and subjected to RNA-seq analysis. High incubation temperature significantly reduced (p<0.05) hatchability but did not affect embryo morphology. Under control temperature, LPS induced differential expression of 41 genes (*adjusted-p*<0.05), including *IL1R2*, *IL18BP*, and *S100A12*, associated with inflammatory modulation and mucosal integrity. In contrast, high-temperature incubation triggered a broad transcriptomic reprogramming in response to LPS, with activation of inflammatory pathways, metabolic processes (glycolysis, Krebs cycle, pentose metabolism), lipid homeostasis, and vesicular trafficking, while simultaneously suppressing genes involved in adaptive immunity, angiogenesis, cell differentiation, and epigenetic regulation. A conserved set of inflammatory genes, including *MMP7*, *PI3*, and *SLC6A14*, was regulated under both thermal conditions, suggesting activation of central defense mechanisms. In conclusion, high incubation temperature did not alter the initial embryonic phenotype but profoundly reshaped the transcriptomic response to LPS, highlighting the intestinal molecular plasticity and its potential implications for immunometabolic adaptation under future stress conditions.

Keywords: immunology; inflammation; metabolism; transcriptomics; quail

Introduction

The success of embryonic development in birds depends on several environmental factors, with incubation temperature being one of the major determinants of chick quality and survival. Japanese quail (Coturnix coturnix japonica) are commonly used to study embryonic development because of their fast life cycle and ease of handling. Thermal conditions during incubation exert lasting effects on the growth, physiology, and adaptive capacity of individuals (Farner, 1960; Griffith et al., 2017; Jiang et al., 2023). Thermal manipulation during the embryonic period has been explored as a strategy to induce beneficial adaptive responses, such as increased resistance to thermal stress and modulation of essential metabolic pathways. Temperature variations can also trigger epigenetic changes, including alterations in DNA methylation, histone acetylation, and histone methylation, directly influencing gene expression (Chaudhary; Mishra, 2024; Al Amaz; Mishra, 2024). Such mechanisms are recognized as important mediators of phenotypic plasticity, allowing organisms to adjust their physiology in response to environmental challenges (Thompson; Nilsson; Skinner, 2020; Li et al., 2022).

Also noteworthy, the immune system of birds can be shaped by exposure to immune challenges. Lipopolysaccharides (LPSs), structural components of the cell wall of Gram-negative bacteria, are widely used to induce acute inflammatory responses in experimental models. This stimulus activates signaling cascades that lead to the production of pro-inflammatory cytokines and reactive oxygen species, triggering metabolic and immunological responses that, albeit vital for survival, may compromise productive performance (Wang et al., 2022; Bi et al., 2022; Tong et al., 2023).

Interactions between thermal conditions experienced during embryogenesis and exposure to immunological challenges in the postnatal phase represent a promising area of research, particularly in poultry farming. In poultry research, great efforts are dedicated to developing strategies to enhance the resilience and well-being of birds. The current study aimed to evaluate the combined effects of incubation temperature (37.5 versus 39 °C) and post-hatch LPS-induced immunological challenges on gene expression in quail. For this, changes in the jejunal transcriptome were analyzed using RNA sequencing, integrating differential expression data with gene ontology and metabolic pathway analyses (Yu et al., 2012). This investigation aims to contribute to our understanding of the molecular mechanisms underlying stress adaptation, providing insights for improving management practices and production efficiency in poultry systems.

Material and methods

The experiment was conducted at the Iguatemi Experimental Farm, State University of Maringá, Maringá, Paraná, Brazil. All procedures were approved by the local Animal Ethics Committee (protocol No. 8954270323).

845 Layer production

846 For the collection of fertile eggs, 200 one-day-old female Japanese quail (*C. coturnix*
847 *japonica*) chicks were reared under conventional conditions until 98 days of age (14 weeks, see
848 the flowchart in Figure 1). During this period, bird growth and laying rates were monitored
849 continuously. Mating began in the 15th week of life. From the 16th week onward, fertile eggs
850 were collected daily over a 10-day period. Cocks (n = 100, adjusted for weight, at a ratio of 1
851 male to 2 female birds) interacted with hens for 1 h a day. Parental effects were minimized by
852 adopting a rotation scheme. Throughout the experiment, all birds were maintained under
853 conventional breeding conditions.

854 Eggs were collected daily, identified, weighed, and stored under controlled conditions
855 (16 °C and 78% relative humidity). During the experiment, layers were housed in individual
856 cages, with *ad libitum* access to water and feed. The diet was formulated to meet the nutritional
857 requirements of birds, as described by Rostagno *et al.* (2011), and contained 2899 kcal kg^{-1}
858 metabolizable energy, 20.7% crude protein, 3.151% calcium, and 0.33% available phosphorus.
859 The lighting regime was set at 17 h of light per day.

860

861 Egg incubation and embryonic development

862 On the last day of collection, eggs were acclimated to room temperature, stored in fruit
863 nets for identification, and assigned to one of two incubation temperature treatments. In the
864 control group, eggs were incubated at 37.5 °C and 60% relative humidity. In the high-
865 temperature (HT) group, eggs were incubated at 39 °C and 60% relative humidity.

866 Eggs from both groups were incubated in the same incubator model (Chocmaster Luna
867 240), which was preconfigured to reach the experimental temperatures of each treatment.
868 During incubation, eggs were maintained in a horizontal position and automatically turned

every 2 h until day 15. The hatching phase was monitored every 3 h, beginning on day 16 (hour 384) and continuing until day 17 (hour 408). At the end of the 17-day incubation period, unhatched eggs were opened and classified as unfertilized eggs or dead embryos. The total hatching rate (Total number of eggs hatched/Total number of eggs incubated × 100) and the fertile egg hatching rate (Total number of fertile eggs hatched/Total number of fertile eggs incubated × 100) were calculated.

Six eggs at embryonic day 17 (E17) were collected from both groups and used to evaluate parameters related to embryonic development, including egg weight, embryo weight, yolk sac weight, and embryo length. The percentage of yolk sac utilization was calculated by dividing the total weight of the yolk sac by the weight of the chick without the yolk sac, then multiplying by 100. The gastrointestinal tract was measured from the point where the esophagus enters the oropharynx to the junction of the large intestine with the cloaca.

Chick performance

Chick physical quality was assessed based on weight, length, and physical characteristics, following the method described by Tona *et al.* (2003). Subsequently, chicks were identified and grouped according to the incubation treatment. Chicks were housed in brooder rings heated by lamps and fed a starter diet formulated according to Rostagno *et al.* (2011) (2899 kcal kg^{-1} metabolizable energy and 20.7% crude protein). Water was available *ad libitum*. Chicks were reared under conventional conditions until 25 days of age.

At 25 days of age, birds were weighed and assigned to two treatments: an unchallenged group and an LPS challenge group. Birds in the LPS group received an intraperitoneal injection containing 100 µL of *Escherichia coli* O111:B4 LPS (Sigma–Aldrich, Brazil) at a dose of 100 µg kg^{-1} body weight. Birds in the unchallenged group were injected intraperitoneally with

100 μL of saline. At 3.5 h after inoculation, all birds were euthanized by cervical dislocation for sample collection.

The experiment was conducted in a completely randomized design with a 2 × 2 factorial arrangement. During incubation, eggs were divided into two temperature treatments: control (37.5 °C) and high temperature (39 °C). At 25 days of age, birds from each group were further divided into two inoculation treatments, namely unchallenged and LPS-challenged groups.

Bird weight (g), heart weight (g), relative heart weight (g, calculated as absolute heart weight ÷ bird weight), spleen weight (g), relative spleen weight (g, calculated as absolute spleen weight ÷ bird weight), and intestine length (cm, measured from the point of insertion of the esophagus into the oropharynx to the junction of the large intestine with the cloaca) were recorded. Jejunum tissue was collected and immediately frozen in liquid nitrogen at −80 °C for gene expression analysis via mRNA sequencing.

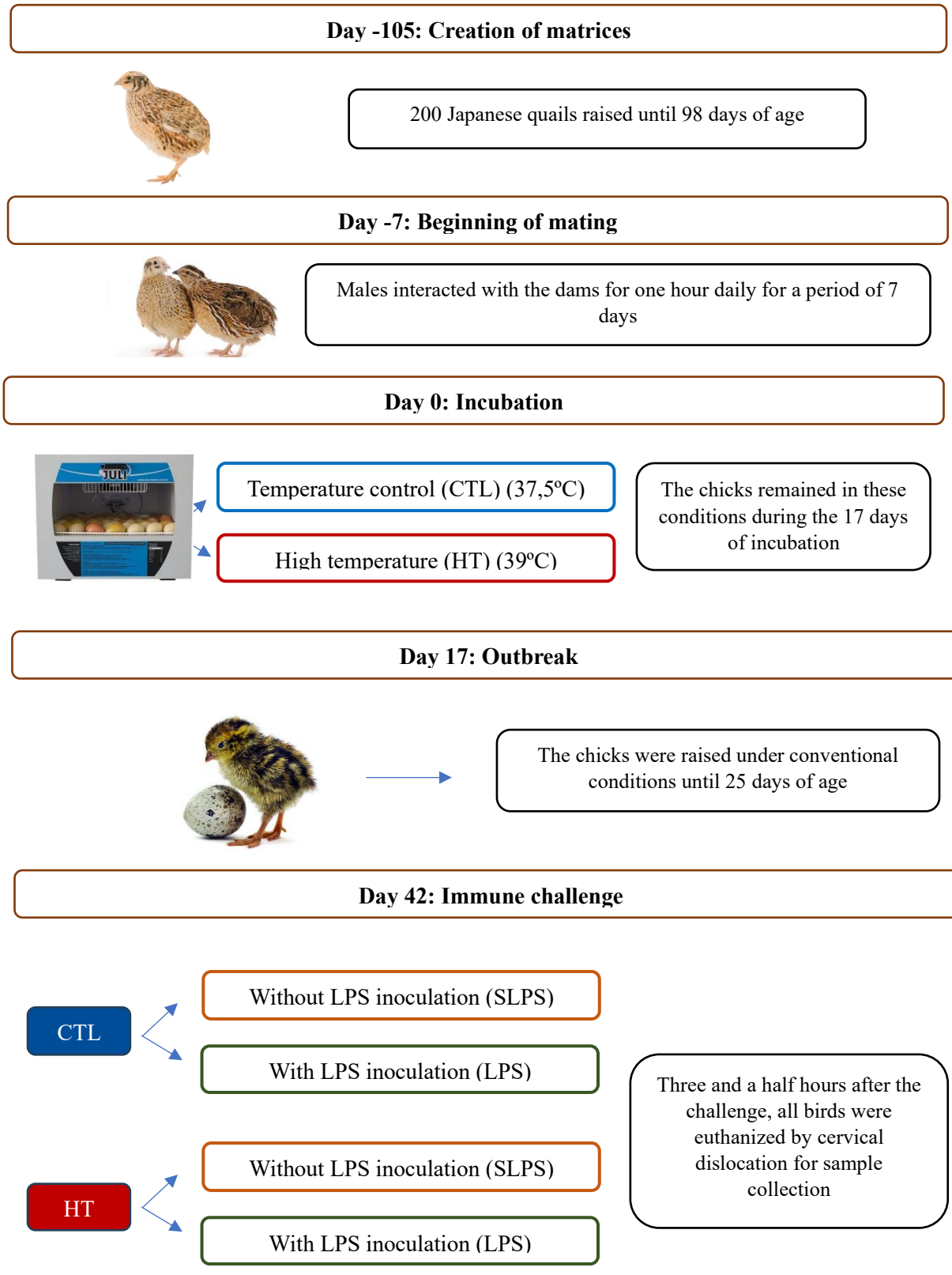

Flowchart 1. Experimental design

941 Statistical analysis of phenotypic data

942 Data were tested for normality and homogeneity of variances using the Shapiro–Wilk
943 and Bartlett tests, respectively. When assumptions were met, two-way analysis of variance
944 (ANOVA) was performed to assess the effects of incubation temperature, LPS challenge, and
945 their interaction. As no significant interaction was observed, treatment means were compared
946 using the *t*-test, with a significance level of 5%. All analyses were conducted using R software
947 version 4.5.0.

948

949 RNA sequencing

950 RNA sequencing was performed using jejunum fragments from 25-day-old Japanese
951 quail. The results were compared as follows: (i) control incubation temperature with LPS
952 challenge versus control incubation temperature without LPS challenge and (ii) high incubation
953 temperature with LPS challenge versus high incubation temperature without LPS challenge.

954

955 mRNA preparation

956 Total RNA was isolated from jejunum specimens using Trizol® reagent (Invitrogen,
957 Carlsbad, CA, USA) at a ratio of 1 mL per 100 mg of tissue, as per the manufacturer's
958 instructions. RNA quantification was performed by spectrophotometric reading at 260 nm, and
959 RNA integrity was confirmed by electrophoresis on 1% agarose gel under ultraviolet light. Total
960 RNA samples were subjected to next-generation sequencing using the Illumina platform.

961

962 Quality control, mapping, and quantification of expression

963 The readings obtained in the sequencing were processed with BBDuk, which is part of
964 the BBTools package version 39.06 (Bushnell, 2023), to remove low-quality bases and Illumina

adapters. This procedure was adopted to minimize potential errors or noise in the following steps. The reads were then mapped to the reference genome using STAR version 2.7.11b (Dobin *et al.*, 2013) to identify their genomic origin and associate them with specific genes. Gene-level read counts were generated using featureCounts version 2.0.8 (Liao; Smyth; Shi, 2014), reflecting the expression level of each gene. The genome and annotation used as reference for mapping and quantification of expression correspond to GCF_001577835.2_Coturnix_japonica_2.1 (Morris *et al.*, 2020), available at https://ftp.ncbi.nlm.nih.gov/genomes/all/GCF/001/577/835/GCF_001577835.2_Coturnix_japonica_2.1.

Differential expression analysis

After gene-level read counts were obtained, differential gene expression analysis was performed using DESeq2 version 1.42.0 (Love; Huber; Anders, 2014), an R/Bioconductor package (Gentleman *et al.*, 2004; Huber *et al.*, 2015). Briefly, the process involved the following steps: (i) using the counts from each library to estimate normalization factors for sequencing depth per sample and the associated dispersion, fitting a negative binomial model; (ii) modeling the data using a generalized linear model with the quasi-likelihood method (Lund *et al.*, 2012) adjusted for the negative binomial; (iii) applying an independent filtering procedure (Bourgon, Gentleman and Huber, 2010) to reduce the number of tests performed and increase the statistical power of the analysis; and (iv) performing a Wald test to assess differential expression for the contrasts of interest. *p*-values were adjusted using the false discovery rate (FDR) method to control for false positives (Benjamini; Hochberg, 1995). Genes with FDR < 0.05 were considered differentially expressed.

989 Functional analysis of differentially expressed genes (DEGs)

990 Functional analysis of DEGs was performed using the clusterProfiler package version
991 4.5.0 (Yu *et al.*, 2012) in the R environment (R Core Team, 2023), with the org.Gg.eg.db
992 annotation database (Carlson, 2019) for *Gallus gallus*. Gene symbols were converted to Entrez
993 IDs using the bitr() function to ensure compatibility with functional enrichment tools and
994 standardize annotation terms.

995 Gene ontology (GO) enrichment analysis was conducted across three main domains:
996 biological processes, molecular functions, and cellular components. The parameter ont = "ALL"
997 allowed simultaneous evaluation of all three categories. The Benjamini–Hochberg adjustment
998 method (pAdjustMethod = "BH") was applied to correct multiple comparisons and reduce false
999 positives. Significantly enriched terms were selected using a cutoff of adjusted *p*-value
1000 (pvalueCutoff = 0.05) and a threshold of *q*-value (qvalueCutoff = 0.05) for improved statistical
1001 reliability. The option readable = TRUE was used to convert Entrez IDs into gene symbols
1002 recognized by the Vertebrate Gene Nomenclature Committee (VGNC) (Jones *et al.*, 2023),
1003 facilitating biological interpretation.

1004 The results were processed and organized in a dataframe, with each GO term ranked by
1005 significance (−log10(FDR)), enabling identification of the most relevant pathways. The
1006 dotplot() function of the enrichplot package was used for visualization, highlighting the most
1007 enriched terms in each GO domain with a color gradient representing statistical significance
1008 (−log10(FDR)). For a more comprehensive analysis, the emapplot() function was used to
1009 visualize relationships between enriched terms based on semantic similarity
1010 (pairwise_termsim), and the cnetplot() function was used to explore connections between genes
1011 and biological pathways, emphasizing terms with lower *p*-values.

1012

Functional analysis of DEGs in the Kyoto Encyclopedia of Genes and Genomes (KEGG)

Functional analysis was performed using a list of DEGs previously identified by RNA sequencing. Genes with adjusted $p < 0.05$ were deemed significant. This criterion was adopted to ensure the selection of genes with biologically relevant and statistically significant changes. For compatibility with the KEGG database, gene symbols were converted to Entrez IDs using the org.Gg.eg.db package specific to *G. gallus*. This step was essential to obtain the correct functional annotation of genes in subsequent analyses. Genes not matched with database genes were excluded from the analysis.

Pathway enrichment analysis for metabolic and signaling pathways was conducted using the clusterProfiler package. Significantly enriched pathways were identified using a threshold of adjusted $p < 0.05$, with Benjamini–Hochberg correction for multiple testing. Additional filters were applied to include only pathways containing between 10 and 500 genes, thereby avoiding selection of pathways that were overly broad or overly specific. For biological interpretation, Entrez IDs were converted back to gene symbols recognized by the VGNC (Jones *et al.*, 2023), enabling more intuitive identification of genes associated with each pathway. Redundancies were reduced by consolidating overlapping pathways through simplification approaches.

Results

Embryonic performance

As shown in Table 1, the total hatching rate was significantly affected by incubation temperature ($p = 0.01128$). Eggs incubated at the control temperature showed a higher total hatching rate (68.50% ± 3.08%) than those incubated at high temperature (56.62% ± 3.43%).

Similarly, the hatching rate of fertile eggs was also significantly higher in the control group (74.75% ± 3.17%) than in the high-temperature group (64.58% ± 3.81%), with $p = 0.042285$.

Table 1. Hatching rate of eggs incubated at control temperature and high temperature

Incubation	Total hatch rate (%)	SE*	Hatching rate of fertile eggs (%)	SE
Control	68.504[a]	3.08	74.754[a]	3.17
High temperature	56.617[b]	3.43	64.583[b]	3.81
P value	0.011128		0.042285	

*Values are presented with mean and standard error (SE). [ab]Different letters in the same column indicate significant differences by Student's t-test ($p<0.05$).

There were no significant differences ($p > 0.05$) in intestine length, embryo weight, egg weight, yolk sac weight, or yolk sac utilization between control and high-temperature groups (Table 2). Thus, exposure to a high incubation temperature did not significantly influence the morphological or physiological performance of the analyzed embryos.

Table 2. Performance of embryos incubated at control temperature and high temperature

Incubation	Bowel length (cm)	SE*	Embryo weight (g)	SE	Egg weight (g)	SE	Yolk sac weight (g)	SE	Yolk sac utilization (%)	SE
Control	86.201	1.69	6.085	0.14	10.248	0.25	1.780	0.10	29.316	1.64
High temperature	80.458	5.07	5.370	0.51	9.846	0.34	1.592	0.13	31.113	2.72
P value	0.30113		0.20094		0.36369		0.28455		0.58147	

*Values are presented with mean and standard error (SE).

Chick performance

No interaction effect of temperature and challenge on chick performance was observed. Therefore, the results are reported as the main effects of each factor. Table 3 presents the results of the LPS challenge. LPS inoculation significantly influenced relative spleen weight, which was higher in the challenged group (0.052% ± 0.00) than in the unchallenged group (0.039% ± 0.00) ($p = 0.039034$). Additionally, no significant differences were observed in absolute or

relative heart weights, absolute spleen weight, bird weight at 17 days, or intestine length ($p > 0.05$).

Table 1. Effect of LPS on progeny performance

Inoculation	Heart weight (g)	SE*	Relative heart weight (%)	SE	Spleen weight (g)	EP	Relative spleen weight (%)	SE	Bird weight at 17 days (g)	SE	Bowel length (cm)	SE
LPS¥	1.104	0.03	1.039	0.03	0.054	0.01	0.052[a]	0.01	104.387	3.33	46.545	1.28
SLPS	1.072	0.03	1.064	0.02	0.041	0.02	0.039[b]	0.02	103.342	2.55	43.000	1.53
P value	0.52783		0.58228		0.053801		0.039034		0.80635		0.21908	

*Values are presented with mean and standard error (SE). [ab]Different letters in the same column indicate significant differences by Student's t-test ($p<0.05$). ¥LPS (With LPS inoculation); SLPS (Without LPS inoculation).

As shown in Table 4, incubation temperature did not significantly affect performance parameters ($p > 0.05$). No statistical differences were observed between the control and high-temperature groups in absolute or relative heart weights, absolute or relative spleen weights, body weight at 17 days, or intestine length.

Table 4. Effect of incubation temperature on progeny performance

Incubation	Heart weight (g)	SE*	Relative heart weight (%)	SE	Spleen weight (g)	EP	Relative spleen weight (%)	SE	Bird weight at 17 days (g)	SE	Bowel length (cm)	SE
Control	1.091	0.03	1.061	0.03	0.051	0.01	0.049	0.01	103.163	2.35	43.272	1.71
High temperature	1.085	0.03	1.042	0.02	0.045	0.01	0.042	0.01	104.566	3.47	45.272	1.09
P value	0.90401		0.68223		0.43538		0.30347		0.74186		0.33787	

*Values are presented with mean and standard error (SE). ¥CTL (Control temperature); AT (High temperature).

DEG identification

In this experiment, Japanese quail eggs were incubated under control and high temperature conditions. At 25 days of age, birds from both groups were inoculated with LPS or saline. The effect of LPS challenge was compared within each incubation temperature.

Gene expression analysis revealed distinct transcriptional regulation patterns between experimental groups. A total of 41 DEGs were identified in the control temperature group

(Control + LPS versus Control + Unchallenged), of which 22 were upregulated and 19 were downregulated based on log2 fold-change (log2FC) values (Figure 1A). In the high-temperature group (High Temperature + LPS versus High Temperature + Unchallenged), LPS inoculation resulted in 845 DEGs (Figure 1B), with 405 upregulated and 440 downregulated genes.

The global distribution of DEGs was visualized using a volcano plot (Figure 1). The *X*-axis represents log2FC values, indicating both the direction and magnitude of gene regulation, whereas the *Y*-axis shows statistical significance as −log10 of the adjusted *p*-value. Upregulated genes, shown in red, cluster on the right side of the plot, reflecting increased expression, whereas downregulated genes, shown in blue, appear on the left, indicating strong suppression. The great concentration of points with high *Y*-axis values underscores the robustness of the analysis and highlights the presence of important genes.

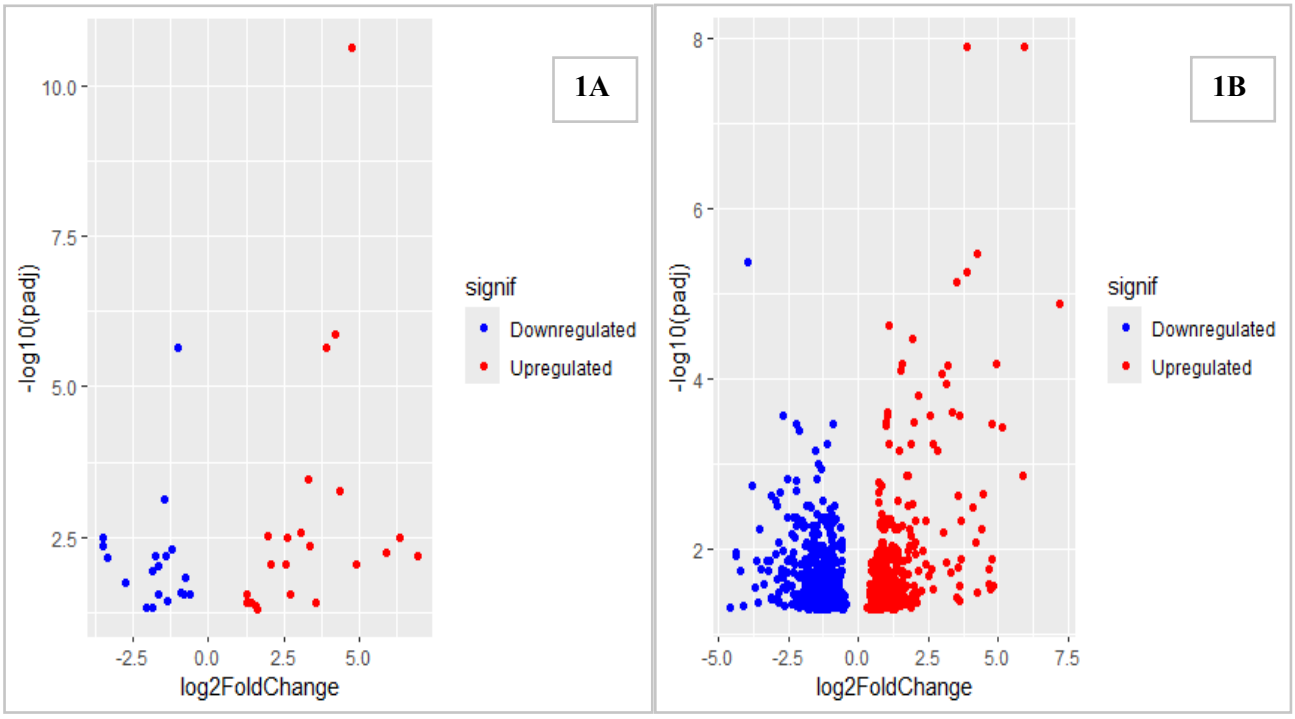

Figure 1. Volcano plot of DEGs expressed in the contrasts CTL+LPS vs CTL+SLPS; and AT+LPS vs AT+SLPS. Scatter plots (volcano plots) representing the differentially expressed genes in the jejunum of Japanese quails. On the left (1A), results of the comparison between the group incubated at control temperature without and with LPS. On the right (1B), comparison between the group incubated at high temperature with and without LPS. The X-axis represents the log2Foldchange (log2FC) values, while the Y-axis indicates the statistical significance (-log10 of

the adjusted p-value). Upregulated genes are highlighted in red and downregulated genes in blue (adjusted p-value < 0.05).

Heatmaps generated from RNA sequencing data are commonly used to analyze gene expression in different biological samples. These heatmaps visually represent gene expression levels, with each row corresponding to a gene and its log2FC value. The heatmap comparing Control + LPS versus Control + Unchallenged (Figure 2) shows positively regulated DEGs, with log2FC values ranging from 1.28 to 6.93. Some of the most highly expressed genes include those involved in solute transport (*SLC5A12* and *SLC13A1*), immune response and inflammation (*IL1R2* and *IL18BP*), and cell surface functions (*PDCD1LG2* and *ZPLD1*). The presence of interleukins and immunity-associated genes supports the hypothesis of inflammatory pathway activation in response to the experimental challenge. Negatively regulated DEGs in the same comparison group exhibit log2FC values ranging from −0.65 to −3.50. Genes showing the greatest suppression include those involved in energy metabolism and lipid oxidation (*GPD1*), regulation of inflammation and immune response (*SAMHD1*), and nutrient transport (*SLC2A15*).

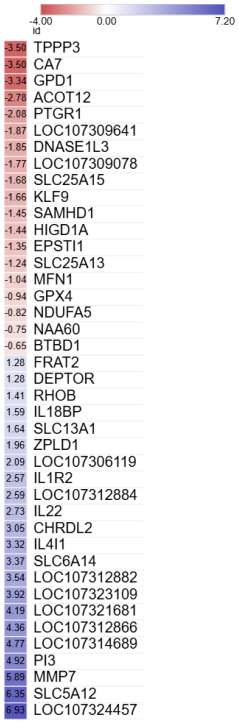

Figure 2. Heatmap of DEGs expressed in CTL+LPS vs. CTL+SLPS from most suppressed to most expressed. Heatmap representing the levels of differential gene expression in the jejunum of Japanese quails subjected to incubation at control temperature and inoculation with lipopolysaccharide (LPS). The values correspond to the log2Foldchange (log2FC) of the differentially expressed genes. The color scale ranges from red (suppressed genes) to blue (overexpressed genes), as indicated in the top bar. Only genes with statistically significant differential expression were included (adjusted $p < 0.05$).

In the heat map comparing DEGs between High Temperature + LPS and High Temperature + Unchallenged (Figure 3) groups, log2FC values ranged from 7.19 to 0.31 for upregulated genes and from −0.43 to −4.59 for downregulated genes. Among the genes overexpressed in LPS-inoculated quail were LPCAT3, PANK3, PIGM, PGAP2, ITCH, CUL4A, PSMA1, and PSMA7. Some of these genes perform essential functions, including participation in the organophosphate pathway (LPCAT3 and PANK3), protein anchoring to the membrane (PIGM and PGAP2), and degradation of misfolded proteins (ITCH, CUL4A, PSMA1, and PSMA7). Among the downregulated genes, notable examples included GATA2, VEGFC, FLT1, SOX9, CHD4, DNMT3A, and MIER1. These genes are involved in cellular adaptation (GATA2, VEGFC, FLT1, and SOX9) and transcriptional repression (CHD4, DNMT3A, and MIER1).


-4.60 0.00 id
-4.55 LOC116653011
-4.39 LOC107322899
-4.37 ABCA7
-4.21 LOC107323914
-4.19 LOC107305760
-3.97 LOC116653763
-3.78 LOC107321450
-3.67 LOC107321408
-3.63 LOC116652412
-3.56 SCARA5
-3.53 RRAD
-3.50 PAX5
-3.36 LOC107314463
-3.25 THRB
-3.19 GABRR3
-3.18 VWCE
-3.12 ADGRV1
-3.09 LRRC56
-3.08 LOC107312653
-2.95 CRLF2
-2.94 ACOT12
-2.93 LOC107308033
-2.89 SLC24A2
-2.88 GNAZ
-2.87 ERBB4
-2.86 NPPC
-2.85 LOC107322197
-2.83 TPPP3
-2.80 PPP1R13B
-2.75 LOC107310501
-2.72 THBS4
-2.70 SPIC
-2.68 TTBK2
-2.68 ONECUT2
-2.67 GPR176
-2.65 CELF4
-2.65 LOC107309013
-2.62 ADAMTS19
-2.60 CDHR1
-2.55 LOC107311589
-2.54 NPR1
-2.54 PPARGC1B
-2.52 DYTN
-2.52 LOC107316155
-2.50 0.00 id
-2.48 LOC107319226
-2.40 ZBTB20
-2.38 LOC107317866
-2.35 HYDIN
-2.34 DPT
-2.34 SYT1
-2.32 LOC107308034
-2.31 LOC107309482
-2.30 ND5
-2.30 PAMR1
-2.28 LOC107325870
-2.25 CNTLN
-2.25 ENPP2
-2.25 COL27A1
-2.23 PLXDC2
-2.23 SOCS2
-2.22 LOC107307883
-2.22 MLXIPL
-2.22 SLC16A8
-2.22 SETBP1
-2.22 LOC107306152
-2.20 COL25A1
-2.20 ITIH5
-2.17 ADAMTS6
-2.15 SOX9
-2.14 SLC23A1
-2.12 ADAMTS10
-2.11 GRIA4
-2.09 TAF1C
-2.09 LOC107318670
-2.08 LOC107321567
-2.05 LOC107316020
-2.05 COX3
-2.05 DGKG
-2.04 CYTB
-2.02 DNASE1L3
-2.01 LOC107306577
-2.00 GPRIN2
-2.00 ND3
-1.97 PALM2AKAP2
-1.95 ANKDD1B
-1.94 LOC116653670
-1.94 ANTXR1
-1.91 ND2
-2.00 0.00 id
-1.91 ANKRD13B
-1.91 ND1
-1.90 UBXN10
-1.90 TRPM6
-1.89 PROC
-1.89 LOC107307130
-1.89 THBD
-1.89 ANXA1
-1.88 ATP6
-1.88 LOC107319556
-1.87 CTBP2
-1.86 IRF5
-1.86 ND4
-1.86 ST3GAL4
-1.86 LOC107305832
-1.85 ACTA2
-1.85 ZC3H15
-1.84 PRKN
-1.83 ASPN
-1.83 CCDC171
-1.82 RIMBP2
-1.82 TLL1
-1.81 FHOD3
-1.80 PDLIM3
-1.79 PDE4D
-1.79 LOC107306118
-1.79 COX1
-1.78 AHDC1
-1.78 KIAA0040
-1.77 SOX18
-1.77 ROBO2
-1.76 MAMDC2
-1.76 PLXNA2
-1.76 KLHL14
-1.74 LOC107307386
-1.74 DACH1
-1.73 TBX2
-1.73 HMCN1
-1.72 LOC107317182
-1.72 FLT1
-1.72 UBE2T
-1.71 NFIA
-1.70 SVEP1
-1.70 DNMT3A
-2.00 0.00 id
-1.99 FBXL17
-1.98 TXNDC16
-1.98 VEGFC
-1.97 CELF2
-1.96 MAP3K6
-1.96 PTPRB
-1.95 HRH1
-1.95 PROX1
-1.95 LOC107314966
-1.94 PTPRD
-1.94 ABI3BP
-1.94 RASGRF2
-1.93 LOC107308109
-1.92 LOC107306990
-1.92 LOC107306356
-1.91 AMH
-1.91 CKS2
-1.90 PSD3
-1.90 RAPGEF4
-1.90 GHR
-1.89 GATA2
-1.89 MN1
-1.88 UNC13D
-1.88 MEF2C
-1.88 KRT18
-1.87 LOC107312593
-1.86 TRMT10B
-1.86 NRG1
-1.86 NKIRAS1
-1.86 ADGRA1
-1.85 GRB10
-1.85 MED18
-1.84 BAHCC1
-1.84 CCDC30
-1.83 SYK
-1.83 TMEM154
-1.83 LOC107325926
-1.82 LOC107317376
-1.82 LOC107307770
-1.82 PREX2
-1.82 KCNB1
-1.82 EXOSC4
-1.81 ITGA1
-1.81 FAM219A
-2.00 0.00 id
-1.50 ETFRF1
-1.50 CAMK2B
-1.49 DHFR
-1.49 LOC107324334
-1.49 SAMD4A
-1.48 FAM172A
-1.48 CAMK1D
-1.48 KAT6B
-1.47 LOC107306164
-1.46 MAST4
-1.45 NSMF
-1.45 TGFBI
-1.45 ZNF462
-1.45 POLQ
-1.44 MEX3B
-1.44 ADAMTS5
-1.44 PLCXD3
-1.43 LIME1
-1.43 RFX3
-1.42 FYB1
-1.42 PKD2
-1.42 LFNG
-1.42 SLC25A12
-1.41 ANTXRL
-1.40 KLF12
-1.39 NPB
-1.38 LOC107307406
-1.38 LOC107320199
-1.37 GYPC
-1.37 NFIB
-1.36 SREK1IP1
-1.36 CCSER1
-1.35 SH3BP1
-1.35 LOC107307630
-1.35 MALT1
-1.34 TUT7
-1.34 ULK1
-1.33 AOPEP
-1.33 LOC107306830
-1.32 FOCAD
-1.32 CTIF
-1.32 NUFIP2
-1.32 CPLANE1
-1.31 SREK1
-2.00 0.00 id
-1.22 LOC107309078
-1.21 BBS7
-1.21 RPP25L
-1.21 CDK6
-1.21 LOC107323801
-1.21 PTMS
-1.20 RPS23
-1.20 COL21A1
-1.19 SRFBP1
-1.19 GAL3ST1
-1.18 ZFHX3
-1.18 DNAJC12
-1.18 APTX
-1.18 MYO19
-1.18 LOC107307407
-1.18 LOC107312125
-1.17 LOC107320083
-1.17 IPO11
-1.17 NR6A1
-1.17 SLC44A3
-1.17 SPI1
-1.17 ZRANB3
-1.16 FOXN3
-1.16 S1PR1
-1.16 BASP1
-1.16 PARD3B
-1.15 PTPRK
-1.15 CCN2
-1.15 MBNL2
-1.15 SDC2
-1.14 PBX1
-1.14 ZEB2
-1.13 MBNL3
-1.13 SLITRK6
-1.13 DOCK8
-1.12 MAP3K8
-1.12 NOL6
-1.12 ARNTL2
-1.11 DEF6
-1.11 ZMIZ2
-1.10 FER
-1.10 SMAD7
-1.10 CEP85L
-1.10 CHM
-2.00 0.00 id
-1.09 MGAT4A
-1.09 CLK3
-1.09 COMP
-1.08 MBD4
-1.08 ZSWIM6
-1.08 PARP8
-1.08 FBXL2
-1.07 KMT2A
-1.06 LOC107307373
-1.06 PTCH1
-1.06 KLHL3
-1.05 CUNH19orf47
-1.05 NOL9
-1.05 HEXIM1
-1.04 IGFBP5
-1.04 NAA35
-1.04 RCSD1
-1.04 SPRY2
-1.04 AK6
-1.03 FHOD1
-1.03 NDUFA1
-1.03 FLAD1
-1.03 CARMIL3
-1.02 NBEAL2
-1.01 HOOK3
-1.01 SRF
-1.01 LOC107320961
-1.01 FBXO22
-1.01 LOC107309158
-1.01 CEMIP2
-1.01 TOX2
-1.00 PIK3R1
-1.00 SRRT
-0.99 DGUOK
-0.98 FBXO11
-0.98 MIER3
-0.97 SKI
-0.97 ANKRD52
-0.96 TMCC1
-0.96 WDR55
-0.96 LOC107312940
-0.96 NDUFAF2
-0.95 MTREX
-0.95 SMARCA2
-2.00 0.00 id
-0.96 RBBP6
-0.94 SEMA4D
-0.93 TMEM11
-0.93 ABCA2
-0.93 NR2F2
-0.93 ELK3
-0.93 RICTOR
-0.93 TLNRD1
-0.93 NFATC1
-0.92 B4GALT1
-0.92 ECPAS
-0.92 TRIM8
-0.92 DDX3X
-0.92 RP9
-0.92 CLOCK
-0.92 LMNB1
-0.91 RASA1
-0.91 OFD1
-0.90 ZNF142
-0.89 CUX1
-0.89 ABCB8
-0.89 TIMP3
-0.89 PJA2
-0.89 PRKCE
-0.88 NUMA1
-0.88 MAMLD1
-0.87 GRAMD2A
-0.87 MRPL54
-0.87 IL6ST
-0.86 ORC3
-0.86 XPO6
-0.86 PTK2
-0.86 IKZF2
-0.86 IP6K1
-0.85 SIK2
-0.85 RNF44
-0.85 LOC107310851
-0.83 NIPBL
-0.82 SSH2
-0.82 RAP1GDS1
-0.82 CHD4
-0.81 ATXN1
-0.81 GTF3A
-0.80 NCOA3
-2.00 0.00 id
-0.78 PDE12
-0.78 STRN
-0.77 TCTA
-0.77 MAP4
-0.76 AP3D1
-0.75 TERF2IP
-0.74 UXS1
-0.74 C6H10orf88
-0.73 FOXK2
-0.72 AMMECR1L
-0.70 LOC107310736
-0.70 PPP3CA
-0.69 SGSM2
-0.69 LOC107312573
-0.69 WIPF2
-0.68 HCFC2
-0.67 SUZ12
-0.66 UPF2
-0.65 MYO9B
-0.65 CHD1
-0.64 RIN2
-0.64 PITRM1
-0.63 ANKRD17
-0.62 SKIL
-0.62 INPP5A
-0.62 MACO1
-0.61 DENND5A
-0.60 MFN1
-0.60 EGLN1
-0.59 PBRM1
-0.59 RPS6KA6
-0.58 MOB3A
-0.58 WNK1
-0.58 PCCA
-0.57 DPY19L3
-0.56 HIPK1
-0.56 MIER1
-0.55 ETV6
-0.54 USP22
-0.53 LOC107306504
-0.51 TIMM13
-0.50 UVRAG
-0.46 PRRC2C
-0.43 DRG1

1125

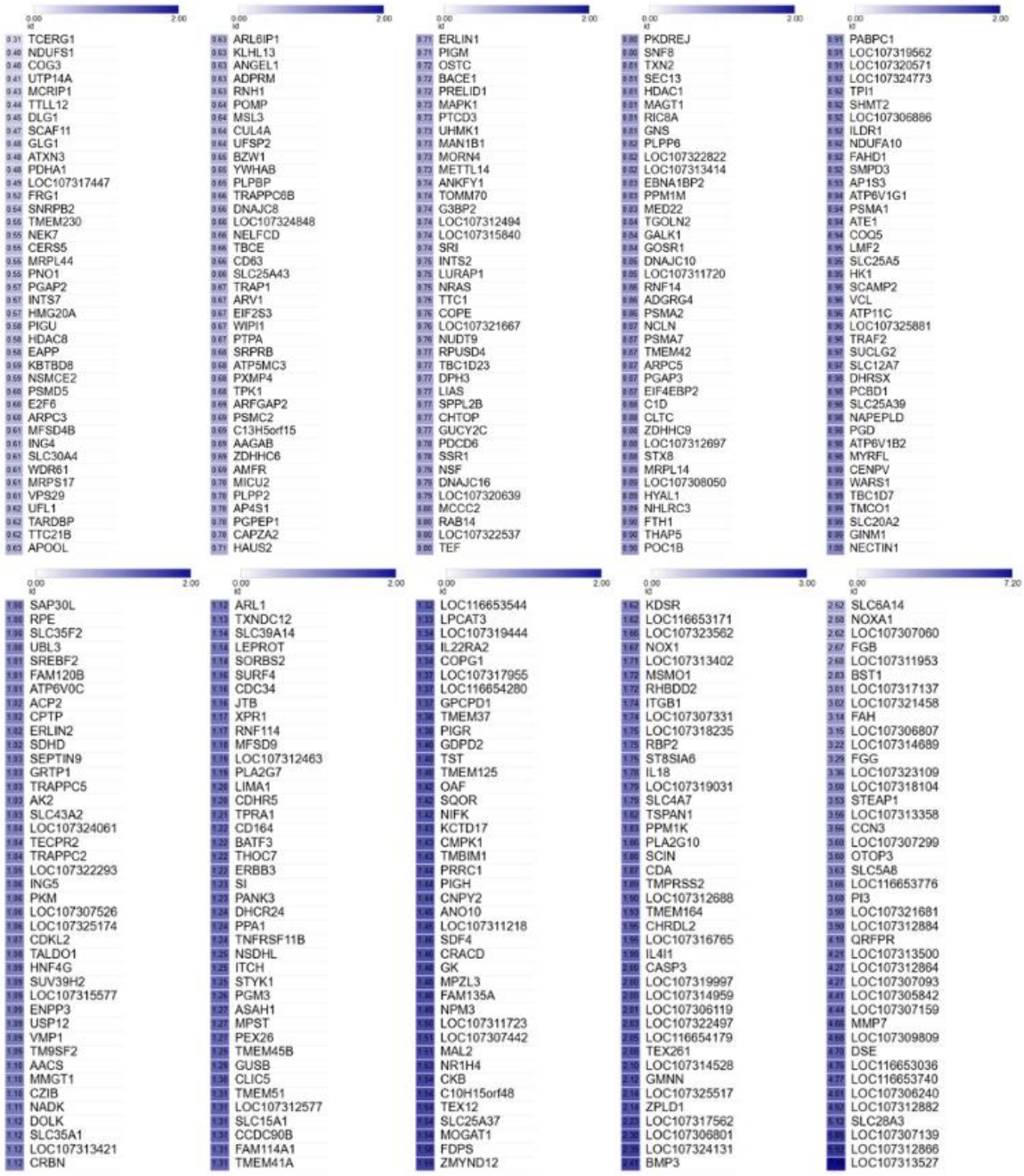

Figure 3. Heatmap of DEGs expressed in AT+LPS vs. AT+SLPS from most suppressed to most expressed. Heatmap representing differential gene expression levels in the jejunum of Japanese quails subjected to high-temperature incubation and inoculation with lipopolysaccharide (LPS). Values correspond to the log2Foldchange (log2FC) of differentially expressed genes. The color scale ranges from red (suppressed genes) to blue (overexpressed genes), as indicated in the top bar. Only genes with statistically significant differential expression were included (adjusted $p < 0.05$).

Effect of LPS inoculation within the control temperature group

Functional annotation using GO was grouped into three main domains: biological process (Table 5), cellular component (Table 6), and molecular function (Table 7). These domains describe the gene's biological function, its role at the molecular level, and its cellular localization, respectively.

The graphs in Figure 4 (A–D) illustrate the functional enrichment analysis of DEGs between Control + LPS and Control + Unchallenged, that is, genes differentially expressed in quail incubated at control temperature and inoculated with LPS. For upregulated genes, the cellular component and molecular function domains were significantly enriched (adjusted $p < 0.05$). In the cellular component domain (Figure 4A), enriched genes were predominantly associated with extracellular structures, such as exosomes, vesicles, and the cell surface, suggesting active signaling and intercellular communication mechanisms. In the molecular function domain (Figure 4B), terms related to cytokine binding and symporter activity were prominent, emphasizing the activation of pathways involved in immune response and molecular transport. For downregulated genes, the biological process and molecular function domains were enriched (adjusted $p < 0.05$). In the biological process domain (Figure 4C), DEGs were strongly associated with nucleotide and purine metabolism, amino acid transport, and oxidative processes such as NADH and NAD^+ metabolism. Suppression of these genes may indicate a reduction in essential metabolic pathways, reflecting a redirection of cellular metabolism in response to the immune challenge. Finally, in the molecular function domain (Figure 4D), the activity of transmembrane L-amino acid transporters was enriched.

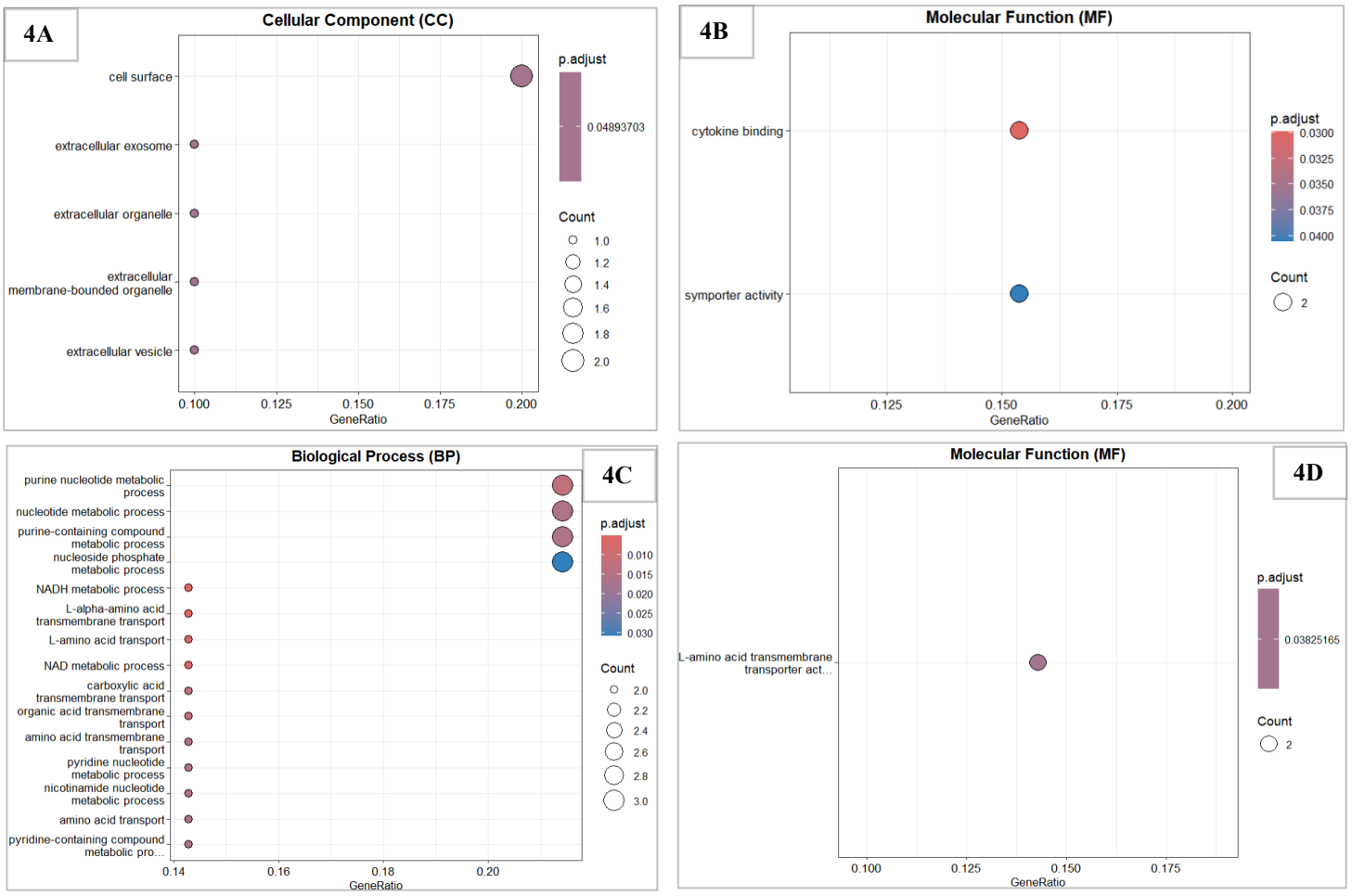

Figure 4. GO enrichment analysis of DEGs upregulated in CTL+LPS vs CTL+SLPS. Figure 4A: Cellular component of overexpressed DEGs. Figure 4B: Molecular function of overexpressed DEGs. Figure 4C: Biological process of suppressed DEGs. Figure 4D: Molecular function of suppressed DEGs. The figures individually present the GeneRatio (proportion of genes in a dataset that are associated with a specific enrichment term) on the X-axis and the enrichment terms on the Y-axis. The circles are associated in size with the gene count and in color with the adjusted p-value.

The biological processes enriched for genes downregulated in LPS-inoculated quail were primarily related to energy metabolism and amino acid transport (Table 5). The most significant term was NADH metabolic process (GO:0006734, adjusted $p = 0.0052$), involving *SLC25A13* and *GPD1*. Amino acid transport processes were also prominent, including L-α-amino acid transmembrane transport (GO:1902475, adjusted $p = 0.0052$) and L-amino acid transport (GO:0015807, adjusted $p = 0.0066$), both mediated by *SLC25A13* and *SLC25A15*.

Furthermore, genes involved in nucleotide metabolism were suppressed, such as those associated with the purine nucleotide metabolic process (GO:0006163, adjusted $p = 0.0123$), including *SLC25A13*, *SAMHD1*, and *GPD1*, and the broader term nucleotide metabolic process (GO:0009117, adjusted $p = 0.0161$). Notably, *SLC25A13* emerged as a central regulator, repeatedly associated with multiple metabolic and transport pathways. Adjusted *p*-values, ranging from 0.0052 to 0.0161, indicated a coordinated downregulation of these biological pathways in response to LPS-induced immune stress.

Table 5. Biological process of DEGs suppressed in CTL+LPS vs CTL+SLPS

ID:PB	Description	geneID	p-ajusted
GO:0006734	NADH metabolic process	*SLC25A13/GPD1*	0.00516
GO:1902475	L-alpha amino acid transmembrane transport	*SLC25A13/SLC25A15*	0.00516
GO:0015807	L-amino acid transport	*SLC25A13/SLC25A15*	0.00665
GO:0019674	NAD metabolic process	*SLC25A13/GPD1*	0.00665
GO:1905039	carboxylic acid transmembrane transport	*SLC25A13/SLC25A15*	0.01230
GO:1903825	organic acid transmembrane transport	*SLC25A13/SLC25A15*	0.01230
GO:0006163	purine nucleotide metabolic process	*SLC25A13/SAMHD1/GPD1*	0.01230
GO:0003333	amino acid transmembrane transport	*SLC25A13/SLC25A15*	0.01570
GO:0009117	nucleotide metabolic process	*SLC25A13/SAMHD1/GPD1*	0.01610
GO:0019362	pyridine nucleotide metabolic process	*SLC25A13/GPD1*	0.01610
GO:0046496	nicotinamide nucleotide metabolic process	*SLC25A13/GPD1*	0.01610
GO:0006865	amino acid transport	*SLC25A13/SLC25A15*	0.01610
GO:0072524	pyridine-containing compound metabolic process	*SLC25A13/GPD1*	0.01610
GO:0072521	purine-containing compound metabolic process	*SLC25A13/SAMHD1/GPD1*	0.01610
GO:0006753	nucleoside phosphate metabolic process	*SLC25A13/SAMHD1/GPD1*	0.03070
GO:0055086	nucleobase-containing small molecule metabolic process	*SLC25A13/SAMHD1/GPD1*	0.03630
GO:0046434	organophosphate catabolic process	*SAMHD1/GPD1*	0.03660
GO:1901136	carbohydrate derivative catabolic process	*SAMHD1/GPD1*	0.03660
GO:0046942	carboxylic acid transport	*SLC25A13/SLC25A15*	0.03710
GO:0015849	organic acid transport	*SLC25A13/SLC25A15*	0.03710

Analysis of the enrichment of cellular components for upregulated DEGs in LPS-inoculated quail revealed the most significant terms, as shown in Table 6. *PDCD1LG2* was associated with the cell surface (GO:0009986), along with *ZPLD1*. The gene *S100A12* showed strong associations with terms related to extracellular vesicles, including extracellular exosome (GO:0070062), extracellular organelle (GO:0043230), extracellular membranous organelle (GO:0065010), and extracellular vesicle (GO:1903561), suggesting potential involvement in intercellular communication via exosomes.

Table 6. Cellular component of DEGs overexpressed in CTL+LPS vs CTL+SLPS

ID:CC	Description	geneID	p-ajusted
GO:0009986	cell surface	*PDCD1LG2/ZPLD1*	0.04890
GO:0070062	extracellular exosome	*S100A12*	0.04890
GO:0043230	extracellular organelle	*S100A12*	0.04890
GO:0065010	extracellular membrane-bound organelle	*S100A12*	0.04890
GO:1903561	extracellular vesicle	*S100A12*	0.04890

Table 7 presents the main terms for molecular function of DEGs in LPS-inoculated quail. Among the upregulated genes were *IL1R2* and *IL18BP*, associated with cytokine binding (GO:0019955, adjusted $p = 0.03$). *SLC5A12* and *SLC13A1* were related to symporter activity (GO:0015293, adjusted $p = 0.0406$), acting on molecular import. The downregulated genes *SLC25A13* and *SLC25A15* were related to L-amino acid transmembrane transporter activity (GO:0015179, adjusted $p = 0.0383$).

Table 7. Molecular function of DEGs regulated in CTL+LPS vs CTL+SLPS

Overexpressed genes			
ID:FM	**Description**	**geneID**	**p-ajusted**
GO:0019955	cytokine binding	*IL1R2/IL18BP*	0.03000
GO:0015293	symporter activity	*SLC5A12/SLC13A1*	0.04060
Suppressed genes			
GO:0015179	L-amino acid transmembrane transporter activity	*SLC25A13/SLC25A15*	0.03830

The integrated enrichment map (emapplot) illustrates connectivity between significantly enriched GO biological terms, allowing identification of interrelated functional groupings. Figure 5A presents an emapplot based on genes upregulated in LPS-inoculated quail. Significant integrations (adjusted $p < 0.05$) were observed between terms related to extracellular components, including organelle, vesicle, exosome, and delimiting membrane. The map also revealed enriched genes (adjusted $p < 0.05$) in non-linked terms, such as cell surface and cytokine binding.

Figure 5B shows a network characterized by strong interconnectivity (adjusted $p < 0.03$) among terms such as purine nucleotide metabolic process, phosphate nucleoside metabolic process, nucleotide metabolic process, and NADH metabolic process, indicating coordinated suppression of these pathways in LPS-inoculated quail. This metabolic reprogramming in the quail jejunum in response to LPS challenge reflects a complex balance between maintaining basic cellular functions, such as intercellular communication and molecular import, and mounting an effective immune response.

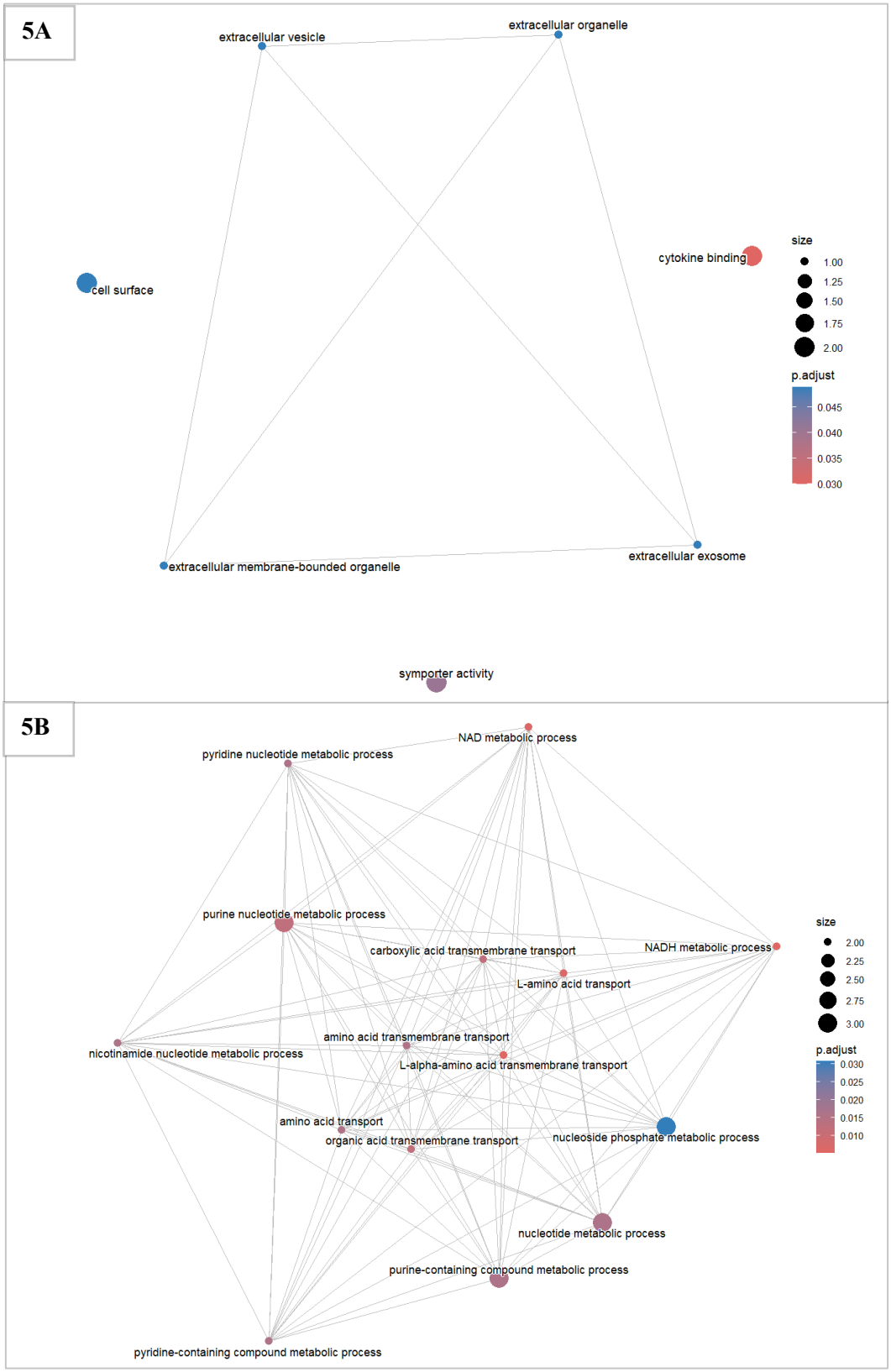

Figure 5. Integrated enrichment map of DEGs in CTL+LPS vs CTL+SLPS. Figure 5A: Integrated enrichment map of overexpressed genes. Figure 5B: Integrated enrichment map of suppressed genes. Nodes represent GO terms, where lines indicate interactions between terms, and the circle (node) corresponds by size to the number of associated genes, and by coloring to the adjusted p-value.

The network graph (cnetplot) lists the most important genes within a biological context and relates them to GO terms. Figure 6A shows the relationship of genes upregulated (adjusted $p < 0.05$) in LPS-inoculated quail with enriched terms. The gene *S100A12* is related to extracellular vesicle, extracellular exosome, external limiting membrane, and extracellular organelle. The *PDCD1LG2* and *ZPLD1* genes are linked to the term cell surface. Figure 6B shows the network of integrations (adjusted $p < 0.05$) between downregulated genes and essential metabolic processes in LPS-inoculated quail. *SLC25A15*, *SLC25A13*, and *GPD1* emerged as central elements in the analysis, demonstrating a strong connection between metabolite transport and energy production. *SLC25A15* is directly associated with three crucial transport processes: carboxylic acid transmembrane transport, L-amino acid transport, and L-α-amino acid transport. Additionally, *SLC25A13* is strongly linked to NAD and NADH metabolism, key components in redox reactions and cellular energy production. Finally, *GPD1* complements this metabolic network by also participating in NADH metabolism, underscoring the importance of this redox system in cellular processes.

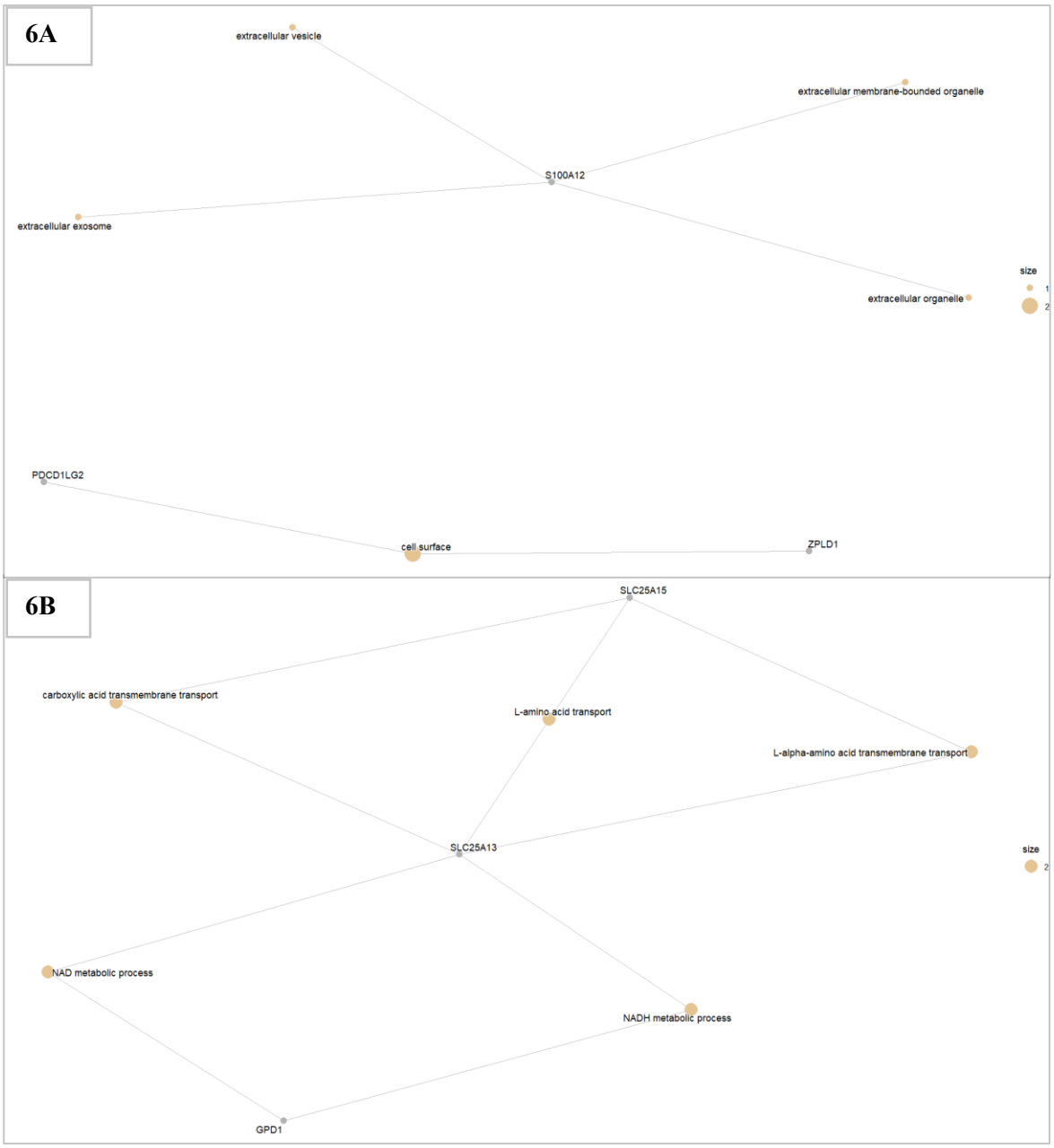

Figure 6. Network graph of DEG enrichment in CTL+LPS vs. CTL+SLPS. Figure 6A: Enrichment network of overexpressed DEGs. Figure 6B: Enrichment network of suppressed DEGs. The larger, orange-colored nodes represent GO terms. The smaller, gray nodes correspond to the genes involved in the respective biological processes present in the figure. The sizes of the functional nodes are proportional to the number of associated genes, as indicated in the lateral legend. Edges connect each gene to the GO terms to which they contributed significantly in the enrichment test.

Effect of LPS inoculation within the high-temperature group

This GO analysis was explored in two categories: biological process (Tables 8 and 9) and cellular component (Table 10). This approach allowed elucidating not only the biological functions of the identified genes but also their subcellular localization. For upregulated genes, both the biological process and cellular component domains were enriched (adjusted $p < 0.05$). Figure 7A shows the enriched biological process terms, which include organophosphate metabolic processes, encompassing both biosynthesis and ubiquitin-dependent degradation pathways. The notable presence of GPI-anchored protein biosynthesis in this group underscores the crucial role of these proteins in cell signaling and adhesion. Concurrently, a marked enrichment in protein degradation pathways was observed, particularly those mediated by the ubiquitin-proteasome system and post-translational modifications. Analysis of the cellular component domain (Figure 7B) complemented these findings, revealing that the upregulated genes are predominantly located in strategic subcellular compartments.

The Golgi apparatus and endoplasmic reticulum emerged as key sites, with emphasis on their membrane substructures. Associations with coated vesicles and specialized protein complexes, such as the endopeptidase complex and the nuclear complex, suggest an active reorganization of protein processing and transport systems in response to LPS stimulation. Analysis of downregulated genes revealed enrichment only in the biological process domain (adjusted $p < 0.05$). Figure 7C shows terms such as negative regulation of DNA-templated transcription, negative regulation of RNA biosynthetic process, and circulatory system development. This combination of terms suggests a conservative cellular strategy, in which energy is prioritized and conserved under conditions of thermal stress.

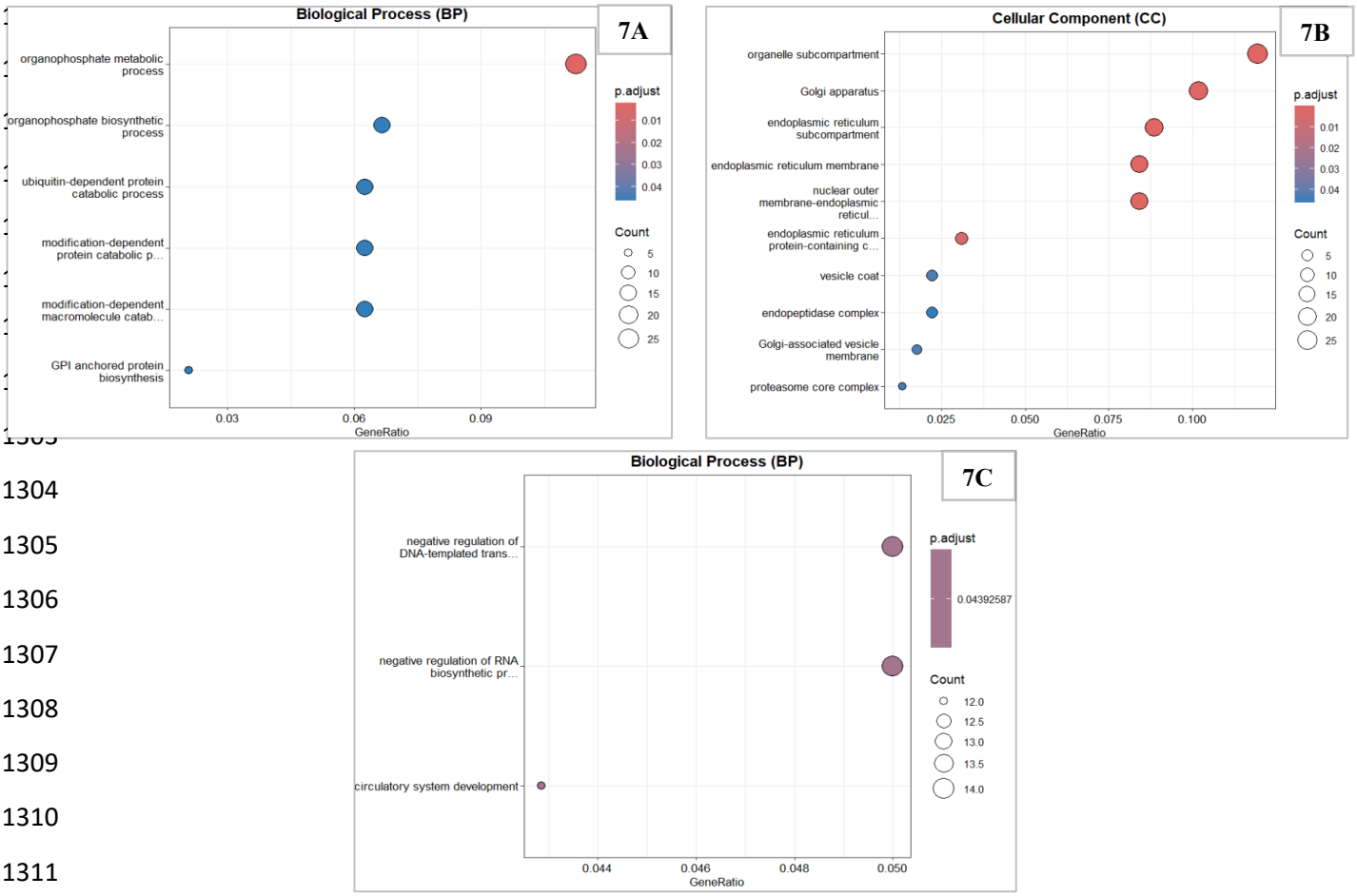

Figure 7. GO enrichment analysis of DEGs upregulated in AT+LPS vs AT+SLPS. Figure 7A: Biological process of overexpressed DEGs. Figure 7B: Cellular component of overexpressed DEGs. Figure 7C: Biological process of suppressed DEGs. The figures individually present the GeneRatio (proportion of genes in a dataset that are associated with a specific enrichment term) on the X-axis and the enrichment terms on the Y-axis. The circles are associated in size with the gene count and in color with the adjusted p-value.

Enrichment analysis of biological processes revealed significant alterations in pathways related to organophosphate metabolism and inflammatory response among genes upregulated in LPS-inoculated quail (Table 8). The most enriched term, GO:0019637 (organophosphate metabolism, adjusted $p = 0.00220$), included 27 genes involved in energy metabolism and cell signaling, such as *SPDF*, *CKB*, *PGM3*, and *NADK*. These findings suggest that thermal stress during incubation, potentially exacerbated by LPS exposure, induces metabolic reprogramming, increasing the demand for organophosphates to sustain energy homeostasis (via ATP) and support membrane phospholipid synthesis under stress conditions.

Enrichment of the term GO:0090407 (organophosphate biosynthetic process, adjusted $p = 0.00462$), involving genes such as *LPCAT3* and *PANK3*, supports the hypothesis that high incubation temperatures activate organophosphate biosynthesis pathways, potentially to compensate for cellular damage or replace signaling molecules. Additionally, the term GO:0180046 (GPI-anchored protein biosynthesis, adjusted $p = 0.00462$) highlighted genes such as *PIGM* and *PGAP2*, suggesting that thermal stress during incubation may modulate protein anchoring to the membrane, a critical mechanism for cell communication during inflammatory responses.

Ubiquitination-dependent protein degradation pathways (GO:0006511, adjusted $p = 0.00462$) were also enriched, related to genes such as *ITCH* and *CUL4A*, as well as proteasome subunit genes (*PSMA1* and *PSMA7*). Possibly, exposure of the embryo to heat and later to LPS activated the degradation of poorly coiled or damaged proteins, a protective mechanism against cellular stress. The overlap of these genes with terms such as GO:0019941 (modification-dependent protein catabolic process) supports the idea that ubiquitination is a conserved response during conditions of combined stresses (thermal and inflammatory).

Table 8. Biological processes of DEGs overexpressed in AT+LPS vs AT+SLPS

ID:PB	Description	geneID	p-ajusted
GO:0019637	organophosphate metabolic process	*PLA2G10/FDPS/CKB/PIGH/CMPK1/GPCPD1/LPCAT3/PGM3/PANK3/DOLK/NADK/ENPP3/TALDO1/AK2/ATP6V1B2/PGD/NAPEPLD/SUCLG2/HK1/SMPD3/TPI1/PGAP3/GUCY2C/PIGM/PLPP2/TPK1/PGAP2*	0.00220
GO:0090407	organophosphate biosynthetic process	*FDPS/CKB/PIGH/CMPK1/LPCAT3/PGM3/PANK3/DOLK/NADK/AK2/TPI1/PGAP3/GUCY2C/PIGM/TPK1/PGAP2*	0.04620
GO:0006511	ubiquitin-dependent protein catabolic process	*KCTD17/ITCH/RNF114/CDC34/ATE1/PSMA1/NHLRC3/PSMA7/PSMA2/RNF14/SNF8/AMFR/PSMC2/CUL4A/UFL1*	0.04620
GO:0180046	gpi-anchored protein biosynthesis	*PIGH/PGAP3/PIGM/PIGU/PGAP2*	0.04620

GO:0019941	modification-dependent protein catabolic process	*KCTD17/ITCH/RNF114/CDC34/ATE1/PSMA1/NHLRC3/PSMA7/PSMA2/RNF14/SNF8/AMFR/PSMC2/CUL4A/UFL1*	0.04620
GO:0043632	modification-dependent macromolecule catabolic process	*KCTD17/ITCH/RNF114/CDC34/ATE1/PSMA1/NHLRC3/PSMA7/PSMA2/RNF14/SNF8/AMFR/PSMC2/CUL4A/UFL1*	0.04620

For genes downregulated in LPS-inoculated quail, Table 9 shows significant enrichment of biological processes related to circulatory system development, negative regulation of gene transcription, and extracellular matrix organization.

The results demonstrated significant activation (adjusted $p < 0.05$) of circulatory system development (GO:0072359), negative regulation of DNA-templated transcription (GO:0045892), and negative regulation of RNA biosynthetic process (GO:1902679). *GATA2*, *VEGFC*, *FLT1*, and *SOX9* are examples of genes associated with these processes. They play critical roles in angiogenesis and vascularization, suggesting active vascular adaptation in response to thermal and immune stress. In parallel, genes such as *CHD4*, *DNMT3A*, and *MIER1*, involved in transcriptional repression, were suppressed in quail chicks inoculated with LPS. Suppression of these genes may indicate an adaptive response that prioritizes the expression of pro-inflammatory or defense-related genes, thereby relaxing control over transcription under stress conditions.

Table 9. Biological processes of DEGs suppressed in AT+LPS vs AT+SLPS

ID:PB	Description	geneID	p-ajusted
GO:0072359	circulatory system development	*NIPBL/S1PR1/MEF2C/GATA2/PTPRB/VEGFC/FLT1/SOX18/PDLIM3/FHOD3/ANXA1/SOX9*	0.04390
GO:0045892	negative regulation of dna-influenced transcription	*MIER1/ATXN1/CHD4/NR2F2/SEMA4D/MIER3/HEXIM1/BASP1/PER2/CRY2/GATA2/DNMT3A/SOX9/THRB*	0.04390
GO:1902679	negative regulation of rna biosynthetic processes	*MIER1/ATXN1/CHD4/NR2F2/SEMA4D/MIER3/HEXIM1/BASP1/PER2/CRY2/GATA2/DNMT3A/SOX9/THRB*	0.04390

Regarding cellular components (Table 10), for the genes overexpressed in LPS-challenged chicks, the enriched terms were mainly associated with the endoplasmic reticulum. The most significant term was organelle subcompartment (GO:0031984, adjusted p <0.00001) including 27 genes such as *KDSR*, *PIGH*, *PGAP3*, and *PIGU*. This finding suggests the structural reorganization of organelles in response to thermal and immune stress. Specifically, strong enrichment was observed in endoplasmic reticulum subcompartment (GO:0098827, adjusted p <0.00001) and endoplasmic reticulum membrane (GO:0005789, adjusted p = 0.00001), involving genes associated with lipid metabolism (*KDSR* and *MOGAT1*), protein anchoring (*PIGH*, *PGAP3*, and *PIGU*), and response to misfolded proteins (*ERLIN2* and *UFL1*).

The nuclear outer membrane-endoplasmic reticulum membrane network (GO:0042175, adjusted p = 0.00001) was also affected, indicating changes in communication between these compartments. Enrichment was observed in the Golgi apparatus (GO:0005794, adjusted p = 0.00004), with the differential expression of genes such as *COPG1* and *CLTC*, involved in vesicular transport and post-translational protein modification. Protein degradation pathways were also modulated, notably in the proteasome core complex (GO:0005839, adjusted p = 0.00442), including the subunits *PSMA1*, *PSMA7*, and *PSMA2*, indicating an increased demand for the removal of damaged proteins under stress conditions.

Table 10. Cellular components of DEGs overexpressed in AT+LPS vs AT+SLPS

ID:CC	Description	geneID	p-adjusted
GO:0031984	organelle subcompartment	*KDSR/MOGAT1/PIGH/DOLK/MMGT1/ERLIN2/TMCO1/MYRFL/ATP11C/SCAMP2/LMF2/PGAP3/NCLN/GOSR1/MAGT1/RAB14/NSF/SSR1/TBC1D23/BACE1/OSTC/ERLIN1/SRPRB/ARV1/UFL1/PIGU/PGAP2*	0.00001
GO:0098827	endoplasmic reticulum subcompartment	*KDSR/MOGAT1/PIGH/DOLK/MMGT1/ERLIN2/TMCO1/MYRFL/LMF2/PGAP3/NCLN/MAGT1/SSR1/OSTC/ERLIN1/SRPRB/ARV1/UFL1/PIGU/PGAP2*	0.00001

GO:0005789	endoplasmic reticulum membrane	*KDSR/MOGAT1/PIGH/DOLK/MMGT1/ERLIN2/TMCO1/MYRFL/LMF2/PGAP3/NCLN/MAGT1/SSR1/OSTC/ERLIN1/SRPRB/UFL1/PIGU/PGAP2*	0.00001
GO:0042175	endoplasmic reticulum-outer nuclear membrane network	*KDSR/MOGAT1/PIGH/DOLK/MMGT1/ERLIN2/TMCO1/MYRFL/LMF2/PGAP3/NCLN/MAGT1/SSR1/OSTC/ERLIN1/SRPRB/UFL1/PIGU/PGAP2*	0.00001
GO:0005794	golgi apparatus	*TMBIM1/COPG1/XPR1/ARL1/SLC35A1/MMGT1/TRAPPC5/ATP11C/SCAMP2/AP1S3/ZDHHC9/CLTC/GOSR1/RAB14/NSF/TBC1D23/COPE/BACE1/ZDHHC6/ARV1/PGAP2/GLG1/COG3*	0.00048
GO:0140534	endoplasmic reticulum protein-containing complex	*PIGH/MMGT1/MAGT1/OSTC/PIGM/SRPRB/PIGU*	0.00364
GO:0030660	golgi-associated vesicle membrane	*COPG1/AP1S3/CLTC/COPE*	0.04310
GO:0030120	vesicle coat	*COPG1/AP1S3/CLTC/SEC13/COPE*	0.04310
GO:0005839	proteasome core complex	*PSMA1/PSMA7/PSMA2*	0.04420
GO:1905369	endopeptidase complex	*PSMA1/PSMA7/PSMA2/PSMC2/PIGU*	0.04650

The integrated enrichment map (emapplot) of DEGs overexpressed in quail chicks subjected to thermal stress during incubation and inoculated with LPS is shown in Figure 8A. Three main axes are evident: activation of the proteostasis system, dynamic remodeling of membrane organelles, and metabolic reprogramming with cell signaling. The significant enrichment of the proteasome core complex (adjusted $p < 0.04$) and ubiquitin-dependent degradation pathways underscores the critical role of proteostasis under stress conditions. The presence of proteasomal subunits and ubiquitination factors suggests an increased degradation of damaged proteins.

Terms such as endoplasmic reticulum membrane (adjusted $p < 0.04$) and endoplasmic reticulum subcompartment ($p < 0.04$) were enriched with genes involved in post-translational modification and response to misfolded proteins. Enrichment of the Golgi apparatus (adjusted $p < 0.04$) and associated structures (vesicle lining and Golgi-associated vesicle membrane) is

indicative of alterations in vesicular traffic, which is essential for secretion of inflammatory mediators and cellular repair. Genes such as *COPG1* and *CLTC* (involved in vesicle transport) can facilitate communication between organelles during stress. Organophosphate metabolism (adjusted $p < 0.04$) emerged as a central pathway, with genes linked to ATP synthesis (*NADK*), phospholipids (*LPCAT3*), and GPI anchors (*PIGM*).

Figure 8B shows the integrated enrichment map of suppressed DEGs in LPS-inoculated quail. Among the main enriched terms (adjusted $p < 0.05$), there was a clear interconnection between negative regulation of DNA-templated transcription and negative regulation of transcription by RNA. Furthermore, circulatory system development was evidenced.

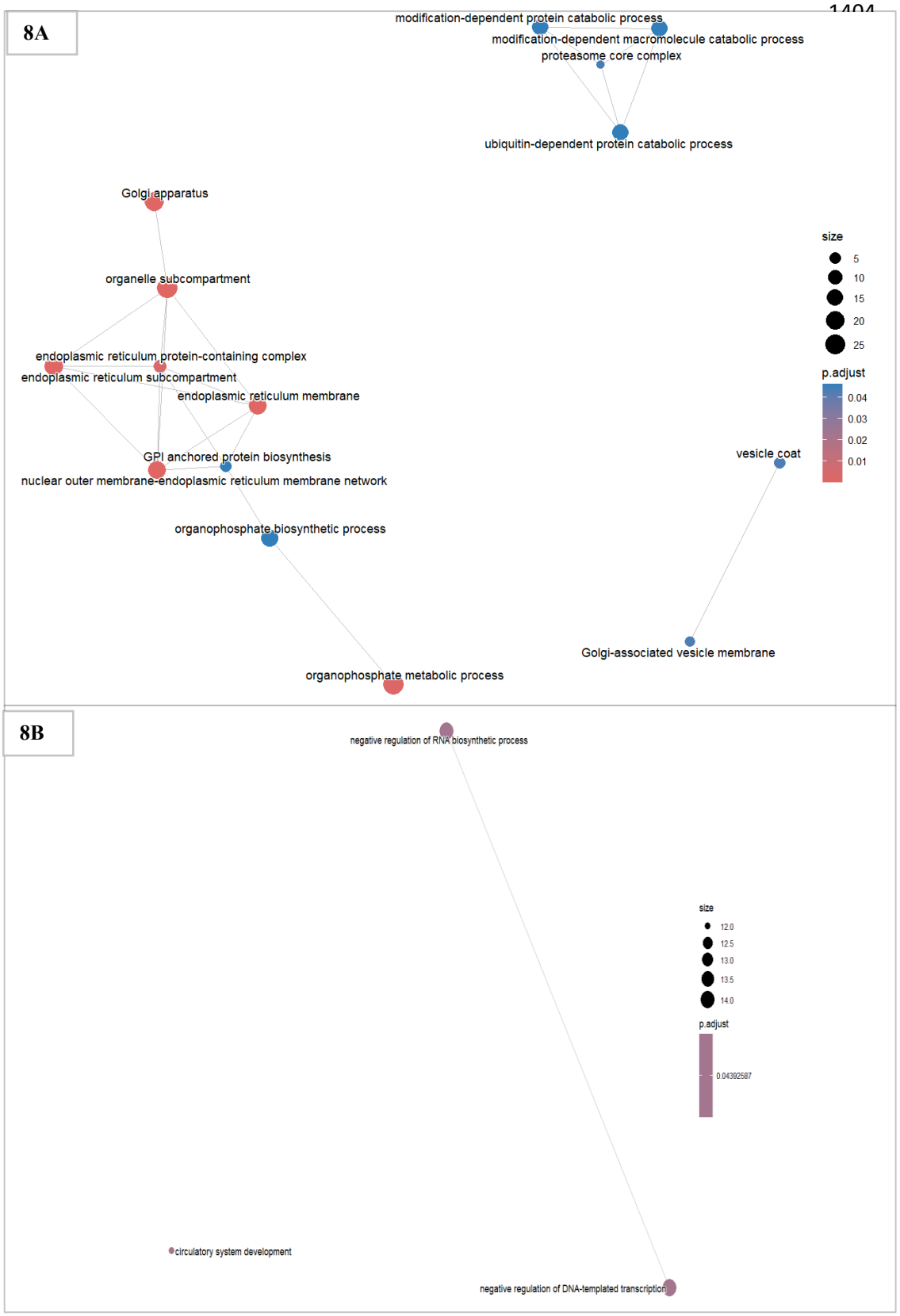

Figure 8. Integrated enrichment map of DEGs in AT+LPS vs AT+SLPS. Figure 8A: Integrated enrichment map of overexpressed genes. Figure 8B: Integrated enrichment map of suppressed genes. Nodes represent GO terms.

where lines indicate interactions between terms. and the circle (node) corresponds by size to the number of associated genes and by color to the adjusted p-value.

Analysis of the DEG network in LPS-inoculated quail revealed two distinct functional groups. The first group (Figure 9A, upper left) encompassed processes related to organophosphate metabolism and biosynthesis, including genes such as *CMPK1*, *PGD*, *HK1*, *DOLK*, *PGAP2*, *PGAP3*, *PIGH*, *PIGM*, and *PIGU*, associated with cell signaling, energy metabolism, and protein anchoring to the cell membrane, especially by GPI. In the second group (Figure 9A, lower right), ubiquitin-dependent protein catabolism processes were observed, with genes such as *PSMA1*, *RNF14*, *ITCH*, *CUL4A*, and *PSMC2*, essential for the selective degradation of proteins via proteasome, which is crucial for protein homeostasis and cellular stress response.

Figure 9B shows the network of downregulated DEGs in LPS-challenged quail. Two groups were identified. The first (top) is associated with circulatory system development, involving genes such as *VEGFC*, *FLT1*, *PTPRB*, *MEF2C*, *S1PR1*, *SOX18*, and *GATA2*, suggesting a possible impact on vascular formation due to induced systemic inflammation. The second group (bottom) is related to negative regulation of transcription and RNA biosynthetic processes, encompassing genes such as *CHD4*, *MIER1*, *THRB*, *NR2F2*, *SEMA4D*, *DNMT3A*, *CRY2*, and *BASP1*. This finding indicates a cellular functional suppression in response to thermal and immune stress. *SOX9* and *GATA2* appear in both groups, underscoring their dual relevance in the physiological response of quail.

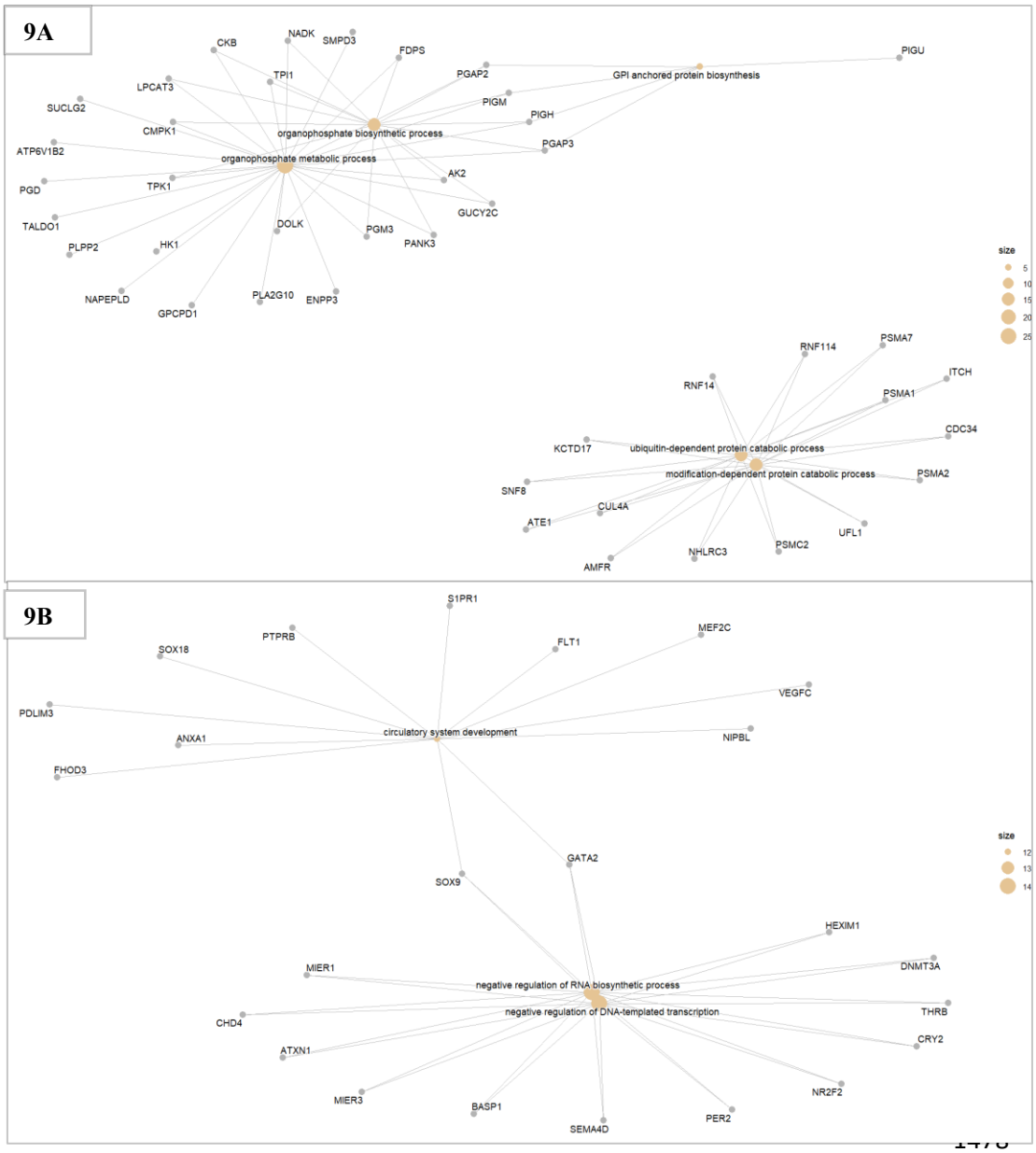

Figure 9. Network graph of DEGs in AT+LPS vs. AT+SLPS. Figure 9A: Enrichment network of overexpressed DEGs. Figure 9B: Enrichment network of suppressed DEGs. The larger orange nodes represent the GO terms; the smaller gray nodes correspond to the genes involved in the respective biological processes present in the figure. The sizes of the functional nodes are proportional to the number of associated genes. as indicated in the lateral legend. Edges connect each gene to the GO terms to which they contributed significantly in the enrichment test.

Genes modulated by LPS exposure according to incubation temperature

The effect of LPS exposure was evaluated within the different incubation temperature groups to better understand its influence on intestinal gene expression in Japanese quail. The analysis identified 20 common DEGs in LPS-challenged chicks from both thermal treatments

(control and high temperature) (Table 11), indicating a set of genes whose modulation was induced by the LPS stimulus, regardless of incubation temperature.

Among these genes, 13 were overexpressed in chicks from the control temperature and high temperature groups, in particular MMP7 (log2FC = 4.66 and 5.88, respectively), involved in the remodeling of the extracellular matrix; PI3 (protease inhibitor 3 gene), a protease inhibitor with immunoregulatory function (log2FC = 3.68 and 4.91); and SLC6A14, an amino acid transporter related to the inflammatory response (log2FC = 2.51 and 3.36). Other genes also showed consistent induction, such as IL4I1, related to modulation of immune responses, and CHRDL2, involved in cell differentiation mediated by bone morphogenetic proteins. Additionally, seven genes were suppressed, including MFN1 (mitofusin 1), related to mitochondrial dynamics (log2FC = −0.60 and −1.03); DNASE1L3, associated with extracellular DNA degradation (log2FC = −2.02 and −1.84); and ACOT12, involved in fatty acid metabolism (log2FC = −2.94 and −2.78). The consistency in the repression of these genes suggests a possible downgrade of metabolic and mitochondrial maintenance pathways in response to LPS.

These findings demonstrated that, although incubation at high temperature significantly increased the total number of genes modulated by LPS, there remains a robust and conserved core inflammatory response. This core consists of genes that were responsive to LPS under both environmental conditions and are essential for innate immunity, transport, and metabolism.

Table 11. DEGs common to CTL + LPS vs CTL + SLPS and AT + LPS vs AT + SLPS contrasts

Gene ID	Description	Log2FoldChange	
		CTL+LPS vs CTL+SLPS	AT+LPS vs AT+SLPS
Overexpressed genes			
MMP7	degrades extracellular matrix components	4.661412	5.885439
PI3	anti-inflammatory activity	3.682538	4.916192
LOC107314689	antimicrobial defense protein	3.215632	4.773523

LOC107312866	epithelial secretory protein	5.916072	4.362927
LOC107321681	involvement in the immune response	3.899021	4.192006
LOC107323109	associated with extracellular signaling	3.359889	3.923222
LOC107312882	involvement with antimicrobial function	4.918488	3.537924
SLC6A14	associated with intestinal inflammation	2.517060	3.365530
IL4I1	involved in modulating the adaptive immune response	1.986800	3.317761
CHRDL2	involved in epithelial differentiation	1.946798	3.045061
LOC107312884	extracellular matrix regulatory protein	3.899713	2.593708
LOC107306119	possible epithelial secreted protein	2.013980	2.087660
ZPLD1	involved in epithelial adhesion and integrity	2.139733	1.960277
	Suppressed genes		
MFN1	participates in mitochondrial fusion and energy homeostasis	-0.60195	-1.03524
LOC107309078	involved in mitochondrial organization	-1.21531	-1.76968
DNASE1L3	involved in apoptosis and immunity	-2.02369	-1.84935
LOC107309641	mitochondrial regulatory factor	-1.26793	-1.86782
ACOT12	involved in fatty acid metabolism and detoxification	-2.94015	-2.78039
TPPP3	related to cytoskeletal stability	-3.50452	-3.50452

Functional analysis of DEGs in KEGG

KEGG is a database used for systematic analysis of genetic functions, linking genomic and functional information. It allows categorizing a set of genes based on the metabolic pathways in which they participate or the functions they perform (Kanehisa and Goto, 2000; Feng *et al.*, 2025). The genes suppressed in quail incubated at the control temperature and inoculated with LPS, namely *GPX4* and *PTGR1* (Table 12), are related to the arachidonic acid metabolic pathway (adjusted p = 0.014367), indicating a reduction in the production of inflammatory mediators. Table 12 also lists the genes upregulated in quail incubated at high temperature and inoculated with LPS. Enrichment analysis revealed that upregulated genes were mainly associated with intracellular degradation (lysosome pathway, adjusted p = 0.018314). Additionally, pathways indicative of metabolic reprogramming were identified, involving membrane modifications and cell signaling, such as the GPI anchor biosynthesis pathway.

Table 12. KEGG analysis of the cellular process of DEGs

Contrast	Pathway	Gene	p-adjusted

CTL+LPS *vs* CTL+SLPS	**Suppressed**		
	Arachidonic acid metabolism	*GPX4/PTGR1*	0.01436
AT+LPS *vs* AT+SLPS	**Overexpressed**		
	Lysosome	*GUSB/ASAH1/CD164/ACP2/ ATP6V0C/AP1S3/HYAL1/CL TC/GNS/AP4S1/CD63*	0.01831
	Glycosylphosphatidylinositol (GPI)-anchor biosynthesis	*PIGH/PGAP3/PIGM/PIGU/ PGAP2*	0.01905

Discussion

Influence of incubation temperature on quail embryos

The results showed that high-temperature incubation significantly influenced total hatching rate (56.62% versus 68.50%) and fertile egg hatching rate (64.58% versus 74.75%). Accordingly, previous research has shown that an increase in temperature during incubation can impact embryo survival and hatchability (Lin *et al.*, 2017; Abdelfattah, 2019; Carvalho *et al.*, 2020; Yalcin; Sezen; Shah, 2022). The observed reduction in hatching rate can be attributed to heat stress induced by high temperature, which affects physiological processes critical to embryonic development, such as respiration, osmotic regulation, and energy metabolism (Lourens et al., 2007). Thermal stress is known to alter gas exchange through the eggshell, leading to hypoxia and metabolic acidosis, factors that can increase embryonic mortality, especially in the final stages of incubation (Jimoh et al., 2023). Thus, the lower hatching rate observed in the high-temperature group suggests that embryos experienced difficulties adapting to the adverse thermal condition imposed during development.

On the other hand, despite the effect on hatching rates, no significant differences ($p > 0.05$) were observed in the morphological or physiological parameters of the surviving embryos, including intestine length, embryo weight, egg weight, yolk sac weight, and yolk sac utilization. These findings indicate that, although the high incubation temperature reduced hatching success, surviving embryos exhibited morphological traits comparable to those

incubated under control conditions. Similar results were reported by Carvalho *et al.* (2020), who observed that embryos exposed to thermal variations during incubation had higher mortality; however, among survivors, there were no significant differences in body weight. This pattern may be explained by natural selection imposed by thermal stress, where only the most resilient embryos complete development, retaining morphological traits similar to those of individuals not exposed to the stressor.

Furthermore, the lack of differences in yolk sac utilization suggests that embryo metabolism and nutrient absorption were not significantly affected by high temperature (Van *et al.*, 2020), highlighting that thermal stress primarily impacted hatching rates rather than the morphometry of surviving embryos.

Effect of incubation temperature and immune stress on chicks

LPS inoculation significantly impacted ($p < 0.05$) variables associated with the immune response of quail chicks, particularly with regard to the spleen. The higher absolute and relative weights of the spleen (0.054 g and 0.052%, respectively) among Japanese quail inoculated with LPS may reflect immune system activation. The spleen plays a central role in the innate and adaptive immune response of birds (John, 1994). LPS, a component of the cell wall of Gram-negative bacteria, is a potent immunomodulatory agent capable of inducing systemic inflammatory responses, leading to hypertrophy of lymphoid organs, such as the spleen (Scanes, 2020).

Interestingly, no significant changes in absolute or relative weight of the heart, as well as body weight or intestine length, were found in LPS-challenged chicks. These results suggest that although the immune challenge promoted specific alterations in the spleen, it did not

produce enough systemic impact to affect overall morphological development or alter cardiovascular or intestinal traits.

Incubation temperature did not significantly affect ($p>0.05$) the growth performance of quail chicks. Parameters such as absolute and relative weights of the heart and spleen, body weight, and intestine length were similar between chicks incubated at control or high temperatures. Although elevated incubation temperature reduced the hatching rate, as previously demonstrated, no detectable or latent effects on the physiological performance of chicks were observed up to the post-hatch evaluation. Similar findings were reported by Berntsen and Bech (2021), who observed no changes in morphological development or long-term effect on basal metabolic rate in birds exposed to adverse thermal conditions during incubation.

Effect of LPS challenge on the jejunum of Japanese quail subjected to control temperature during egg incubation

LPS inoculation induced the differential expression of 41 genes in the jejunum of Japanese quail, with a balanced distribution between overexpressed (22) and suppressed (19) genes. This pattern reflects a functional equilibrium between immune activation and modulation, with each molecular component contributing specifically to the physiological context of the intestinal tissue.

The immune response in the jejunum demonstrated sophisticated self-limiting strategies aimed at containing collateral damage to the intestinal epithelium. One of the main elements of this regulation was *IL1R2* (adjusted $p = 0.0300$), expressed in goblet cells (Li *et al.*, 2023). Its overexpression has been described as a marker of infection by Gram-negative bacteria, as observed in various animal models challenged with LPS, such as mice and wild ducks (Lang *et*

al., 2016; Jax *et al.*, 2021; Kim; Lee, 2024). Additionally, *IL18BP* (adjusted $p = 0.0300$), of the immunoglobulin family (Wang, 2024), was also significantly overexpressed. Studies in murine models have shown that its administration under inflammatory conditions contributes to the reduction of exacerbated immune activity (Novick *et al.*, 1999; Harms *et al.*, 2017).

The gene *S100A12* (adjusted $p = 0.0489$) deserves mention among the overexpressed genes, being previously described as a marker of epithelial and leukocyte activation in different contexts of intestinal inflammation (Chiou *et al.*, 2016; Ronaldo *et al.*, 2020; Yang *et al.*, 2001; Singh; Rai; Agrawal, 2022; Wang *et al.*, 2023). The upregulation of *PDCD1LG2* (adjusted $p = 0.0489$) highlights the involvement of lymphocyte modulation mechanisms in jejunal tissue. Its participation has been described in infectious contexts and humoral responses, with a potential role in inflammatory containment (Tanaka *et al.*, 2018; Chen *et al.*, 2014). Additionally, *ZPLD1* (adjusted $p = 0.0489$) exhibited increased expression; its previously reported association with intestinal epithelial barrier homeostasis in mice (Vijayakumar *et al.*, 2019) suggests a role in tissue responses to inflammatory stress.

The observed changes also indicate metabolic reprogramming in enterocytes. The suppression of *GPD1* (adjusted $p = 0.00516$) suggests modulation of energy metabolism, as described by Oh *et al.* (2024) and Kishimoto *et al*. (2021), potentially reflecting an adaptation to the inflammatory microenvironment. Similarly, *SAMHD1* (adjusted $p = 0.0161$) was downregulated; its inactivation has been associated with increased genomic vulnerability and cell apoptosis under stress conditions (Eudald *et al.*, 2022; Rentoft *et al.*, 2016).

Modulation of mitochondrial transporters was also observed. The downregulation of *SLC25A13* and *SLC25A15* (adjusted $p = 0.0383$) suggests an impact on energy metabolism and mitochondrial activity, as described by Chen *et al*. (2019), Ryan and Luke (2017), and Zhang *et al.* (2023). These changes align with the metabolic reprogramming typical of inflammation

(Warburg effect) (Kurmi; Haigis, 2020). By contrast, genes involved in the transport and utilization of alternative substrates were upregulated. The overexpression of *SLC5A12* (adjusted $p = 0.0406$) and *SLC13A1* (adjusted $p = 0.0406$) indicates compensatory strategies for metabolic support and antioxidant protection against inflammatory challenge (Petersen *et al.*, 2022; Barnes *et al.*, 2017).

Figure 6A shows the significant integration between terms related to extracellular components, indicating a coordinated activation of structures involved in intercellular transport and communication, especially via exosomes, potentially modulating inflammatory and immune signals. Figure 6B, on the other hand, reveals functional interconnection between nucleotide metabolism pathways, suggesting a coordinated inactivation of these pathways in the face of inflammatory challenge, possibly aimed at energy conservation and adaptation to stress.

In Figure 7A, genes such as *S100A12* are associated with extracellular vesicle release and immune modulation, whereas *PDCD1LG2* and *ZPLD1* indicate participation in cell recognition and adaptive immune signaling. Finally, Figure 7B highlights suppressed genes, such as *SLC25A15*, *SLC25A13*, and *GPD1*, which are essential for metabolite transport and mitochondrial energy metabolism. The pattern suggests a prioritization of immune functions over metabolic activity in response to the inflammatory stimulus. Overall, this functional dissociation reflects a potential redirection of cellular metabolism during the inflammatory response.

Effect of LPS challenge on Japanese quail subjected to high temperature during egg incubation

Analysis of gene expression in the gut of Japanese quail incubated at high temperature and inoculated with LPS revealed a coordinated modulation of genes associated with

inflammatory processes, cellular stress, metabolism, and maintenance of epithelial homeostasis. The significant expression of *PLA2G10* (adjusted $p = 0.00220$) highlights the importance of arachidonic acid in the response to combined stress, corroborating previous studies that identified this phospholipase as a mediator of fatty acid release during inflammatory processes (Jurivich *et al.*, 1996; Curfs *et al.*, 2008). In parallel, *NAPEPLD* activation (adjusted $p = 0.00220$) indicates the involvement of endogenous anti-inflammatory endocannabinoid pathways (Lefort *et al.*, 2020). Upregulation of *BACE1* (adjusted $p < 0.0000$) is also noteworthy. The gene plays a role in intestinal inflammation and is associated with angiogenesis, immunological and antimicrobial properties, and inflammatory response in macrophages, as recently elucidated (Taylor *et al.*, 2022).

The activation patterns of *AP1S3*, *ZDHHC6*, and *ZDHHC9* (adjusted $p = 0.0004$) suggest active remodeling of membrane microdomains during inflammation (Mahil *et al.*, 2016; Shimell *et al.*, 2019; Salaun; Tomkinson; Chamberlain, 2023). This mechanism seems to be amplified by the positive co-regulation of *MAGT1* and *MMGT1* (adjusted $p < 0.0000$), consistent with their role as key signaling modulators of immune cells (Matsuda-Lennikov *et al.*, 2019), particularly in lymphocyte activation (Goytain; Quamme, 2008).

Transcriptional analysis also revealed the reprogramming of lipid metabolism in the gut of Japanese quail, possibly aimed at maintaining mucosal integrity under adverse conditions. Activation of *LPCAT3*, *GPCPD1*, *SMPD3*, and *PLPP2* (adjusted $p = 0.00220$), together with *MOGAT1* and *KDSR* (adjusted $p < 0.0000$), demonstrates an integrated response to maintain lipid homeostasis under adverse conditions (Garoby-Salom *et al*., 2014; Liss *et al*., 2018; Lutkewitte *et al.*, 2019; Reed *et al*., 2022; Tang *et al*., 2022; Adam *et al*., 2024; Chen *et al*., 2024). Similarly, Sedghi *et al.* (2024) identified the importance of *LPCAT3* in preserving membrane fluidity during inflammatory processes in poultry.

The expression pattern of *ARV1* (adjusted $p < 0.0000$) underscores the importance of cholesterol homeostasis, confirming previous observations about its role in the vesicular transport of sterols (Palmer *et al.*, 2016). The positive regulation of *TMBIM1* (adjusted $p = 0.0004$) and *ATP11C* (adjusted $p = 0.0004$) elucidates mechanisms of cellular protection against endoplasmic reticulum stress and ionic imbalances, as described in studies with mammalian models (Doycheva *et al.*, 2019).

The identified expression patterns also indicated the reprogramming of intestinal energy metabolism. The significant induction of *SPDF* (adjusted $p = 0.00220$) and *PGD* and *TALDO1* (adjusted $p = 0.00220$) indicates activation of the pentose-phosphate pathway, suggesting an increase in the production of NADPH and ribose-5-phosphate to meet the demands of cell biosynthesis under adverse conditions (Lin *et al.*, 2015). Together, the glycolytic enhancement evidenced by the expression of *HK1* and *TPI1* (adjusted $p = 0.00220$) reveals the prioritization of rapid ATP production. Accordingly, the concomitant activation of *SUCLG2* (adjusted $p = 0.00220$) indicates efficient coupling between glycolysis and the Krebs cycle, ensuring the continuous flow of metabolic intermediates (Hu *et al.*, 2023). The coordinated activation of genes such as *AK2*, *CMPK1*, *PANK3*, *TPK1*, *CKB*, and *NADK* (adjusted $p = 0.00220$) is related to the regulation of critical cofactors. According to previous studies, these genes act to maintain cellular energy homeostasis, ensuring the continuous availability of ATP, CoA, and NAD^+, even under stress conditions (Suzuki *et al.*, 2004; Uda *et al.*, 2006; Elbow; Manoel, 2020).

The adaptive response of the endoplasmic reticulum was demonstrated by the activation of *PGM3* (adjusted $p = 0.0462$) and *DOLK* (adjusted $p = 0.00220$). These genes, associated with the *N*-glycosylation pathway, are essential for protein modification under cellular stress (Yang *et al.*, 2024). Induction of GPI anchor synthesis genes (*PIGH*, *PGAP2*, *PGAP3*, *PIGM*,

and *PIGU*, adjusted $p = 0.00220$) suggests structural adaptation of cell membranes, which is crucial for the maintenance of cell signaling under adverse conditions (Naseer *et al*., 2016; Nguyen *et al*., 2018; Farooqi *et al*., 2023; Torres *al*., 2024). Genes related to protein quality control, such as *ERLIN1*, *ERLIN2*, and *TMCO1* (adjusted $p < 0.0000$), are involved in the degradation of poorly coiled receptors, functioning as a negative feedback mechanism to control the inflammatory response (Wang *et al.*, 2016). Protein translocation and folding machinery were also activated, as demonstrated by the increased expression of *OSTC*, *SRPRB*, and *SSR1* (adjusted $p < 0.0000$).

The ubiquitin-proteasome system was significantly activated, as indicated by the upregulation of proteasomal subunits *PSMA1*, *PSMA2*, *PSMA7*, and *PSMC2* (adjusted $p = 0.0462$). This response likely reflects an adaptation to the accumulation of misfolded proteins arising from cellular stress (Hershko; Ciechanover, 1998). Such a pattern aligns with the classical proteotoxic stress response, in which the ubiquitin-proteasome system serves as the primary protein quality control system (Tanaka, 2009). The coordinated expression of multiple E3 ligases, including *ITCH*, *RNF114*, *RNF14*, *CDC34*, *CUL4A*, *AMFR*, *UFL1*, *ATE1*, *KCTD17*, *SNF8*, and *NHLRC3* (adjusted $p = 0.0462$), suggests the activation of selective mechanisms for recognizing and labeling damaged proteins (Chiu *et al*., 2008; Cocklin *et al*., 2011; Han *et al*., 2013; Ingham *et al*., 2014; Hannah; Zhou, 2015; Kashina, 2015; Mentrup *et al*., 2017; Nakajima; Raz, 2020; Yang *et al*., 2022; Wolfe *et al*., 2022; Shin *et al*., 2023; Brugger *et al*., 2024).

In the intracellular transport axis, components of the clathrin-coated vesicle complex and proteins associated with vesicular traffic were activated (adjusted $p < 0.0004$), including *COPG1*, *COPE*, *SEC13*, *GOSR1*, *SCAMP2*, *RAB14*, *NSF*, and *ARL1*. This response suggests an intense reorganization of the endomembrane system, possibly aiming to increase the

transport capacity of essential components such as proteins and lipids and facilitate the removal of damaged proteins (Junutula *et al*., 2004; Torres; Rosa-Ferreira; Munro, 2014; Niu *et al*., 2014; Chen *et al*., 2021; Liu *et al*., 2023). In parallel, activation of genes of the Golgi apparatus, namely *COG3*, *SLC35A1*, *TBC1D23*, *TRAPPC5*, and *ARL1* (adjusted $p < .00001$), indicates a specific adaptation of this organelle, crucial for post-translational modification processes (Ma *et al*., 2020; Liu *et al*., 2024; Papaioannou *et al*., 2023; Liu *et al*., 2025).

Regarding epithelial homeostasis, genes associated with preservation of the intestinal barrier were activated, including *GUCY2C*, *ATP6V1B2*, *LMF2*, *GLG1*, *NCLN*, *MYRFL*, *XPR1*, and *ENPP3* (adjusted $p < 0.0020$). Concomitantly, some components of the immune response were downregulated, such as *SASH3*, *SYK*, and *DOCK8* and inflammatory modulators *HRH1* and *ANXA1* (adjusted $p = 0.04390$) (Mocsai; Ruland; Victor, 2010; Wang *et al.*, 2015; Li; Richardson, 2016; Novoa *et al.*, 2017; Han *et al.*, 2020; Borza *et al.*, 2021; Renan *et al.*, 2023; Chen *et al.*, 2025).

The analysis revealed the suppression of genes related to angiogenesis (*VEGFC*, *FLT1*, *PTPRB*, *SOX18*, *PLXNA2*, and *S1PR1*, adjusted $p = 0.04390$), indicating impaired intestinal vascularization, which could limit tissue perfusion and nutrient delivery (Duffy; Bouchier-hayes; Harmey, 2015; Olbromski; Okołów; Dzięgiel, 2018; Zhao *et al*., 2018; Weng *et al*., 2019; Winfree *et al*., 2024; Wang *et al*., 2024). Epithelial differentiation and renewal could also be affected with the suppression of essential transcription factors, such as *MEF2C*, *GATA2*, *SOX9*, *NR2F2*, *THRB*, and *BASP1* (adjusted $p = 0.04390$). These findings corroborate previous research showing that these genes regulate intestinal epithelial homeostasis (Symon; Harley, 2017; Wang *et al.*, 2019; Moorhouse *et al.*, 2022; Iris; Pater; Zhang, 2023; Rehman *et al.*, 2023; Ward; Sjulson; Batista-Brito, 2024). Some epigenetic genes were also suppressed, including *CHD4*, *MIER1*, *MIER3*, *DNMT3A*, *ATXN1*, *HEXIM1*, and *NIPBL* (adjusted $p = 0.04390$),

which indicates a profound impact on transcriptional plasticity, possibly compromising the adaptive capacity of intestinal cells (Didonna *et al.*, 2020; Lv *et al.*, 2023; Yan; Liu; Yuan, 2024).

Circadian regulation was also significantly affected, as evidenced by suppression of *PER2* and *CRY2* (adjusted $p = 0.04390$). These genes are central components of the circadian molecular oscillator, and their dysregulation can impact several physiological processes, including intestinal motility and nutrient absorption (Chang *et al.*, 2019; Sokolowska *et al.*, 2020; Wiertsema *et al.*, 2021; Tobias; Sadiq, 2022). In poultry, disturbance of the circadian rhythm is consistently associated with reductions in weight gain and feed efficiency (Helm; Greives; Zeman, 2024).

Finally, the reduced expression of genes involved in neuroimmune communication, namely *SLITRK6* and *SEMA4D* (adjusted $p = 0.04390$), and cytoskeleton organization, such as *PDLIM3* and *FHOD3* (adjusted $p = 0.04390$), points to disturbances in the integration between the enteric nervous system and immune system (Smith *et al.*, 2014; Mir *et al.*, 2023), as well as in the maintenance of epithelial architecture (Wu *et al.*, 2021). Such alterations may have significant implications for intestinal function, potentially compromising from epithelial barrier integrity to local immune response.

Inflammatory response to LPS, regardless of incubation temperature

A total of 19 genes were expressed in LPS-challenged chicks from both incubation groups. Among the overexpressed genes (13 genes), *MMP7* deserves mention, as it is involved in inflammatory processes, and was detected with high expression levels (log2FC = 4.66 and 5.88) in both treatments (Liao *et al.*, 2021). Similarly, *PI3*, related to immune regulation, showed strong induction (log2FC = 3.68 and 4.91) (Cao *et al.*, 2020). Another highly expressed

gene was *SLC6A14*, associated with metabolism. It was highly expressed (log2FC = 2.51 and 3.36) in chicks from both groups (Ahmadi *et al.*, 2018). Genes such as *IL4I1*, related to immune response (Sadik *et al.*, 2020), and *CHRDL2*, involved in cell signaling (Wang *et al.*, 2022), exhibited increased expression.

Among the genes suppressed in LPS-challenged chicks incubated at control and high temperatures (7 genes), the following deserve mention: *MFN1*, related to mitochondrial function (log2FC = −0.60 and −1.03) (Alghamdi, 2024); *DNASE1L3*, involved in DNA degradation (log2FC = −2.02 and −1.84) (Chan *et al.*, 2020); and *ACOT12*, related to lipid metabolism (log2FC = −2.94 and −2.78) (Lu *et al.*, 2019).

The fact that these genes were modulated in chicks from both incubation treatments (control and high temperature) demonstrates the presence of a conserved functional core of inflammatory response to LPS. This core encompasses genes that are critical for innate immunity, solute transport, and metabolic regulation. The findings underscore that, although high incubation temperatures may increase the total number of modulated genes, LPS exposure alone is sufficient to activate an essential set of biological responses that remain stable even under adverse physiological conditions.

KEGG pathways modified by LPS exposure and incubation temperature

Comparative analysis of quail chicks incubated at the control temperature and later inoculated with LPS revealed the negative regulation of the arachidonic acid metabolic pathway (adjusted p = 0.014367), with suppression of *GPX4* and *PTGR1*. This pathway is directly involved in the production of pro-inflammatory eicosanoids, such as prostaglandins and leukotrienes (Higgins; Lees, 1984; Wang *et al.*, 2021). Such repression suggests a negative

modulation of the biosynthesis of inflammatory lipid mediators, which may represent an adaptive response of inflammation containment triggered by the immune challenge.

By contrast, in quail chicks subjected to high temperature during incubation and later challenged with LPS, positive changes in gene expression were observed in pathways associated with catabolic processes and cell restructuring. The lysosome pathway was enriched (adjusted p = 0.018314), and a set of genes was activated, including *GUSB*, *ASAH1*, *CD164*, *ACP2*, *ATP6V0C*, *AP1S3*, *HYAL1*, *CLTC*, *GNS*, *AP4S1*, and *CD63*. These genes are involved in the degradation of cellular components, macromolecule recycling, and response to intracellular damage, suggesting an intensification of lysosomal activity as an adaptation mechanism to heat and inflammatory stress.

Additionally, the GPI anchor biosynthesis pathway was enriched (adjusted p = 0.019050), with increased expression of *PIGH*, *PGAP3*, *PIGM*, *PIGU*, and *PGAP2*. These lipid anchors are responsible for attaching proteins to the outer face of the plasma membrane, playing a central role in the modulation of cell signaling, adhesion, and intercellular recognition (Paulick; Bertozzi, 2008). Activation of this pathway suggests reconfiguration of cell membrane architecture and functional reorganization of intestinal cells as part of an adaptive response to challenges imposed by high-temperature incubation and inflammation.

Conclusion

The results of this study demonstrate that high incubation temperature exerts significant impacts on embryonic development by reducing hatching rates. Nevertheless, embryos that complete development under these adverse conditions display morphological and physiological traits comparable to those incubated at control temperatures, suggesting a selective process that favors more resistant individuals.

By contrast, immune challenge with LPS elicited a coordinated inflammatory response in the quail gut, with activation of genes involved in immunomodulation, energy metabolism, and tissue repair. Notably, the combination of high incubation temperature and LPS exposure resulted in the suppression of genes associated with immune response, angiogenesis, and cell differentiation, indicating a possible limitation of intestinal adaptive capacity. However, this constraint was not accompanied by detectable phenotypic alterations, suggesting that the observed effects reflect molecular adjustments that do not cause functional impairment. A core set of inflammatory genes was consistently modulated by LPS exposure, regardless of incubation temperature, underscoring the existence of conserved pathogen-response pathways. These findings highlight the complex interplay between thermal stress and inflammation during embryonic development and provide novel insights into the mechanisms underlying immune resistance and intestinal programming in birds.

References

ABDELFATTAH, M. Effect of thermal manipulation during incubation and spraying japanese quail eggs with ascorbic acid on embryogenesis and phsiological responses of hatch chicks. **Egyptian Poultry Science**, v. 39, n. 2, p. 479–499, 30 jun. 2019. DOI: 10.21608/epsj.2019.39281

ABEYWANSHA; HUANG, W.; YE, X.; NAWROCKI, A.; LAN, X.; JANKOWSKY, E.; TAYLOR, D. J.; ZHANG, Y. The structural basis of tRNA recognition by arginyl-tRNA-protein transferase. **Nature Communications**, v. 14, n. 1, 19 abr. 2023. DOI: https://doi.org/10.1038/s41467-023-38004-8

ADAM, S. Y. *et al.* Dietary Organic Zinc Supplementation Modifies the Oxidative Genes via RORγ and Epigenetic Regulations in the Ileum of Broiler Chickens Exposed to High-Temperature Stress. **Antioxidants**, v. 13, n. 9, p. 1079, 4 set. 2024. DOI: https://doi.org/10.3390/antiox13091079

AHMADI, S.; XIA, S.; WU, Y.-S.; PAOLA, M. D.; KISSOON, R.; LUK, C.; LIN, F.; DU, K.; ROMMENS, J.; BEAR, C. E. SLC6A14, an amino acid transporter, modifies the primary CF defect in fluid secretion. **eLife**, v. 7, 13 jul. 2018. DOI: https://doi.org/10.7554/eLife.37963

AL AMAZ, S.; MISHRA, B. Embryonic thermal manipulation: a potential strategy to mitigate heat stress in broiler chickens for sustainable poultry production. **Journal of Animal Science**

and Biotechnology BioMed Central Ltd, 1 dez. 2024. DOI: https://doi.org/10.1186/s40104-024-01028-1

ALGHAMDI, A. A detailed review of pharmacology of MFN1 (mitofusion-1)-mediated mitochondrial dynamics: Implications for cellular health and diseases. **Saudi Pharmaceutical Journal**, v. 32, n. 4, p. 102012, abr. 2024. DOI: https://doi.org/10.1016/j.jsps.2024.102012

ALLMANN, S. *et al.* Cytosolic NADPH Homeostasis in Glucose-starved Procyclic Trypanosoma brucei Relies on Malic Enzyme and the Pentose Phosphate Pathway Fed by Gluconeogenic Flux. **Journal of Biological Chemistry**, v. 288, n. 25, p. 18494–18505, jun. 2013. DOI: https://doi.org/10.1074/jbc.M113.462978

ARASHIKI, N.; NIITSUMA, K.; SEKI, M.; TAKAKUWA, Y.; NAKAMURA, F. ATP11C T418N, a gene mutation causing congenital hemolytic anemia, reduces flippase activity due to improper membrane trafficking. **Biochemical and Biophysical Research Communications**, v. 516, n. 3, p. 705–712, ago. 2019. DOI: https://doi.org/10.1016/j.bbrc.2019.06.092

ARONSON, B. E.; STAPLETON, K. A.; KRASINSKI, S. D. Role of GATA factors in development, differentiation, and homeostasis of the small intestinal epithelium. **AJP Gastrointestinal and Liver Physiology**, v. 306, n. 6, p. G474–G490, 17 jan. 2014. DOI: 10.1152/ajpgi.00119.2013

BAO, P.; KODRA, A.; MARJANA TOMIC-CANIC; GOLINKO, M. S.; EHRLICH, H. P.; BREM, H. The Role of Vascular Endothelial Growth Factor in Wound Healing. **Journal of Surgical Research**, v. 153, n. 2, p. 347–358, 13 maio 2008. DOI: 10.1016/j.jss.2008.04.023
BARNES, S. K.; EIBY, Y. A.; LEE, S.; LINGWOOD, B. E.; DAWSON, P. A. Structure, organization and tissue expression of the pig SLC13A1 and SLC13A4 sulfate transporter genes. **Biochemistry and Biophysics Reports**, v. 10, p. 215–223, 13 abr. 2017. DOI: 10.1016/j.bbrep.2017.04.005

BENJAMINI, Y.; HOCHBERG, Y. Controlling the False Discovery Rate: A Practical and Powerful Approach to Multiple Testing, **Journal of the Royal Statistical Society: Series B (Methodological)** 57: 289-300., 1995. DOI: https://doi.org/10.1111/j.2517-6161.1995.tb02031.x

BERNTSEN, H. H.; BECH, C. Incubation temperature and physiological aging in the zebra finch. **PLoS ONE**, v. 16, n. 11, p. e0260037–e0260037, 29 nov. 2021. DOI: https://doi.org/10.1371/journal.pone.0260037

BI, S.; QU, Y.; SHAO, J.; ZHANG, J.; LI, W.; ZHANG, L.; NI, J.; CAO, L. Ginsenoside Rg3 Ameliorates Stress of Broiler Chicks Induced by Escherichia coli Lipopolysaccharide. **Frontiers in Veterinary Science**, v. 9, 8 abr. 2022. DOI: 10.3389/fvets.2022.878018

BIGGS, C. M.; SEVGI KELES; CHATILA, T. A. DOCK8 deficiency: Insights into pathophysiology, clinical features and management. **Clinical Immunology**, v. 181, p. 75–82, 16 jun. 2017. DOI: 10.1016/j.clim.2017.06.003

BLACKMORE, T. M.; MERCER, C. F.; PATERNO, G. D.; GILLESPIE, L. L. The transcriptional cofactor MIER1-beta negatively regulates histone acetyltransferase activity of the CREB-binding protein. **BMC Research Notes**, v. 1, n. 1, p. 68, 2008. DOI: 10.1186/1756-0500-1-68

BORZA, R.; SALGADO-POLO, F.; MOOLENAAR, W. H.; ANASTASSIS PERRAKIS. Structure and function of the ecto-nucleotide pyrophosphatase/phosphodiesterase (ENPP) family: Tidying up diversity. Journal of Biological Chemistry, v. 298, n. 2, p. 101526–101526, 24 dez. 2021. DOI: https://doi.org/10.1016/j.jbc.2021.101526

BOURGON, R.; GENTLEMAN, R.; HUBER, W. Independent filtering increases detection power for high-throughput experiments. **Proceedings of the National Academy of Sciences of the United States of America**, v. 107, n. 21, p. 9546-9551, 2010. DOI: https://doi.org/10.1073/pnas.0914005107

BRUGGER, M. *et al.* Bi-allelic variants in SNF8 cause a disease spectrum ranging from severe developmental and epileptic encephalopathy to syndromic optic atrophy. **The American Journal of Human Genetics**, v. 111, n. 3, p. 594–613, mar. 2024.

BUSHNELL, B. **BBTools**: a suite of fast, multithreaded bioinformatics tools designed for analysis of DNA and RNA sequence data. 2023. Software version 39.06. Disponível em: http://sourceforge.net/projects/bbmap.

CAI, J. *et al.* TMBIM1 promotes proliferation and attenuates apoptosis in glioblastoma cells by targeting the p38 MAPK signalling pathway. **Translational Oncology**, v. 19, p. 101391, maio 2022. https://doi.org/10.1016/j.tranon.2022.101391

CAO, F.; WEERD, S. DE; CHEN, D.; ZWINDERMAN, M. R. H.; WOUDEN, P. E. VAN DER; DEKKER, F. J. Induced protein degradation of histone deacetylases 3 (HDAC3) by proteolysis targeting chimera (PROTAC). **European Journal of Medicinal Chemistry**, v. 208, p. 112800, dez. 2020. DOI: 10.1016/j.ejmech.2020.112800

CARLSON, M. **org.Gg.eg.db: Genome wide annotation for Gallus gallus**. Bioconductor, 2019. Disponível em: https://bioconductor.org/packages/org.Gg.eg.db/.

CARPENTIERI, G. *et al.* Dominantly acting variants in ATP6V1C1 and ATP6V1B2 cause a multisystem phenotypic spectrum by altering lysosomal and/or autophagosome function. **Human Genetics and Genomics Advances**, v. 5, n. 4, p. 100349, out. 2024. DOI: https://doi.org/10.1016/j.xhgg.2024.100349

CARVALHO, A. V.; CHRISTELLE HENNEQUET-ANTIER; CROCHET, S.; BORDEAU, T.; COUROUSSÉ, N.; CAILLEAU-AUDOUIN, E.; PASCAL CHARTRIN; DARRAS, V. M.; ZERJAL, T.; COLLIN, A.; COUSTHAM, V. Embryonic thermal manipulation has short and long-term effects on the development and the physiology of the Japanese quail. **PLoS ONE**, v. 15, n. 1, p. e0227700–e0227700, 23 jan. 2020. DOI: https://doi.org/10.1371/journal.pone.0227700

CHAN, R. W. Y. *et al.* Plasma DNA Profile Associated with DNASE1L3 Gene Mutations: Clinical Observations, Relationships to Nuclease Substrate Preference, and In Vivo Correction. **The American Journal of Human Genetics**, v. 107, n. 5, p. 882–894, nov. 2020. DOI: https://doi.org/10.1016/j.ajhg.2020.09.006

CHANG, A.-M. *et al.* Chronotype Genetic Variant in PER2 is Associated with Intrinsic Circadian Period in Humans. **Scientific Reports**, v. 9, n. 1, 29 mar. 2019. DOI: https://doi.org/10.1038/s41598-019-41712-1

CHAUDHARY, A.; MISHRA, B. Systemic effects of heat stress on poultry performances, transcriptomics, epigenetics and metabolomics, along with potential mitigation strategies. **World's Poultry Science Journal Taylor and Francis Ltd**., 2024. DOI: 10.1080/00439339.2024.2364884

CHEN, C.; TSENG, C.; CHO, J. J.; LEE, Y.; KAO, C.; CHENG, Y.; HONG, Y.; CHO, C. Heat shock induces expression of OSTC/DC2, a novel subunit of oligosaccharyltransferase, *in vitro* and *in vivo*. **The Kaohsiung Journal of Medical Sciences**, v. 30, n. 5, p. 219–223, 2 mar. 2014. DOI: https://doi.org/10.1016/j.kjms.2014.01.003

CHEN, J.-L.; ZHANG, Z.-H.; LI, B.-X.; CAI, Z.; ZHOU, Q.-H. Bioinformatic and functional analysis of promoter region of human SLC25A13 gene. **Gene**, v. 693, p. 69–75, 30 jan. 2019. DOI: https://doi.org/10.1016/j.gene.2019.01.023

CHEN, L.; HE, J.; WANG, M.; SHE, J. Structure and function of human XPR1 in phosphate export. **Nature Communications**, v. 16, n. 1, 26 mar. 2025. DOI: https://doi.org/10.1038/s41467-025-58195-6

CHEN, S. *et al.* Role of Gpcpd1 in intestinal alpha-glycerophosphocholine metabolism and trimethylamine N-oxide production. **Journal of Biological Chemistry**, p. 107965–107965, 1 nov. 2024. DOI: 10.1016/j.jbc.2024.107965

CHEN, S.; CHEN, N.; MIAO, B.; PENG, J.; ZHANG, X.; CHEN, C.; ZHANG, X.; CHANG, L.; DU, Q.; HUANG, Y.; TONG, D. Coatomer protein COPε, a novel NS1-interacting protein, promotes the replication of Porcine Parvovirus via attenuation of the production of type I interferon. **Veterinary Microbiology**, v. 261, p. 109188–109188, 27 jul. 2021. DOI: https://doi.org/10.1016/j.vetmic.2021.109188

CHIOU, J. W.; FU, B.; CHOU, R.-H.; YU, C. Blocking the Interactions between Calcium-Bound S100A12 Protein and the V Domain of RAGE Using Tranilast. **PLoS ONE**, v. 11, n. 9, p. e0162000–e0162000, 6 set. 2016. DOI: https://doi.org/10.1371/journal.pone.0162000

CHIU, C. G.; ST-PIERRE, P.; NABI, I. R.; WISEMAN, S. M. Autocrine motility factor receptor: a clinical review. **Expert Review of Anticancer Therapy**, v. 8, n. 2, p. 207–217, fev. 2008. DOI: 10.1586/14737140.8.2.207

COCKLIN, R.; HEYEN, J.; LARRY, T.; TYERS, M.; GOEBL, M. New Insight Into the Role of the Cdc34 Ubiquitin-Conjugating Enzyme in Cell Cycle Regulation via Ace2 and Sic1. **Genetics**, v. 187, n. 3, p. 701–715, 1 mar. 2011. DOI: 10.1534/genetics.110.125302

CODO, A. C.; MANOEL, P. AK2 deficiency: An awkward tale for B cells. **Journal of Allergy and Clinical Immunology**, v. 146, n. 1, p. 74–76, 1 jul. 2020. DOI: 10.1016/j.jaci.2020.04.060

CRESPO-BARRETO, J.; FRYER, J. D.; SHAW, C. A.; ORR, H. T.; ZOGHBI, H. Y. Partial Loss of Ataxin-1 Function Contributes to Transcriptional Dysregulation in Spinocerebellar Ataxia Type 1 Pathogenesis. **PLoS Genetics**, v. 6, n. 7, p. e1001021–e1001021, 8 jul. 2010. DOI: https://doi.org/10.1371/journal.pgen.1001021

CURFS; GHESQUIERE, S. A. I.; VERGOUWE, M. N.; INGEBORG; GIJBELS, M. J. J.; GREAVES, D. R.; VERBEEK, J. S.; HOFKER, M. H.; MENNO. Macrophage Secretory Phospholipase A2 Group X Enhances Anti-inflammatory Responses, Promotes Lipid Accumulation, and Contributes to Aberrant Lung Pathology. **Journal of Biological Chemistry**, v. 283, n. 31, p. 21640–21648, 30 maio 2008. DOI: 10.1074/jbc.M710584200

DELMONTE, O. M. *et al. SASH3*variants cause a novel form of X-linked combined immunodeficiency with immune dysregulation. **Blood**, v. 138, n. 12, p. 1019–1033, 19 abr. 2021. DOI: 10.1182/blood.2020008629

DIDONNA, A. et al. Ataxin-1 regulates B cell function and the severity of autoimmune experimental encephalomyelitis. Proceedings of the National Academy of Sciences, v. 117, n. 38, p. 23742–23750, 2 set. 2020. DOI: https://doi.org/10.1073/pnas.200379811

DOBIN, A.; DAVIS, C. A.; SCHLESINGER, F.; JORG DRENKOW; ZALESKI, C.; JHA, S.; PHILIPPE BATUT; CHAISSON, M.; GINGERAS, T. R. STAR: ultrafast universal RNA-seq aligner. **Bioinformatics**, v. 29, n. 1, p. 15–21, 25 out. 2012. DOI: 10.1093/bioinformática/bts635

DOYCHEVA, D.; KAUR, H.; TANG, J.; ZHANG, J. H. The characteristics of the ancient cell death suppressor, TMBIM6, and its related signaling pathways after endoplasmic reticulum stress. **Journal of Neuroscience Research**, v. 98, n. 1, p. 77–86, maio 2019. DOI: https://doi.org/10.1002/jnr.24434

DUFFY, A. M.; BOUCHIER-HAYES, D. J.; HARMEY, J. H. **Vascular Endothelial Growth Factor (VEGF) and Its Role in Non-Endothelial Cells: Autocrine Signalling by VEGF**. Disponível em: <https://www.ncbi.nlm.nih.gov/books/NBK6482/>. Acesso em: 7 jul. 2025.

EUDALD FELIP *et al.* Modulation of DNA Damage Response by SAM and HD Domain Containing Deoxynucleoside Triphosphate Triphosphohydrolase (SAMHD1) Determines Prognosis and Treatment Efficacy in Different Solid Tumor Types. **Cancers**, v. 14, n. 3, p. 641–641, 27 jan. 2022. DOI: 10.3390/cancers14030641

FARNER, D. S. The Avian Embryo Alexis L. Romanoff. **The Auk**, v. 77, n. 3, p. 358–359, jul. 1960.

FAROOQI, N.; RAHMAN, A.; ALI, Y.; ALI, K.; MUHAMMAD; JONES, D. A.; ABDELKARIM, M.; ULLAH, F.; JALIL, F. Phylogenetic analysis of promoter regions of

human *Dolichol kinase* (DOLK) and orthologous genes using bioinformatics tools. **Open Life Sciences**, v. 18, n. 1, 1 jan. 2023. DOI: 10.1515/biol-2022-0591

FAZIO, A. *et al.* DNA methyltransferase 3A controls intestinal epithelial barrier function and regeneration in the colon. **Nature Communications**, v. 13, n. 1, 21 out. 2022. DOI: https://doi.org/10.1038/s41467-022-33844-2

FENG, Y.; LIU, J.; CHEN, X.; GUO, B.; LEI, M.; ZHU, H.; NI, Y. Changes in goose hypothalamus under different photocycles: RNA-Seq reveals new pathways and molecules. **Poultry Science**, v. 104, n. 5, p. 104883, maio 2025. DOI: https://doi.org/10.1016/j.psj.2025.104883

GAROBY-SALOM, S.; ROUAHI, M.; MUCHER, E.; AUGE, N.; SALVAYRE, R.; NEGRE-SALVAYRE, A. Hyaluronan synthase-2 upregulation protects smpd3-deficient fibroblasts against cell death induced by nutrient deprivation, but not against apoptosis evoked by oxidized LDL. **Redox Biology**, v. 4, p. 118–126, 16 dez. 2014. DOI: https://doi.org/10.1016/j.redox.2014.12.004

GENTLEMAN, R. C. *et al*. Bioconductor: open software development for computational biology and bioinformatics. **Genome Biology**, v. 5, n. 10, p. R80, 2004. DOI: https://doi.org/10.1186/gb-2004-5-10-r80

GOYTAIN, A.; QUAMME, G. A. Identification and characterization of a novel family of membrane magnesium transporters, MMgT1 and MMgT2. **American Journal of Physiology-Cell Physiology**, v. 294, n. 2, p. C495–C502, fev. 2008. DOI: https://doi.org/10.1152/ajpcell.00238.2007

GRIFFITH, O. W.; BRANDLEY, M. C.; WHITTINGTON, C. M.; BELOV, K.; THOMPSON, M. B. Comparative genomics of hormonal signaling in the chorioallantoic membrane of oviparous and viviparous amniotes. **General and Comparative Endocrinology**, v. 244, p. 19–29, 22 abr. 2016. DOI: 10.1016/j.ygcen.2016.04.017

HAN, H. L.; LIU, J.; FENG, X. J.; ZHANG, M.; LIN, Q. F.; WANG, T.; QI, S. L.; XU, T.; HUA, X. J. SSR1 is involved in maintaining the function of mitochondria electron transport chain and iron homeostasis upon proline treatment in Arabidopsis. **Journal of Plant Physiology**, v. 256, p. 153325–153325, 24 nov. 2020. DOI: https://doi.org/10.1016/j.jplph.2020.153325

HAN, J. *et al.* ZNF313 is a novel cell cycle activator with an E3 ligase activity inhibiting cellular senescence by destabilizing p21WAF1. **Cell Death and Differentiation**, v. 20, n. 8, p. 1055–1067, 3 maio 2013. DOI: https://doi.org/10.1038/cdd.2013.33

HAN, P.-F.; CHE, X.-D.; LI, H.-Z.; GAO, Y.-Y.; WEI, X.-C.; LI, P.-C. Annexin A1 involved in the regulation of inflammation and cell signaling pathways. **Chinese Journal of Traumatology**, v. 23, n. 2, p. 96–101, abr. 2020. DOI: https://doi.org/10.1016/j.cjtee.2020.02.002

HANNAH, J.; ZHOU, P. Distinct and overlapping functions of the cullin E3 ligase scaffolding proteins CUL4A and CUL4B. **Gene**, v. 573, n. 1, p. 33–45, 4 set. 2015. DOI: https://doi.org/10.1016/j.gene.2015.08.064

HARMS, R. Z.; CREER, A. J.; LORENZO-ARTEAGA, K. M.; OSTLUND, K. R.; SARVETNICK, N. E. Interleukin (IL)-18 Binding Protein Deficiency Disrupts Natural Killer Cell Maturation and Diminishes Circulating IL-18. **Frontiers in Immunology**, v. 8, 28 ago. 2017. DOI: https://doi.org/10.3389/fimmu.2017.01020

HELM, B.; GREIVES, T.; ZEMAN, M. Endocrine–circadian interactions in birds: implications when nights are no longer dark. **Philosophical Transactions of the Royal Society B: Biological Sciences**, v. 379, n. 1898, 5 fev. 2024. DOI: 10.1098/rstb.2022.0514

HERSHKO, A.; CIECHANOVER, A. THE UBIQUITIN SYSTEM. **Annual Review of Biochemistry**, v. 67, n. 1, p. 425–479, jun. 1998. DOI: https://doi.org/10.1146/annurev.biochem.67.1.425

HIGGINS, A. J.; LEES, P. The acute inflammatory process, arachidonic acid metabolism and the mode of action of anti-inflammatory drugs. **Equine Veterinary Journal**, v. 16, n. 3, p. 163–175, 1 maio 1984. DOI: 10.1111/j.2042-3306.1984.tb01893.x

HU, Q.; XU, J.; WANG, L.; YUAN, Y.; LUO, R.; GAN, M.; WANG, K.; ZHAO, T.; WANG, Y.; HAN, T.; WANG, J. SUCLG2 Regulates Mitochondrial Dysfunction through Succinylation in Lung Adenocarcinoma. **Advanced Science**, v. 10, n. 35, 30 out. 2023. DOI: https://doi.org/10.1002/advs.202303535

HUANG, W.; CHEN, J.; LIU, X.; LIU, X.; DUAN, S.; CHEN, L.; LIU, X.; LAN, J.; ZOU, Y.; GUO, D.; ZHOU, J. MIER3 induces epithelial-mesenchymal transition and promotes breast cancer cell aggressiveness via forming a co-repressor complex with HDAC1/HDAC2/Snail. **Experimental Cell Research**, v. 406, n. 1, p. 112722–112722, 6 jul. 2021. DOI: https://doi.org/10.1016/j.yexcr.2021.112722

HUBER, W. *et al*. Orchestrating high-throughput genomic analysis with Bioconductor. **Nature Methods**, v. 12, n. 2, p. 115-121, 2015. DOI: https://doi.org/10.1038/nmeth.3252

INGHAM, A. B. *et al.* RNF14 is a regulator of mitochondrial and immune function in muscle. **BMC Systems Biology**, v. 8, n. 1, 29 jan. 2014. DOI: https://doi.org/10.1186/1752-0509-8-10

IRIS; PATER, E. DE; ZHANG, W. The role of GATA2 in adult hematopoiesis and cell fate determination. **Frontiers in Cell and Developmental Biology**, v. 11, 14 nov. 2023. DOI: https://doi.org/10.3389/fcell.2023.1250827

JAX, E. *et al.* Health monitoring in birds using bio-loggers and whole blood transcriptomics. **Scientific Reports**, v. 11, n. 1, 24 maio 2021. DOI: https://doi.org/10.1038/s41598-021-

JIANG, B.; HE, Y.; ARMIN ELSLER; WANG, S.; KEATING, J. N.; SONG, J.; KEARNS, S. L.; BENTON, M. J. Extended embryo retention and viviparity in the first amniotes. **Nature Ecology & Evolution**, v. 7, n. 7, p. 1131–1140, 12 jun. 2023. DOI: 10.1038/s41559-023-02074-0

JIMOH, O. A.; DARAMOLA, O. T.; HAFSAT OLOLADE OKIN-AMINU; OJO, O. A. HSP70, adiponectin, leptin, pro-inflammatory cytokines and metabolic hormones of heat-stressed broilers fed herbal supplements. **Journal of Thermal Biology**, v. 117, p. 103681–103681, 22 ago. 2023. DOI: 10.1016/j.jtherbio.2023.103681

JOHN, J. L. The Avian Spleen: A Neglected Organ. **The Quarterly Review of Biology**, v. 69, n. 3, p. 327–351, set. 1994. DOI: 10.1086/418649

JONES, T. E. M.; YATES, B.; BRYONY BRASCHI; GRAY, K.; TWEEDIE, S.; SEAL, R. L.; BRUFORD, E. A. The VGNC: expanding standardized vertebrate gene nomenclature. **Genome biology**, v. 24, n. 1, 12 maio 2023. DOI: 10.1186/s13059-023-02957-2

JUNUTULA, J. R.; DE, A. M.; PEDEN, A. A.; ERVIN, K. E.; ADVANI, R. J.; SUZANNE; KLUMPERMAN, J.; SCHELLER, R. H. Rab14 Is Involved in Membrane Trafficking between the Golgi Complex and Endosomes. **Molecular Biology of the Cell**, v. 15, n. 5, p. 2218–2229, 9 mar. 2004. DOI: https://doi.org/10.1091/mbc.e03-10-0777

JURIVICH, D. A.; S PANGAS; QIU, L.; WELK, J. F. Phospholipase A2 triggers the first phase of the thermal stress response and exhibits cell-type specificity. **The Journal of Immunology**, v. 157, n. 4, p. 1669–1677, 15 ago. 1996. DOI: https://doi.org/10.4049/jimmunol.157.4.1669

KANEHISA, M. e GOTO, S. KEGG: Kyoto Encyclopedia of Genes and Genomes. **Nucleic Acids Research**, v. 28, n.1, p. 27-30, 2000. DOI: 10.1093/nar/28.1.27

KASHINA, A. S. Protein Arginylation: Over 50 Years of Discovery. **Methods in molecular biology**, p. 1–11, 1 jan. 2015. DOI: https://doi.org/10.1007/978-1-4939-2935-1_1

KATO, S. *et al.* Semaphorin 4D, a lymphocyte semaphorin, enhances tumor cell motility through binding its receptor, plexinB1, in pancreatic cancer. **Cancer Science**, v. 102, n. 11, p. 2029–2037, 4 ago. 2011. DOI: 10.1111/j.1349-7006.2011.02053.x

KIM, D. H.; LEE, W.-W. IL-1 Receptor Dynamics in Immune Cells: Orchestrating Immune Precision and Balance. **Immune Network**, v. 24, n. 3, 1 jan. 2024. DOI: https://doi.org/10.4110/in.2024.24.e21

KISHIMOTO, T.; TETSUO MIOKA; ITOH, E.; WILLIAMS, D. E.; ANDERSEN, R. J.; TANAKA, K. Phospholipid flippases and Sfk1 are essential for the retention of ergosterol in the plasma membrane. **Molecular Biology of the Cell**, v. 32, n. 15, p. 1374–1392, 26 maio 2021. DOI: 10.1091/mbc.E20-11-0699

KOWALIK, M. A.; AMEDEO COLUMBANO; PERRA, A. Emerging Role of the Pentose Phosphate Pathway in Hepatocellular Carcinoma. **Frontiers in Oncology**, v. 7, 11 maio 2017. DOI: https://doi.org/10.3389/fonc.2017.00087

KURMI, K.; HAIGIS, M. C. Nitrogen Metabolism in Cancer and Immunity. **Trends in Cell Biology**, v. 30, n. 5, p. 408–424, maio 2020. DOI: 10.1016/j.tcb.2020.02.005

LANG, Y. *et al.* Interleukin-1 Receptor 2. **Shock**, v. 47, n. 1, p. 119–124, 9 ago. 2016. DOI: 10.1097/SHK.0000000000000714

LEE, J.; KIM, J.; SON, K.; PHAM, A.-L.; MIN, J.-Y. Acid phosphatase 2 (ACP2) is required for membrane fusion during influenza virus entry. **Scientific Reports**, v. 7, n. 1, 8 mar. 2017. DOI: https://doi.org/10.1038/srep43893

LEFORT, C. *et al.* Hepatic NAPE-PLD Is a Key Regulator of Liver Lipid Metabolism. **Cells**, v. 9, n. 5, p. 1247–1247, 18 maio 2020. DOI: https://doi.org/10.3390/cells9051247

LI, H.; RICHARDSON, W. D. Evolution of the CNS myelin gene regulatory program. **Brain Research**, v. 1641, p. 111–121, jun. 2016. DOI: https://doi.org/10.1016/j.brainres.2015.10.013

LI, J. *et al.* A Specialized Epithelial Cell Type Regulating Mucosal Immunity and Driving Human Crohn's Disease. 2 out. 2023. DOI: 10.1101/2023.09.30.560293

LI, J. *et al.* TMCO1-mediated Ca2+ leak underlies osteoblast functions via CaMKII signaling. **Nature Communications**, v. 10, n. 1, 8 abr. 2019. DOI: https://doi.org/10.1038/s41467-019-09653-5

LI, X.; WANG, M.; LIU, S.; CHEN, X.; QIAO, Y.; YANG, X.; YAO, J.; WU, S. Paternal transgenerational nutritional epigenetic effect: A new insight into nutritional manipulation to reduce the use of antibiotics in animal feeding. **Animal Nutrition**, v. 11, p. 142–151, dez. 2022. DOI: 10.1016/j.aninu.2022.07.002

LIAO, H.-Y.; DA, C.-M.; LIAO, B.; ZHANG, H.-H. Roles of matrix metalloproteinase-7 (MMP-7) in cancer. **Clinical Biochemistry**, v. 92, p. 9–18, 10 mar. 2021. DOI: https://doi.org/10.1016/j.clinbiochem.2021.03.003

LIAO, P.; HEMMERLIN, A.; BACH, T. J.; CHYE, M.-L. The potential of the mevalonate pathway for enhanced isoprenoid production. **Biotechnology Advances**, v. 34, n. 5, p. 697–713, set. 2016. DOI: 10.1016/j.biotechadv.2016.03.005

LIAO, Y.; SMYTH, G. K.; SHI, W. featureCounts: an efficient general purpose program for assigning sequence reads to genomic features. **Bioinformatics**, v. 30, n. 7, p. 923-930, 2014. DOI: https://doi.org/10.1093/bioinformatics/btt656

LIN, R. *et al.* 6-Phosphogluconate dehydrogenase links oxidative PPP, lipogenesis and tumour growth by inhibiting LKB1–AMPK signalling. **Nature Cell Biology**, v. 17, n. 11, p. 1484–1496, 19 out. 2015. DOI: 10.1038/ncb3255

LIN, Y. M.; S. DRUYAN; S. YAHAV; BRAKE, J. Thermal treatments prior to and during the beginning of incubation affects development of the broiler embryo and yolk sac membranes, and live performance and carcass characteristics. **Poultry Science**, v. 96, n. 6, p. 1939–1947, 25 fev. 2017. DOI: 10.3382/ps/pew467

LISS, K. H. H.; LUTKEWITTE, A. J.; PIETKA, T.; FINCK, B. N.; FRANCZYK, M.; YOSHINO, J.; KLEIN, S.; HALL, A. M. Metabolic importance of adipose tissue monoacylglycerol acyltransferase 1 in mice and humans. **Journal of Lipid Research**, v. 59, n. 9, p. 1630–1639, 31 maio 2018. DOI: https://doi.org/10.1194/jlr.M084947

LIU, L.; GUO, Z.; TIEU, Q.; CASTLE, A.; CASTLE, D. Role of Secretory Carrier Membrane Protein SCAMP2 in Granule Exocytosis. **Molecular Biology of the Cell**, v. 13, n. 12, p. 4266–4278, 1 dez. 2002. DOI: https://doi.org/10.1091/mbc.e02-03-0136

LIU, D.; LUO, S.; LI, Z.; LIANG, G.; GUO, Y.; XU, Y.; CHONG, K. *COG3* confers the chilling tolerance to mediate OsFtsH2-D1 module in rice. **New Phytologist**, v. 241, n. 5, p. 2143–2157, 3 jan. 2024. DOI: 10.1111/nph.19514

LIU, K.; CHEN, Y.; MENG, Y.; WANG, X.; TANG, X.; LI, H.; CHEN, J.; ZHONG, Z. Identification and functional analysis of a novel TBC1D23 pathogenic variant in a Chinese family with pontocerebellar hypoplasia. **Human Genomics**, v. 19, n. 1, 28 jun. 2025. DOI: https://doi.org/10.1186/s40246-025-00782-1

LIU, L.; WANG, D.; LI, X.; ADEYINKA ABIOLA ADETULA; KHAN, A.; ZHANG, B.; LIU, H.; YU, Y.; CHU, Q. Long-lasting effects of lipopolysaccharide on the reproduction and splenic transcriptome of hens and their offspring. **Ecotoxicology and Environmental Safety**, v. 237, p. 113527–113527, 19 abr. 2022. DOI: https://doi.org/10.1016/j.ecoenv.2022.113527

LOURENS, A.; VAN; M.J.W. HEETKAMP; R. MEIJERHOF; KEMP, B. Effects of Eggshell Temperature and Oxygen Concentration on Embryo Growth and Metabolism During Incubation. **Poultry Science**, v. 86, n. 10, p. 2194–2199, 1 out. 2007. DOI: 10.1093/ps/86.10.2194

LOVE, M. I.; HUBER, W.; ANDERS, S. Moderated estimation of fold change and dispersion for RNA-seq data with DESeq2. **Genome Biology**, v. 15, n. 12, p. 550, 2014. DOI: https://doi.org/10.1186/s13059-014-0550-8

LU, M. *et al.* ACOT12-Dependent Alteration of Acetyl-CoA Drives Hepatocellular Carcinoma Metastasis by Epigenetic Induction of Epithelial-Mesenchymal Transition. **Cell Metabolism**, v. 29, n. 4, p. 886-900.e5, 27 jan. 2019. DOI: https://doi.org/10.1016/j.cmet.2018.12.019

LUCKI, N. C.; BANDYOPADHYAY, S.; WANG, E.; MERRILL, A. H.; SEWER, M. B. Acid Ceramidase (ASAH1) Is a Global Regulator of Steroidogenic Capacity and Adrenocortical Gene Expression. **Molecular Endocrinology**, v. 26, n. 2, p. 228–243, 20 jan. 2012. DOI: https://doi.org/10.1210/me.2011-1150

LUNA-PELÁEZ, N.; MARCH-DÍAZ, R.; MARÍA CEBALLOS-CHÁVEZ; GUERRERO-MARTÍNEZ, J. A.; GRAZIOLI, P.; GARCÍA-GUTIÉRREZ, P.; VACCARI, T.; MASSA, V.;

REYES, J. C.; GARCÍA-DOMÍNGUEZ, M. The Cornelia de Lange Syndrome-associated factor NIPBL interacts with BRD4 ET domain for transcription control of a common set of genes. **Cell Death and Disease**, v. 10, n. 8, 18 jul. 2019. DOI: https://doi.org/10.1038/s41419-019-1792-x

LUND, S. P.; NETTLETON, D.; MCCARTHY, D. J.; SMYTH, G. K. Detecting Differential Expression in RNA-sequence Data Using Quasi-likelihood with Shrunken Dispersion Estimates. **Statistical Applications in Genetics and Molecular Biology**, v. 11, n. 5, 22 out. 2012. DOI: https://doi.org/10.1515/1544-6115.1826

LUTKEWITTE, A. J.; MCCOMMIS, K. S.; SCHWEITZER, G. G.; CHAMBERS, K. T.; GRAHAM, M. J.; WANG, L.; PATTI, G. J.; HALL, A. M.; FINCK, B. N. Hepatic monoacylglycerol acyltransferase 1 is induced by prolonged food deprivation to modulate the hepatic fasting response. **Journal of Lipid Research**, v. 60, n. 3, p. 528–538, 5 jan. 2019. DOI: 10.1194/jlr.M089722

LV, Z.; WANG, T.; CAO, X.; SUN, M.; QU, Y. The role of receptor-type protein tyrosine phosphatases in cancer. **Precision Medical Sciences**, v. 12, n. 1, p. 48–57, 2 jan. 2023. DOI:10.1002/prm2.12090

MA, N. X. *et al.* Slc35a1 deficiency causes thrombocytopenia due to impaired megakaryocytopoiesis and excessive platelet clearance in the liver. **Haematologica**, v. 106, n. 3, p. 759–769, 17 abr. 2020. DOI: 10.3324/haematol.2019.225987

MAHIL, S. K. *et al.* AP1S3 Mutations Cause Skin Autoinflammation by Disrupting Keratinocyte Autophagy and Up-Regulating IL-36 Production. **Journal of Investigative Dermatology**, v. 136, n. 11, p. 2251–2259, 4 jul. 2016. DOI: https://doi.org/10.1016/j.jid.2016.06.618

MATSUDA-LENNIKOV, M. *et al.* Magnesium transporter 1 (MAGT1) deficiency causes selective defects in N-linked glycosylation and expression of immune-response genes. **Journal of Biological Chemistry**, v. 294, n. 37, p. 13638–13656, set. 2019. DOI: https://doi.org/10.1074/jbc.RA119.008903

MENTRUP, H. L.; HARTMAN, A.; THAMES, E. L.; BASHEER, W. A.; MATESIC, L. E. The ubiquitin ligase ITCH coordinates small intestinal epithelial homeostasis by modulating cell proliferation, differentiation, and migration. **Differentiation**, v. 99, p. 51–61, 15 dez. 2017. DOI: https://doi.org/10.1016/j.diff.2017.12.003

MIR, M. A. *et al.* Differential expression of SLITRK6 gene as a potential therapeutic target for urothelial carcinoma in particular upper tract cancer. **Gene**, v. 878, p. 147583, ago. 2023. DOI: https://doi.org/10.1016/j.gene.2023.147583

MÓCSAI, A.; RULAND, J.; VICTOR. The SYK tyrosine kinase: a crucial player in diverse biological functions. **Nature reviews. Immunology**, v. 10, n. 6, p. 387–402, 14 maio 2010. DOI: 10.1038/nri2765

MONSON, M. S.; VAN GOOR, A. G.; ASHWELL, C. M.; PERSIA, M. E.; ROTHSCHILD, M. F.; SCHMIDT, C. J.; LAMONT, S. J. Immunomodulatory effects of heat stress and

lipopolysaccharide on the bursal transcriptome in two distinct chicken lines. **BMC Genomics**, v. 19, n. 1, 30 ago. 2018. DOI: 10.1186/s12864-018-5033-y

MOORHOUSE, A. J.; LOATS, A. E.; MEDLER, K. F.; ROBERTS, S. G. E. The BASP1 transcriptional corepressor modifies chromatin through lipid-dependent and lipid-independent mechanisms. **iScience**, v. 25, n. 8, p. 104796–104796, 20 jul. 2022. DOI: https://doi.org/10.1016/j.isci.2022.104796

MORRIS, K. M. *et al*. The quail genome: insights into social behaviour, seasonal biology and infectious disease response. **BMC Biology**, v. 18, n. 1, p. 14, 2020. DOI: https://doi.org/10.1186/s12915-019-0730-9

MUNIZ-SANTOS; LUCIERI-COSTA, G.; MATHEUS; MORAES-DE-SOUZA, I.; ALICE, M.; SILVA, A. R.; CASSIANO FELIPPE GONÇALVES-DE-ALBUQUERQUE. Lipid oxidation dysregulation: an emerging player in the pathophysiology of sepsis. **Frontiers in Immunology**, v. 14, 3 ago. 2023. DOI: 10.3389/fimmu.2023.1224335

NAKAJIMA, K.; RAZ, A. Autocrine motility factor and its receptor expression in musculoskeletal tumors. **Journal of bone oncology**, v. 24, p. 100318–100318, 14 set. 2020. DOI: https://doi.org/10.1016/j.jbo.2020.100318

NASEER, M. I.; RASOOL, M.; JAN, M. M.; CHAUDHARY, A. G.; PUSHPARAJ, P. N.; ABUZENADAH, A. M.; AL-QAHTANI, M. H. A novel mutation in PGAP2 gene causes developmental delay, intellectual disability, epilepsy and microcephaly in consanguineous Saudi family. **Journal of the Neurological Sciences**, v. 371, p. 121–125, 19 out. 2016. DOI: 10.1016/j.jns.2016.10.027

NGUYEN, T. T. M.; MAHIDA, S.; SMITH-HICKS, C.; CAMPEAU, P. M. A*PIGH*mutation leading to GPI deficiency is associated with developmental delay and autism. **Human Mutation**, v. 39, n. 6, p. 827–829, 26 abr. 2018. DOI: 10.1002/humu.23426

NIU, X.; HONG, J.; ZHENG, X.; MELVILLE, D. B.; KNAPIK, E. W.; MENG, A.; PENG, J. The Nuclear Pore Complex Function of Sec13 Protein Is Required for Cell Survival during Retinal Development. **Journal of Biological Chemistry**, v. 289, n. 17, p. 11971–11985, 14 mar. 2014. DOI: 10.1074/jbc.M114.547190

NOVICK, D.; KIM, S.-H.; GIAMILA FANTUZZI; REZNIKOV, L. L.; DINARELLO, C. A.; RUBINSTEIN, M. Interleukin-18 Binding Protein. **Immunity**, v. 10, n. 1, p. 127–136, 1 jan. 1999. DOI: https://doi.org/10.1016/S1074-7613(00)80013-8

NOVILLO, A.; FERNÁNDEZ-SANTANDER, A.; GAIBAR, M.; GALÁN, M.; ROMERO-LORCA, A.; FADOUA EL ABDELLAOUI-SOUSSI; ARCO, P. G. Role of Chromodomain-Helicase-DNA-Binding Protein 4 (CHD4) in Breast Cancer. **Frontiers in Oncology**, v. 11, 26 abr. 2021. DOI: https://doi.org/10.3389/fonc.2021.633233

NOVOA, L. F.; CORZO, L.; SEOANE, S.; CACABELOS, R. A Genomic Approach to Histamine Function. **Journal of Genomic Medicine and Pharmacogenomics,** v. 2, n.1, p. 233-241, 15 fev. 2017. DOI: https://www.researchgate.net/publication/324330896

OH, S.; MAI, X. L.; KIM, J.; GUZMAN, A. C. V. DE; LEE, J. Y.; PARK, S. Glycerol 3-phosphate dehydrogenases (1 and 2) in cancer and other diseases. **Experimental & Molecular Medicine**, v. 56, n. 5, p. 1066–1079, 1 maio 2024. DOI: https://doi.org/10.1038/s12276-024-01222-1

O'NEILL, L. A. J.; KISHTON, R. J.; RATHMELL, J. A guide to immunometabolism for immunologists. **Nature Reviews Immunology**, v. 16, n. 9, p. 553–565, 11 jul. 2016. DOI:10.1038/nri.2016.70

OLBROMSKI, M.; PODHORSKA-OKOŁ□W, M.; DZIĘGIEL, P. Role of the SOX18 protein in neoplastic processes (Review). **Oncology Letters**, v. 16, n. 2, p. 1383-1389, 25 maio 2018. DOI: 10.3892/ol.2018.8819

PALMER, E. E. *et al.* Neuronal deficiency of*ARV1*causes an autosomal recessive epileptic encephalopathy. **Human Molecular Genetics**, p. ddw157, 6 jun. 2016. DOI: https://doi.org/10.1093/hmg/ddw157

PAPAIOANNOU, P.; WALLACE, M. J.; MALHOTRA, N.; MOHLER, P. J.; EL REFAEY, M. Biochemical Structure and Function of TRAPP Complexes in the Cardiac System. **JACC: Basic to Translational Science**, v. 8, n. 12, p. 1599–1612, dez. 2023. DOI: https://doi.org/10.1016/j.jacbts.2023.03.011

PARK, K.-H.; YE, Z.; ZHANG, J.; HAMMAD, S. M.; TOWNSEND, D. M.; ROCKEY, D. C.; KIM, S.-H. 3-ketodihydrosphingosine reductase mutation induces steatosis and hepatic injury in zebrafish. **Scientific Reports**, v. 9, n. 1, 4 fev. 2019. DOI: https://doi.org/10.1038/s41598-018-37946-0

PAULICK, M. G.; BERTOZZI, C. R. The Glycosylphosphatidylinositol Anchor: A Complex Membrane-Anchoring Structure for Proteins. **Biochemistry**, v. 47, n. 27, p. 6991–7000, 17 jun. 2008. DOI: 10.1021/bi8006324

PETERSEN, A. M.; SMALL, C. M.; YAN, Y.; WILSON, C.; BATZEL, P.; BREMILLER, R. A.; BUCK, C. L.; FRANK; CRESKO, W. A.; POSTLETHWAIT, J. H. Evolution and developmental expression of the sodium–iodide symporter (*NIS*,*slc5a5*) gene family: Implications for perchlorate toxicology. **Evolutionary Applications**, v. 15, n. 7, p. 1079–1098, 24 maio 2022. DOI: https://doi.org/10.1111/eva.13424

R CORE TEAM. **R: A language and environment for statistical computing**. Vienna, Austria: R Foundation for Statistical Computing, 2023. Disponível em: https://www.R-project.org/.

RAMPURIA; MOSYAK, L.; ROOT, A. R.; SVENSON, K.; AGOSTINO, M. J.; LAVALLIE, E. R. Molecular insights into recognition of GUCY2C by T-cell engaging bispecific antibody anti-GUCY2CxCD3. **Scientific Reports**, v. 13, n. 1, 17 ago. 2023. DOI: 10.1038/s41598-023-40467-0

REED, A.; TAKA-AKI ICHU; MILOSEVICH, N.; MELILLO, B.; SCHAFROTH, M. A.; OTSUKA, Y.; SCAMPAVIA, L.; SPICER, T. P.; CRAVATT, B. F. LPCAT3 Inhibitors Remodel the Polyunsaturated Phospholipid Content of Human Cells and Protect from Ferroptosis. **ACS Chemical Biology**, v. 17, n. 6, p. 1607–1618, 6 jun. 2022. DOI: 10.1021/acschembio.2c00317

REHMAN, G.; KUMARI, N.; BANO, F.; TYAGI, R. K. Thyroid hormone receptor beta: Relevance in human health and diseases. **Endocrine and Metabolic Science**, v. 13, p. 100144, dez. 2023. DOI: https://doi.org/10.1016/j.endmts.2023.100144

RENTOFT, M. *et al.* Heterozygous colon cancer-associated mutations of *SAMHD1* have functional significance. **Proceedings of the National Academy of Sciences**, v. 113, n. 17, p. 4723–4728, 11 abr. 2016. DOI: 10.1073/pnas.1519128113

RONALDO LIRA-JUNIOR; HOLMSTRÖM, S. B.; CLARK, R.; ZWICKER, S.; MIRJAM MAJSTER; JOHANNSEN, G.; BJÖRN AXTELIUS; SIGVARD ÅKERMAN; SVENSSON, M.; KLINGE, B.; BOSTRÖM, E. A. S100A12 Expression Is Modulated During Monocyte Differentiation and Reflects Periodontitis Severity. **Frontiers in Immunology**, v. 11, 31 jan. 2020. DOI: https://doi.org/10.3389/fimmu.2020.00086

ROSTAGNO, S. H. *et al*. **Composição de Alimentos e Exigências Nutricionais 3 a Edição Editor: Horacio Santiago Rostagno**. [s.l: s.n.]. 2011. Disponível em: https://centrodepesquisasavicolas.wordpress.com/wp-content/uploads/2011/02/tabelas-brasileiras-2011.pdf

RYAN, D. G.; LUKE. Krebs cycle rewired for macrophage and dendritic cell effector functions. **FEBS Letters**, v. 591, n. 19, p. 2992–3006, 7 jul. 2017. DOI: https://doi.org/10.1002/1873-3468.12744

SADIK, A. *et al.* IL4I1 Is a Metabolic Immune Checkpoint that Activates the AHR and Promotes Tumor Progression. **Cell**, v. 182, n. 5, p. 1252-1270.e34, 19 ago. 2020. DOI: https://doi.org/10.1016/j.cell.2020.07.038

SALAUN, C.; TOMKINSON, N. C. O.; CHAMBERLAIN, L. H. The endoplasmic reticulum–localized enzyme zDHHC6 mediates S-acylation of short transmembrane constructs from multiple type I and II membrane proteins. **Journal of Biological Chemistry**, v. 299, n. 10, p. 105201–105201, 1 set. 2023. DOI: https://doi.org/10.1016/j.jbc.2023.105201

SCANES, C. G. Avian Physiology: Are Birds Simply Feathered Mammals? **Frontiers in Physiology**, v. 11, 9 nov. 2020. DOI: https://doi.org/10.3389/fphys.2020.542466

SEDGHI, M.; FATEMEH JAVANMARD; ANVAR AMOOZMEHR; SAEID ZAMANY; MOHAMMADI, I.; KIM, W.; REDDY, S. Lysophospholipid Supplementation in Broiler Breeders' Diet Benefits Offspring's Productive Performance, Blood Parameters, and Hepatic β-Oxidation Genes. **Animals**, v. 14, n. 21, p. 3066–3066, 24 out. 2024. DOI: https://doi.org/10.3390/ani14213066

SHIMELL, J. J. *et al.* The X-Linked Intellectual Disability Gene Zdhhc9 Is Essential for Dendrite Outgrowth and Inhibitory Synapse Formation. **Cell Reports**, v. 29, n. 8, p. 2422-2437.e8, nov. 2019. DOI: 10.1016/j.celrep.2019.10.065

SHIN, M. C.; JUNG, Y. H.; JEONG, Y.; OH, A.-R.; LEE, S. B.; KIM, K. Kctd17-mediated Chop degradation promotes adipogenic differentiation. **Biochemical and Biophysical Research Communications**, v. 653, p. 126–132, abr. 2023. DOI: 10.1016/j.bbrc.2023.02.068

SINGH, H.; RAI, V.; AGRAWAL, D. K. LPS and oxLDL-induced S100A12 and RAGE expression in carotid arteries of atherosclerotic Yucatan microswine. **Molecular Biology Reports**, v. 49, n. 9, p. 8663–8672, 30 jun. 2022. DOI: 10.1007/s11033-022-07703-8

SMITH, E. S. *et al.* SEMA4D compromises blood–brain barrier, activates microglia, and inhibits remyelination in neurodegenerative disease. **Neurobiology of Disease**, v. 73, p. 254–268, 18 out. 2014. DOI: https://doi.org/10.1016/j.nbd.2014.10.008

SOKOLOWSKA, E. *et al.* The circadian gene *Cryptochrome 2* influences stress-induced brain activity and depressive-like behavior in mice. **Genes, Brain and Behavior**, v. 20, n. 4, 26 out. 2020. DOI: https://doi.org/10.1111/gbb.12708

STERTZ, L.; CONTRERAS-SHANNON, V.; MONROY-JARAMILLO, N.; SUN, J.; WALSS-BASS, C. BACE1-Deficient Mice Exhibit Alterations in Immune System Pathways. **Molecular Neurobiology**, v. 55, n. 1, p. 709–717, 21 dez. 2016. DOI: 10.1007/s12035-016-0341-1

SUZUKI, T.; MIZUTA, C.; UDA, K.; ISHIDA, K.; MIZUTA, K.; SONA, S.; COMPAAN, D. M.; ELLINGTON, W. R. Evolution and Divergence of the Genes for Cytoplasmic, Mitochondrial, and Flagellar Creatine Kinases. **Journal of Molecular Evolution**, v. 59, n. 2, p. 218–226, ago. 2004. DOI: https://doi.org/10.1007/s00239-004-2615-x

SYMON, A.; HARLEY, V. SOX9: A genomic view of tissue specific expression and action. **The International Journal of Biochemistry & Cell Biology**, v. 87, p. 18–22, 16 mar. 2017. DOI: https://doi.org/10.1016/j.biocel.2017.03.005

TANAKA, K. The proteasome: Overview of structure and functions. **Proceedings of the Japan Academy Series B**, v. 85, n. 1, p. 12–36, 1 jan. 2009. DOI: 10.2183/pjab.85.12

TANAKA, Y.; MAESHIMA, A. M.; NOMOTO, J.; MAKITA, S.; FUKUHARA, S.; MUNAKATA, W.; MARUYAMA, D.; TOBINAI, K.; KOBAYASHI, Y. Expression pattern of PD-L1 and PD-L2 in classical Hodgkin lymphoma, primary mediastinal large B-cell lymphoma, and gray zone lymphoma. **European Journal of Haematology**, v. 100, n. 5, p. 511–517, mar. 2018. DOI: https://doi.org/10.1111/ejh.13033

TANG, X.; CROMWELL, C. R.; LIU, R.; GODBOUT, R.; HUBBARD, B. P.; MCMULLEN, T. P. W.; BRINDLEY, D. N. Lipid phosphate phosphatase-2 promotes tumor growth through increased c-Myc expression. **Theranostics**, v. 12, n. 13, p. 5675–5690, 1 jan. 2022. DOI: 10.7150/thno.66230

TAYLOR, H. A.; PRZEMYLSKA, L.; CLAVANE, E. M.; MEAKIN, P. J. BACE1: More than just a β-secretase. **Obesity Reviews**, v. 23, n. 7, 4 fev. 2022. DOI: https://doi.org/10.1111/obr.13430

THE GENE ONTOLOGY CONSORTIUM. The Gene Ontology resource: enriching a GOld mine. **Nucleic Acids Research**, v. 49, n. D1, p. D325-D334, 2021. DOI: https://doi.org/10.1093/nar/gkaa1113.

THOMPSON, R. P.; NILSSON, E.; SKINNER, M. K. Environmental epigenetics and epigenetic inheritance in domestic farm animals. **Animal Reproduction Science Elsevier B.V.**, 1 set. 2020. DOI: 10.1016/j.anireprosci.2020.106316

TOBIAS, A.; SADIQ, N. M. **Physiology, Gastrointestinal Nervous Control**. Disponível em: <https://www.ncbi.nlm.nih.gov/books/NBK545268/>. Acesso em: 8 jul. 2025.

TONA, K.; F BAMELIS; B DE KETELAERE; BRUGGEMAN, V.; MORAES, V.; J BUYSE; O ONAGBESAN; E DECUYPERE. Effects of egg storage time on spread of hatch, chick quality, and chick juvenile growth. **Poultry Science**, v. 82, n. 5, p. 736–741, 1 maio 2003. DOI: 10.1093/ps/82.5.736

TONG, Y.; YU, C.; CHEN, S.; ZHANG, X.; YANG, Z.; WANG, T. Trans-anethole exerts protective effects on lipopolysaccharide-induced acute jejunal inflammation of broilers via repressing NF-κB signaling pathway. **Poultry Science**, v. 102, n. 2, p. 102397–102397, 9 dez. 2022. DOI: 10.1016/j.psj.2022.102397

TONG, Y.; YU, C.; CHEN, S.; ZHANG, X.; YANG, Z.; WANG, T. Trans-anethole exerts protective effects on lipopolysaccharide-induced acute jejunal inflammation of broilers via repressing NF-κB signaling pathway. **Poultry Science**, v. 102, n. 2, p. 102397, fev. 2023. DOI: 10.1016/j.psj.2022.102397

TORRES, I. L.; ROSA-FERREIRA, C.; MUNRO, S. The Arf family G protein Arl1 is required for secretory granule biogenesis in Drosophila. **Journal of Cell Science**, 1 jan. 2014. DOI: 10.1242/jcs.122028

TORRES-VALDETANO; VERÓNICA VALLEJO-RUIZ; MILFLORES-FLORES, L.; MARTÍNEZ-MORALES, P. Role of *PIGM* and *PIGX* in glycosylphosphatidylinositol biosynthesis and human health (Review). **Biomedical Reports**, v. 20, n. 4, 5 fev. 2024. DOI: https://doi.org/10.3892/br.2024.1746

UDA, K.; FUJIMOTO, N.; AKIYAMA, Y.; MIZUTA, K.; TANAKA, K.; ELLINGTON, W. R.; SUZUKI, T. Evolution of the arginine kinase gene family. **Comparative Biochemistry and Physiology Part D: Genomics and Proteomics**, v. 1, n. 2, p. 209–218, jun. 2006. DOI: https://doi.org/10.1016/j.cbd.2005.10.007

VAN; INGRID; MITCHELL, M. A.; MOLENAAR, R.; HENRY. A review on yolk sac utilization in poultry. **Poultry Science**, v. 99, n. 4, p. 2162–2175, 8 fev. 2020. DOI: 10.1016/j.psj.2019.11.041

VENKATAKRISHNAN, J.; YUAN, Y.; ZHANG, J.; YU, Y.; HU, Y.-C.; KAO, W. W-Y. Self-complementary AAV vector therapy for treating corneal cloudiness of mucopolysaccharidosis

type VII (MPS VII). **The Ocular Surface**, v. 32, p. 39–47, abr. 2024. DOI: 10.1016/j.jtos.2024.01.002

VIJAYAKUMAR, S.; JONES, S. M.; JONES, T. A.; TIAN, C.; JOHNSON, K. R. Spontaneous mutations of the Zpld1 gene in mice cause semicircular canal dysfunction but do not impair gravity receptor or hearing functions. **Scientific Reports**, v. 9, n. 1, 27 ago. 2019. DOI: https://doi.org/10.1038/s41598-019-48835-5

WANG, B.; WU, L.; CHEN, J.; DONG, L.; CHEN, C.; WEN, Z.; HU, J.; FLEMING, I.; WANG, D. W. Metabolism pathways of arachidonic acids: mechanisms and potential therapeutic targets. **Signal Transduction and Targeted Therapy**, v. 6, n. 1, 26 fev. 2021. DOI: https://doi.org/10.1038/s41392-020-00443-w

WANG, F. Interleukin-18 binding protein: Biological properties and roles in human and animal immune regulation (Review). **Biomedical Reports**, v. 20, n. 6, 9 abr. 2024. DOI: https://doi.org/10.3892/br.2024.1775

WANG, H.; ZANG, C.; LIU, X. S.; ASTER, J. C. The Role of Notch Receptors in Transcriptional Regulation. **Journal of Cellular Physiology**, v. 230, n. 5, p. 982–988, 28 jan. 2015. DOI: 10.1002/jcp.24872

WANG, J. *et al.* NR2F2 loss-of-function mutation is responsible for congenital bicuspid aortic valve. **International Journal of Molecular Medicine**, 31 jan. 2019. DOI: https://doi.org/10.3892/ijmm.2019

WANG, L.; XU, W.; MEI, Y.; WANG, X.; LIU, W.; ZHU, Z.; NI, Z. CHRDL2 promotes cell proliferation by activating the YAP/TAZ signaling pathway in gastric cancer. **Free Radical Biology and Medicine**, v. 193, p. 158–170, nov. 2022. DOI: https://doi.org/10.1016/j.freeradbiomed.2022.09.006

WANG, P.; DAI, X.; JIANG, W.; LI, Y.; WEI, W. RBR E3 ubiquitin ligases in tumorigenesis. **Seminars in Cancer Biology**, v. 67, p. 131–144, 19 maio 2020. DOI: https://doi.org/10.1016/j.semcancer.2020.05.0

WANG, Q.-C. *et al.* TMCO1 Is an ER Ca 2+ Load-Activated Ca 2+ Channel. **Cell**, v. 165, n. 6, p. 1454–1466, 21 maio 2016. DOI: 10.1016/j.cell.2016.04.051

WANG, Q.; THIAM, M.; LISSETTE, A.; WANG, Z.; ZHANG, J.; LI, Q.; WEN, J.; ZHAO, G. Gene Co-Expression Network Analysis Reveals the Hub Genes and Key Pathways Associated with Resistance to Salmonella Enteritidis Colonization in Chicken. **International Journal of Molecular Sciences**, v. 24, n. 5, p. 4824–4824, 2 mar. 2023. DOI: https://doi.org/10.3390/ijms24054824

WANG, X.; LI, C.; WANG, Y.; LI, L.; HAN, Z.; WANG, G. UFL1 Alleviates LPS-Induced Apoptosis by Regulating the NF-κB Signaling Pathway in Bovine Ovarian Granulosa Cells. **Biomolecules**, v. 10, n. 2, p. 260, 9 fev. 2020. DOI: 10.3390/biom10020260

WANG, Y.; FANG, J.; ZENG, H.-F.; ZHONG, J.-F.; LI, H.-X.; CHEN, K.-L. Identification and bioinformatics analysis of differentially expressed milk exosomal microRNAs in milk

exosomes of heat-stressed Holstein cows. **Functional & Integrative Genomics**, v. 22, n. 1, p. 77–87, 27 nov. 2021. DOI: 10.1007/s10142-021-00814-8

WANG, Y.-Q.; REN, Y.; GALE, R. P.; NIU, L.-T.; HUANG, X.-J. Sphingosine-1 phosphate receptor 1 (S1PR1) expression maintains stemness of acute myeloid leukemia stem cells. **Cancer Letters**, v. 600, p. 217158, set. 2024. DOI: https://doi.org/10.1016/j.canlet.2024.217158

WARD, C.; SJULSON, L.; BATISTA-BRITO, R. The function of Mef2c toward the development of excitatory and inhibitory cortical neurons. **Frontiers in Cellular Neuroscience**, v. 18, 23 set. 2024. DOI: https://doi.org/10.3389/fncel.2024.1465821

WATT, S. M.; HANS-JÖRG BÜHRING; SIMMONS, P. J.; ANDREW. The stem cell revolution: on the role of CD164 as a human stem cell marker. **npj Regenerative Medicine**, v. 6, n. 1, 8 jun. 2021. DOI: https://doi.org/10.1038/s41536-021-00143-1

WENG, X.; CHEN, W.; HU, W.; XU, K.; QI, L.; CHEN, J.; LU, D.; SHAO, Y.; ZHENG, X.; YE, C.; ZHENG, S. PTPRB promotes metastasis of colorectal carcinoma via inducing epithelial-mesenchymal transition. **Cell Death and Disease**, v. 10, n. 5, 30 abr. 2019. DOI: https://doi.org/10.1038/s41419-019-1554-9

WIERTSEMA, S. P.; JEROEN VAN BERGENHENEGOUWEN; JOHAN GARSSEN; LEON. The Interplay between the Gut Microbiome and the Immune System in the Context of Infectious Diseases throughout Life and the Role of Nutrition in Optimizing Treatment Strategies. **Nutrients**, v. 13, n. 3, p. 886–886, 9 mar. 2021. DOI: 10.3390/nu13030886

WINFREE, R. L.; NOLAN, E.; KAJ BLENNOW; ZETTERBERG, H.; GIFFORD, K. A.; PECHMAN, K. R.; SCHNEIDER, J.; BENNETT, D. A.; PETYUK, V. A.; JEFFERSON, A. L.; HOHMAN, T. J. Vascular endothelial growth factor receptor-1 (FLT1) interactions with amyloid-beta in Alzheimer's disease: a putative biomarker of amyloid-induced vascular damage. **Neurobiology of Aging**, v. 147, p. 141–149, 25 dez. 2024. DOI: https://doi.org/10.1016/j.neurobiolaging.2024.12.010

WOLFE, R. *et al.* ITCH deficiency clinical phenotype expansion and mitochondrial dysfunction. **Molecular Genetics and Metabolism Reports**, v. 33, p. 100932–100932, 30 out. 2022. DOI: https://doi.org/10.1016/j.ymgmr.2022.100932

WRIGHT, F. A.; BONZERATO, C. G.; SLITER, D. A.; WOJCIKIEWICZ, R. J. H. The erlin2 T65I mutation inhibits erlin1/2 complex–mediated inositol 1,4,5-trisphosphate receptor ubiquitination and phosphatidylinositol 3-phosphate binding. **Journal of Biological Chemistry**, v. 293, n. 40, p. 15706–15714, out. 2018. DOI: https://doi.org/10.1074/jbc.RA118.004547

WU, G.; RUAN, J.; LIU, J.; ZHANG, C.; KANG, L.; WANG, J.; ZOU, Y.; SONG, L. Variant Spectrum of Formin Homology 2 Domain-Containing 3 Gene in Chinese Patients With Hypertrophic Cardiomyopathy. **Journal of the American Heart Association**, v. 10, n. 5, p. e018236, 1 fev. 2021. DOI: 10.1161/JAHA.120.018236

XIURUI LV; MURPHY, K.; MURPHY, Z.; GETMAN, M.; RAHMAN, N.; NAKAMURA, Y.; BLANC, L.; GALLAGHER, P. G.; PALIS, J.; NARLA MOHANDAS; STEINER, L. A. HEXIM1 is an essential transcription regulator during human erythropoiesis. **Blood**, v. 142, n. 25, p. 2198–2215, 22 set. 2023. DOI: 10.1182/blood.2022019495

YALCIN, S.; SEZEN ÖZKAN; SHAH, T. Incubation Temperature and Lighting: Effect on Embryonic Development, Post-Hatch Growth, and Adaptive Response. **Frontiers in Physiology**, v. 13, 13 maio 2022. DOI: https://doi.org/10.3389/fphys.2022.899977

YAN, Z.; LIU, Y.; YUAN, Y. The plasticity of epithelial cells and its potential in the induced differentiation of gastric cancer. **Cell Death Discovery**, v. 10, n. 1, 24 dez. 2024. DOI: https://doi.org/10.1038/s41420-024-02275-x

YANG, L. *et al.* PGM3 insufficiency: a glycosylation disorder causing a notable T cell defect. **Frontiers in Immunology**, v. 15, 24 dez. 2024. DOI: https://doi.org/10.3389/fimmu.2024.1500381

YANG, L.; YANG, T.; WANG, H.; DOU, T.; FANG, X.; SHI, L.; LI, X.; FENG, M. DNMBP-AS1 Regulates NHLRC3 Expression by Sponging miR-93-5p/17-5p to Inhibit Colon Cancer Progression. **Frontiers in Oncology**, v. 12, 27 abr. 2022. DOI: 10.3389/fonc.2022.765163

YANG, Z.; TAO, T.; RAFTERY, M. J.; YOUSSEF, P.; DI GIROLAMO, N.; GECZY, C. L. Proinflammatory properties of the human S100 protein S100A12. **Journal of Leukocyte Biology**, v. 69, n. 6, p. 986–994, 1 jun. 2001. DOI: https://doi.org/10.1189/jlb.69.6.986

YIN, H.; ZHAO, J.; HE, H.; CHEN, Y.; WANG, Y.; LI, D.; ZHU, Q. Gga-miR-3525 Targets PDLIM3 through the MAPK Signaling Pathway to Regulate the Proliferation and Differentiation of Skeletal Muscle Satellite Cells. **International Journal of Molecular Sciences**, v. 21, n. 15, p. 5573–5573, 4 ago. 2020. DOI: 10.3390/ijms21155573

YU, G.; WANG, L.-G.; HAN, Y.; HE, Q.-Y. clusterProfiler: an R Package for Comparing Biological Themes Among Gene Clusters. **OMICS A Journal of Integrative Biology**, v. 16, n. 5, p. 284–287, 28 mar. 2012. DOI: 10.1089/omi.2011.0118.

ZHANG, Q. *et al.* Deficiency in SLC25A15, a hypoxia-responsive gene, promotes hepatocellular carcinoma by reprogramming glutamine metabolism. **Journal of Hepatology**, v. 80, n. 2, p. 293–308, 30 out. 2023. DOI: 10.1016/j.jhep.2023.10.024

ZHAO, M., WANG, Q., LIU, L., GENG, T., GONG, D. Mitochondrial-bound hexokinase 1 can affect the glucolipid metabolism and reactive oxygen species production in goose fatty liver. **Italian Journal of Animal Science**, v. 21 (1), p. 314–323, 2022. DOI https://doi.org/10.1080/1828051X.2022.2029589

ZHAO, S.; ZHANG, X.; YANG, L.; WANG, Y.; JIA, S.; LI, X.; WANG, Z.; YANG, F.; LIANG, M.; WANG, X.; WANG, D. ATP6V0C gene variants were identified in individuals with epilepsy, with or without developmental delay. **Journal of Human Genetics**, v. 68, n. 9, p. 589–597, 10 maio 2023. DOI: https://doi.org/10.1038/s10038-023-01145-1

ZHAO, X.-F. *et al.* PlexinA2 Forward Signaling through Rap1 GTPases Regulates Dentate Gyrus Development and Schizophrenia-like Behaviors. **Cell Reports**, v. 22, n. 2, p. 456–470, 1 jan. 2018. DOI: 10.1016/j.celrep.2017.12.044

ZHU, C.; SOLORZANO, C.; SAHAR, S.; REALINI, N.; FUNG, E.; SASSONE-CORSI, P.; PIOMELLI, D. Proinflammatory Stimuli Control N-Acylphosphatidylethanolamine-Specific Phospholipase D Expression in Macrophages. **Molecular Pharmacology**, v. 79, n. 4, p. 786–792, abr. 2011. DOI: https://doi.org/10.1124/mol.110.070201